


AN ABSTRACT OF THE THESIS OF

BRUCE JOHN HIGGINS for the degree of MASTER OF SCIENCE
in Ocean Engineering presented on June 3, 1976
Title: AN OPERATION STUDY OF THE WHEELWASH DREDGE SANDWICK
Abstract approved by: Signature redacted for privacy.
 Larry S. Slotta

An interesting means of shoal removal has recently been implemented by the U.S. Army Corps of Engineers for use in shallow Pacific Coast tidal inlets and estuaries. In the past, removal of shoaled material has consisted of physical excavation of material, transportation from the site, and placement in a spoils area. The present study considers a method of shoal removal by agitation dredging; the shoaled material is placed into suspension by propeller wash and is then carried downstream by natural currents.

The interrelationships of the variables governing the wheelwash process were investigated by a systematic study of the basic parameters. A determination of the propeller and deflector door hydrodynamics on a modified landing craft, the LCM Sandwick, was undertaken along with documentation of the scour process and altered settling in the propeller wake region. Laboratory models were used to confirm theoretical predictions and for comparison with field measurements regarding scour depths and efficiencies.

An Operation Study
of the Wheelwash Dredge
Sandwick

by

Bruce John Higgins

A THESIS

submitted to

Oregon State University

in partial fulfillment of
the requirements for the
degree of

Master of Ocean Engineering

June 1977

ACKNOWLEDGEMENTS

I wish to express my gratitude to Professors Larry S. Slotta, J. Sergio Montes and Charles K. Sollitt for their guidance and encouragement during this project.

I extend my appreciation to Richard Downs, James Leshuk and Jim McGinnis for their aid in conducting the field and laboratory measurements. Thanks is also given to the crew of the LCM Sandwick for their cooperation in the field whereby their efforts facilitated obtaining prototype information.

The Corps of Engineers, Portland District, provided the financial support for this study to Oregon State University through Contract Number 57-74-C-0087, which is gratefully acknowledged.

List of Symbols

as they appear

U_o	velocity at nozzle
D_o	diameter of nozzle
r	radial direction
Z, z	vertical distance
Z_o	height of jet above bed
U	velocity of the jet
Z_{max}	distance of maximum scour
R_{max}	rim maximum
Z_{core}	length of the core
b	width of the jet
U_c	jet velocity at centerline
U_m, U_{max}	maximum jet velocity
δ	height of $U_{1/2}$ in a wall jet
θ	angle from vertical
Δr	displacement of impingement, for deflected jet
Y_f	height of forward deflected flow
Y_b	height of back deflected flow
U_f	velocity of deflected jet, forward
U_b	velocity of deflected jet, back
ϕ	radial angle
U_s	crossflow

α	amplitude of pulsation
ω, f	frequency of pulsation
t, t^*	time, normalized time
k	$k = 2f/U$
$E(k)$	energy of pulsation
\bar{u}	turbulent velocity component
Q	discharge of the jet
μ	viscosity of the jet
g	gravity
ρ	density of the fluid
ω	pulsation rate
d_s, d	diameter of the sediment
h_1, h	normalizing height
W, w	weight of scoured material
B	constant
V	normalized volume
\bar{W}, \bar{w}	normalized weight
γ_s	specific gravity of the sediment
γ	specific gravity of the fluid
\bar{y}	normalized height
\bar{T}	normalized time
R, \bar{R}	Reynolds number
F, \bar{F}	Froude number
W_s, w_s	fall velocity
L_r	length ratio
D_m, D_{50}	mean diameter of the sediment

List of Figures

<u>Figure</u>		<u>Page</u>
I- 1	The LCM <u>Sandwich</u> , with deflector door raised	2
II- 1	Jet schematic, for reference and symbol definition	7
II- 2	Scour hole schematic, for reference and symbol definition	8
II- 3	Axisymmetric round jet, major features in the entrainment and developments of flow	10
II- 4	Lateral velocity distribution for an axisymmetric round jet	11
II- 5	Decay of centerline velocity	12
II- 6	Dimensionless distribution of mean radial velocities	14
II- 7	Control volume for a deflected, axisymmetric round jet	15
II- 8	Jet deflected by flow	17
II- 9	Variation of jet spread $r_{1/2}/D_o$, and centerline velocity decay	19
II-10	Non-dimensional spectrum at $r/D_o = 0$, $Z/D_o = 12$	20
III- 1	Comparison of critical velocity relationships	24
III- 2	Angle of repose of moderately angular sand grains	25
III- 3	Self-similar scour hole for a plain jet	27
III- 4	Effect of screen on normalized depth of scour, $d = 4\text{mm}$, $F = 2.53$, $R = 2250$	29
IV- 1	Sketch of model hull used in tests	31
IV- 2	Model test circuit	33
IV- 3	Plot of U/U_{\max} for a 10° deflector door	41
IV- 4	Plot of U/U_{\max} for a 20° deflector door	42
IV- 5	Plot of U/U_{\max} for a 30° deflector door	43
IV- 6	Decay of maximum velocity along center plan, with square root of nozzle area	44

<u>Figure</u>		<u>Page</u>
IV- 7	Isovels for 10° deflector door, LCM <u>Sandwick</u> 1:12 scale model	45
IV- 8	Isovels for 20° deflector door, LCM <u>Sandwick</u> 1:12 scale model	46
IV- 9	Settling velocity vs. particle diameter	48
IV-10	Erosion-deposition criteria for uniform particles	49
IV-11	Angle of repose for sand grains	50
IV-12	Four basic scour forms observed for 1:40 model	52
IV-13	Self-similar scour holes for a 20° deflector door angle showing the extremes observed 1:12 model	54
IV-14	Depth of maximum scour for different deflector door angles, 1:12 scale	56
IV-15	Depth of maximum scour for different deflector door angles, 1:40 scale	57
IV-16	Normalized volume scoured vs. normalized time	58
V- 1	Streamlines behind the LCM <u>Sandwick</u> , 10° deflector	64
V- 2	Streamlines behind the LCM <u>Sandwick</u> , 20° deflector	65
V- 3	Velocity profile behind the LCM <u>Sandwick</u> , 10° deflector	66
V- 4	Velocity profile behind the LCM <u>Sandwick</u> , 20° deflector	67
V- 5	Location of scour holes	68
V- 6	North hole, 20 December 1973	70
V- 7	Central hole, 20 December 1973	71
V- 8	South hole, 20 December 1973	72
V- 9	North hole, slope comparisons	73
V-10	Central hole, slope comparisons	74
V-11	South hole, slope comparisons	75
V-12	Volume of material removed vs. time of operation	77
V-13	North hole, 6 February 1974	78

<u>Figure</u>	<u>Page</u>
V-14 North hole, 23 May 1974	79
V-15 Central hole, 6 February 1974	80
V-16 Central hole, 23 May 1974	81
V-17 South hole, 6 February 1974	82
V-18 South hole, 23 May 1974	83
V-19 Fill-in vs. time	86

List of Tables

<u>Table</u>		<u>Page</u>
IV-1	Modeled Parameters	32
IV-2	Pertinent Variables of Jet Discharge	35
IV-3	Pertinent Variables of Scour	37
V-1	Test Summary	61
V-2	Volumes Excavated for Various Tests Conditions	76
V-3	Dredge Hole Accretion	85
V-4	Slope Measurements	87

Table of Contents

	<u>Page</u>
Abstract	ii
Acknowledgements	iii
List of Symbols	iv
List of Figures	vi
List of Tables	ix
I. Introduction	1
Background	1
Purpose and Scope of The Study	1
II. Hydrodynamics of Jets	6
Governing Equations	6
III. Sediment Processes - Scour and Settling	22
Theory of Bed Scour	22
IV. Model Study	30
Background	30
Model Similitude	34
Scaling of Sediments	36
Test Procedure	38
Parameters Measured	39
V. Field Study	60
Background	60
Methods	60
Parameters	63
Soil Property Measurements	84
VI. Conclusions and Recommendations	89
VII. References	91
Appendices: (1) <u>Sandwick</u> Design Information	
(2) Grain Size Distribution	
(3) Model Information	

An Operation Study of the Wheelwash Dredge Sandwick

I. Introduction

Background

The LCM Sandwick, a specially adapted LCM-8 landing craft, has successfully been utilized for maintenance shoal removal of several shallow Oregon waterways (Bechley 1975). This vessel, shown in Figure I-1, does not remove shoaled material by conventional dredging methods. Rather, the vessel depends on the action of its propeller wake to scour and suspend the bed sediments. The suspended material is moved only a short distance away by a combination of propeller wake and by the region's natural currents. The twin propellers of the craft create a high velocity current similar to water jets operating in a static fluid. The wash is directed toward the bed by a deflector door mounted on the vessel's stern. The jet will scour non-consolidated material including sand, gravel and silt. The depth of operation and size of the sediment particles determines the efficiency of this scouring process.

Purpose and Scope of the Study

The study's objective was to determine the operational characteristics and efficiency potential of the LCM Sandwick as a maintenance shoal removal device. Past operations with this craft have easily scoured silts to more than 6 meters, while gravel has successfully been removed only to a depth of 4 meters (Bechley 1975). The scoured material subsequently travels as bed and suspended load with the propeller wash and natural currents. The scoured material eventually settles out downstream. The stream's ability to carry bed load ultimately governs the scoured pattern

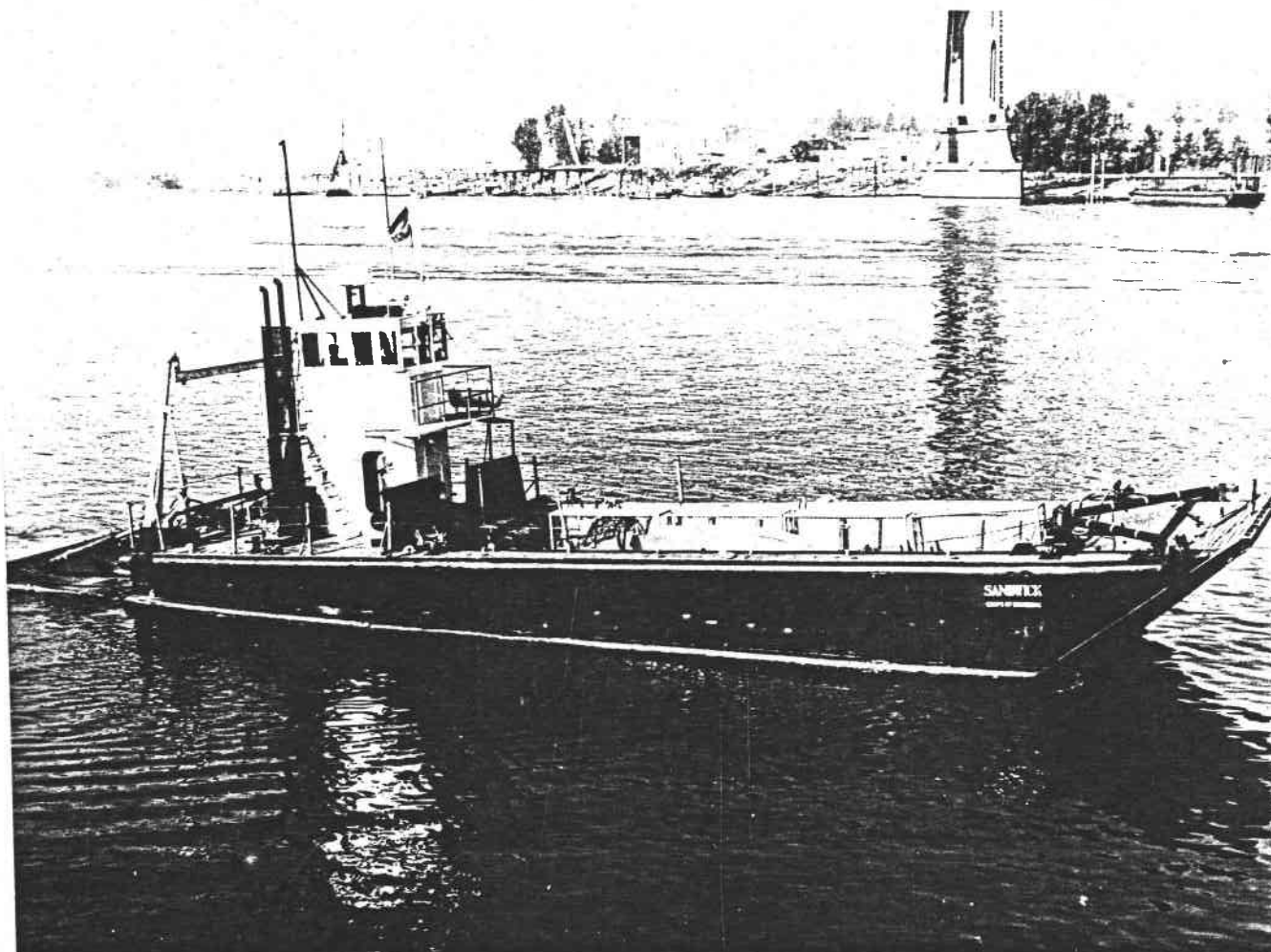


Figure I-1. The LCM Sandwich with deflector door raised.

in the sediment. Depending on the motion of the vessel, either a hole or a channel can be formed in the bed material. Where there are pronounced tidal effects the operation can be properly timed to accelerate the seaward transport of sediments together with the natural stream flow movement.

The LCM Sandwick, as an agitation dredge, was developed from the experience of limited propeller dredging by tugboats in small harbors. In 1969 a patent was issued to the Fred DeVine Diving and Salvage Company of Portland, Oregon for the development of a stern deflector door which would direct the propeller wash downward for scouring bed material. This patent was based on the size, shape and location of the basic components and equipment for propeller wash redirection. DeVine's vessel, the Salvage Chief, was equipped with a deflector door for creating a scoured channel entry across the breaker zone for placement of large ocean outfall pipes (Corps of Engineers 1973). It was found to be most successful, repeatedly transporting over $2,000 \text{ m}^3/\text{hr}$ of suspended sand transport.

The Corps of Engineers received permission to use DeVine's patent to develop and test the device for shoal removal. They retained the original propellers and power plant of the LCM Sandwick and added a deflector door and an improved anchoring system for making the craft a shoal removal device. The deflector door, a hydraulic flap on the stern of the vessel, has improved the erosion potential of the LCM Sandwick. Together with the vessel's anchoring system, the deflector door and rudder are moved either independently or in conjunction to aim the propeller wash. The LCM can be positioned with an anchor extending from each corner of the ship or from a central anchor placed

straight astern of the vessel. This enables the operator to control the vessel, directing the propeller wash at shoaled materials. The LCM Sandwick can commute between sites as a normal craft with the deflector door retracted, out of the water. Optimum operating characteristics were desired for suggesting improved operations of existing vessels and perhaps for the design of other craft for wheel-wash dredging. Tradeoffs in design, such as made originally on converting the LCM Sandwick, are common in naval architectural developments.

The LCM Sandwick received only minor alterations for the present application; but due to potential economic advantages of this method of dredging, future craft may be built specifically for agitation dredging.

The three objectives of this study were to determine the hydrodynamical efficiency of propeller-deflector door combinations, to document the scour process and bed material transport by a propeller as affected by depth and to observe the altered settling of the scoured material in the propeller wake region. To understand the operation and mechanics of propeller wash shoal removal, several approaches were initiated: theoretical, scale model and field measurement. The theoretical approach considered the hydrodynamics of the propeller wash as affected by a deflector door. The scale model studies were conducted to test the theories and to evaluate different configurations of the components. Field measurements and actual process observations were undertaken to determine the relative effectiveness of propeller wash systems.

Most of the information reported here has resulted from studies of physical models; investigations involving actual vessel modifications would be unreasonably expensive. Scale models, under static fluid conditions, were used to study variations of deflector door angle, speed of propeller rotation and depth of the water on scour hole creation. Less emphasis was placed on other factors, but preliminary tests were conducted to determine the importance of the direction of propeller rotation, the motion of the vessel while on its anchors and the length of the deflector door. Documentation of actual scour holes and of velocity distributions behind the LCM Sandwich were conducted near Garabaldi Harbor on Tillamook Bay and near Charleston Harbor on Coos Bay.

II. Hydrodynamics of Jets

Governing Equations

Theory on jets discharging into still water has been satisfactorily defined; many investigations have documented test data on jet discharges (Harsha 1971, Donalson and Snedeker 1971, and others). In this study, no attempt was made to conduct further investigations of such flows; rather a review of previously published information was to be applied for predicting the potential of scour by a jet-propeller wash analogy. Such information would provide concepts to aid in interpreting and predicting field and model findings. The highlights of water jet dredging are discussed in the following section, paralleling the approach of Slotta and Montes (1975).

A simplified theoretical approach to the jet flow analysis is used to typify jet erosion. The jet is assumed to discharge to a submerged condition. A schematic of a simple jet system (Figure II-1) is used to define symbols and serves to give reference to features of the jet flow pattern. The discharge velocity, U_0 , comes from a tube of diameter D_0 directed at the bed. The coordinate system for the jet is r in the radial direction and z , positive downward, in the vertical direction. The elevation of the discharge tube above the bed is Z_0 and the velocity of the jet is U .

A schematic of the scour hole, presented in Figure II-2, serves for defining other symbols and to illustrate features of a simple scour pattern. The scoured bed reaches a maximum depth Z_{\max} , with a characteristic rim radius R_{\max} . The scour pattern has a shape dependent on the strength of the jet; scour pattern II would result from a strong jet striking the bed, while scour pattern I would appear if the jet

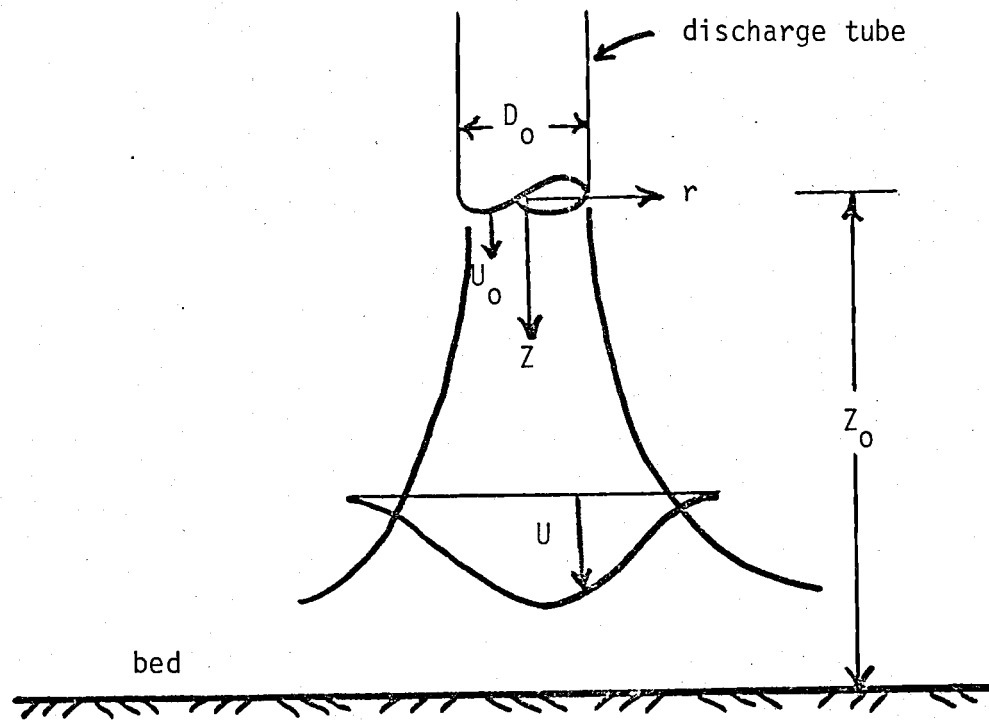


Figure II-1. Jet schematic for reference and symbol definition.

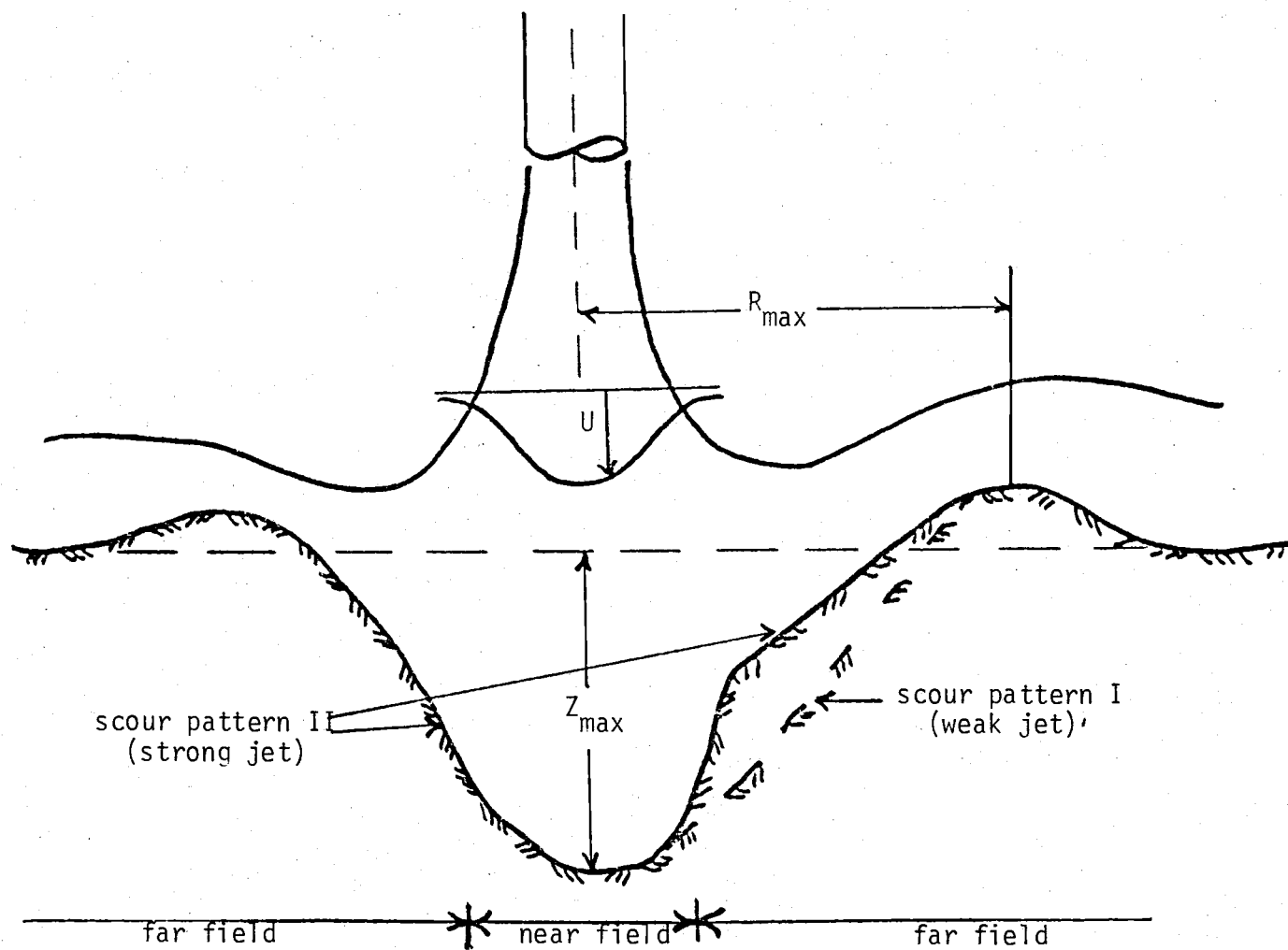


Figure II-2. Scour hole schematic for reference and symbol definition, follows Westrich (1974).

were weak. Two regions exist which influence the flow near the bed. The near field is the region where jet impingement is very dominant and where the bed is nearly horizontal. The far field region receives substantial bed alteration and the velocity of the flow there is substantially reduced because of contact with the bed.

The jet's flow characteristics change immediately as the fluid leaves the tube; Figure II-3 illustrates the flow development as it exhausts from the tube. The flow proceeds through three regions in the development of the jet: the core region, the transition region and the fully developed region. The core region is of the length Z_{core} , where the maximum discharge velocity is observed. The flow, of width b , spreads out in the transition region, entraining more fluid. Farther from the tube, the flow pattern becomes a stable, symmetric shape in the fully developed region; the centerline velocity of the jet is U_c .

The distribution of lateral velocity in the fully developed region forms a pattern independent of the distance of the flow from the tube. Harsha's (1971) work (Figure II-4) shows a typical relationship of the fluid velocity to the radial distance from the tube's centerline. This curve is normalized both in the centerline velocity and in the distance from the tube. This typical relationship is useful in predicting the characteristics of a jet flow in the fully developed region. Also it is known that the jet's strength decays on traveling through the medium and eventually becomes undetectable. Harsha (1971) compiled the results of several investigators in order to correlate the centerline velocity decay with the distance from the tube (Figure II-5). The decay rate is logarithmic in both velocity and distance traveled and, therefore, plots linearly on a log-log graph. It should be noted

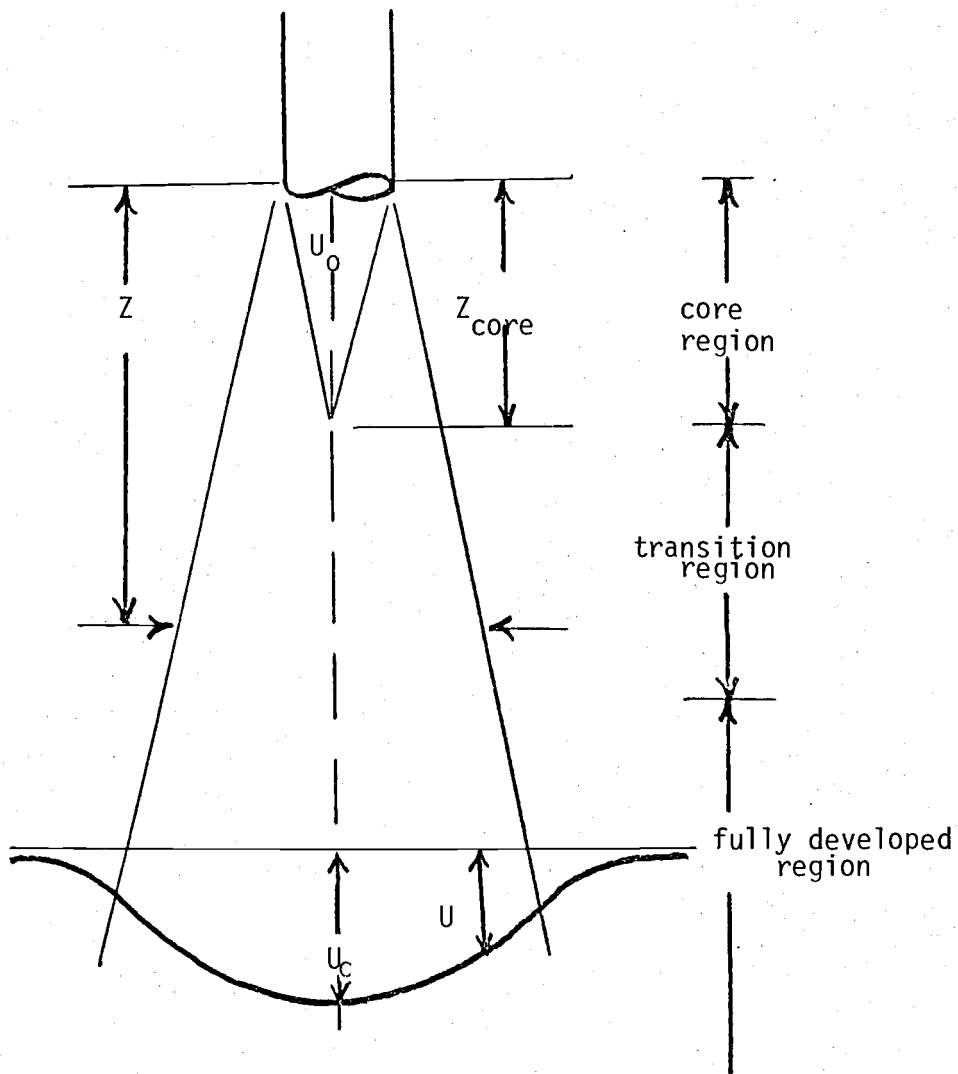


Figure II-3. Axisymmetric round jet, major features in the entrainment and development of flow.

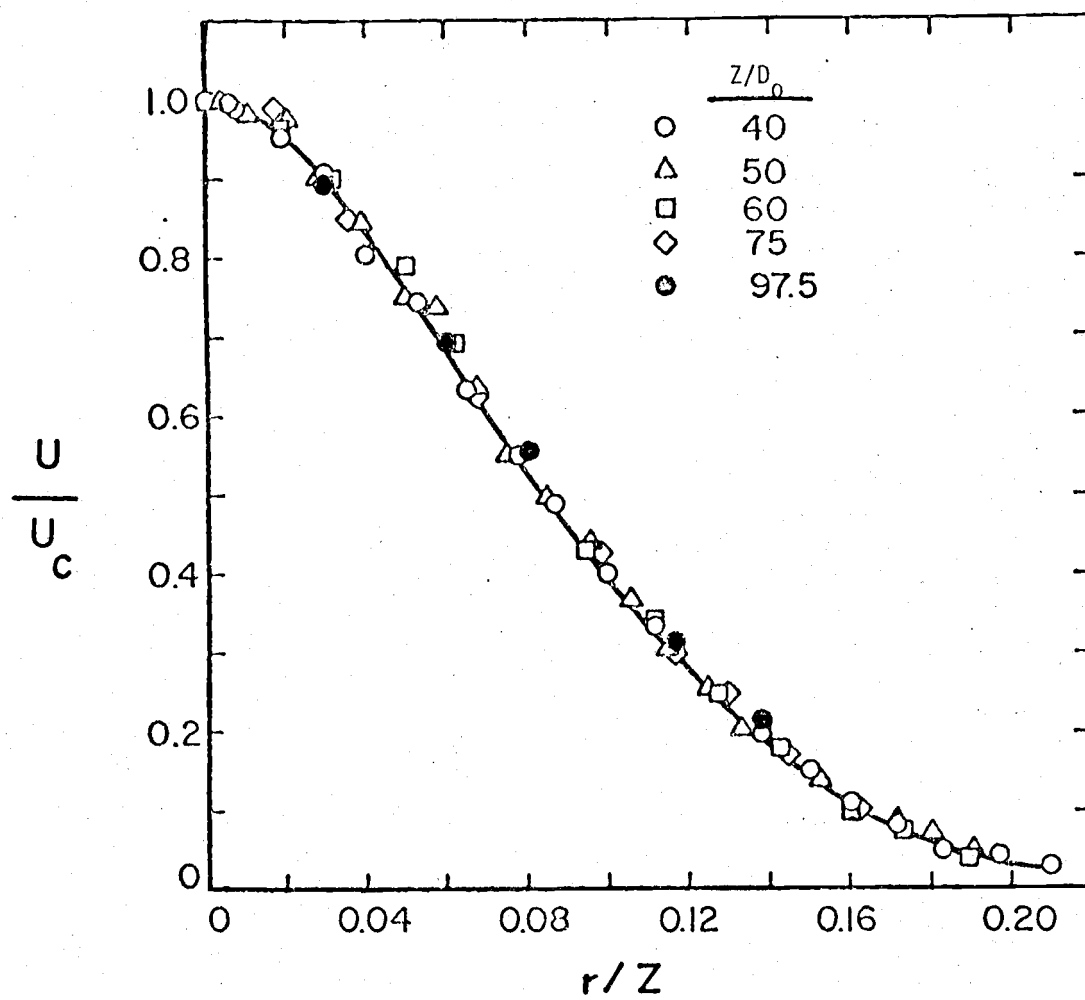


Figure II-4. Lateral velocity distribution for an axisymmetric round jet, from Harsha (1971).

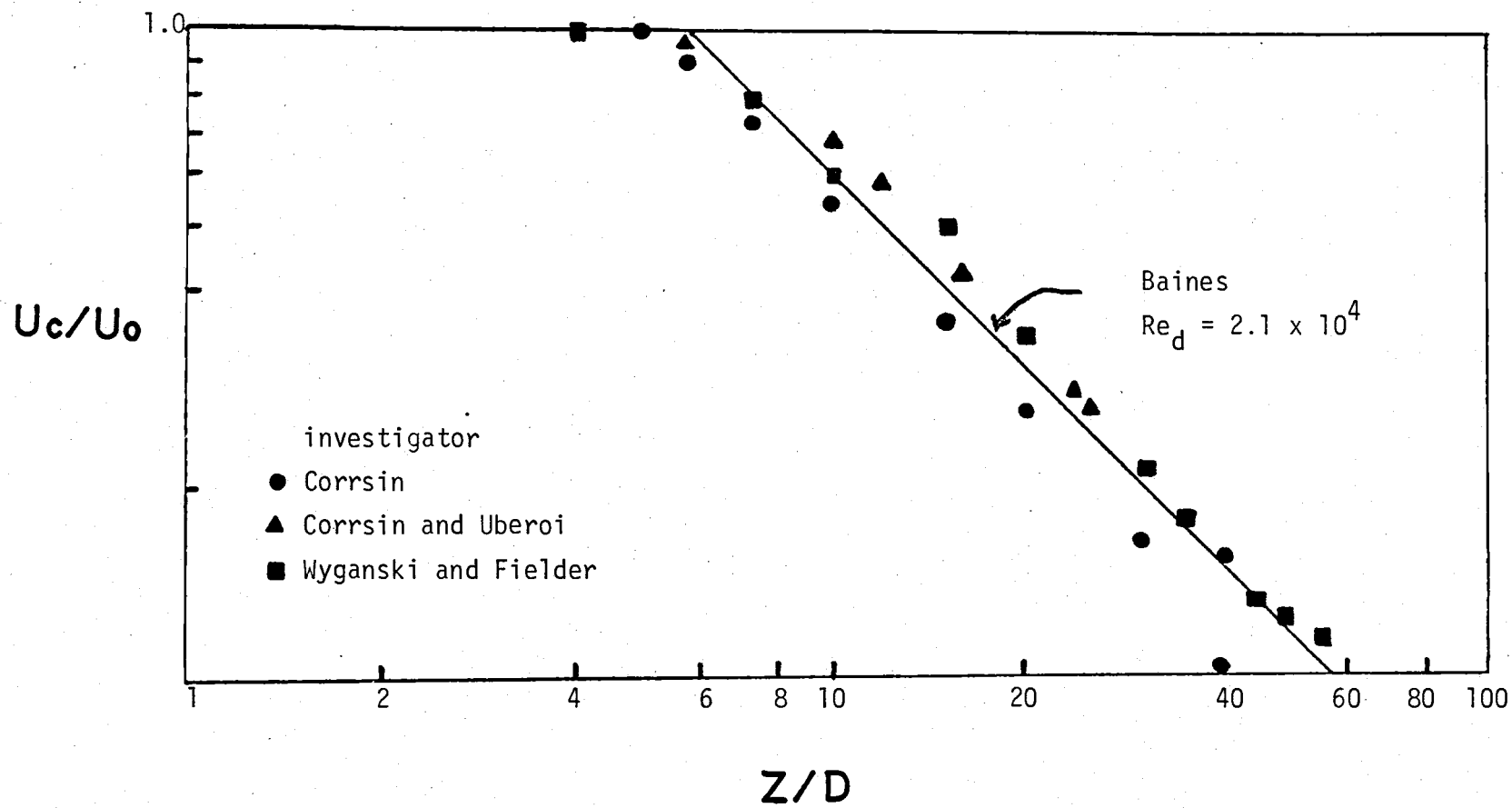


Figure II-5. Decay of centerline velocity from Harsha (1971).

that the core region extends about three tube diameters, and the transition region ends six tube diameters from the tube. About eleven tube diameters distance from the tube, the centerline velocity is about $0.5 U_c$.

To extend this introduction regarding basic jet flow to the scour-jet applications, it will be helpful to examine the characteristics of jets impacting a solid surface. The jet under consideration impinges normally to the bed. In dealing with axisymmetric jet spread, the flow would be symmetric about the vertical jet axis. The deflected jet's spreading flow is broken into two regions: the near field and the far field. In the far field, the deflected or spread jet behaves as a wall jet (Figure II-6). This jet flow along a boundary causes the jet velocity to decrease and is known as a wall jet; see Figure II-6. A wall jet has three characteristic dimensions: U_m is the maximum velocity and δ is the height of the $U_m/2$ point farther above the surface. Bradbury's (1972) curve (Figure II-6) shows normalized data both with respect to height using δ and to velocity using U_m . The plotted data (Figure II-6) was taken at different heights and radial distances from the jet nozzle and shows a self-similar form. The curve is observed to apply over a wide range of values as seen in the limited spread of normalized plotted data points.

If the jet is deflected at an angle from the vertical, the flow will no longer be axisymmetric. In the following illustration (Figure II-7) the details of a deflected jet are sketched. The centerline velocity is, as before, U_c which is at angle θ from the vertical. The point of highest velocity is deflected downstream, Δr , and would be the center of the ellipse in the righthand illustration. The flow has a height Y_f in the downstream or forward direction, and a height Y_b , in the backflow

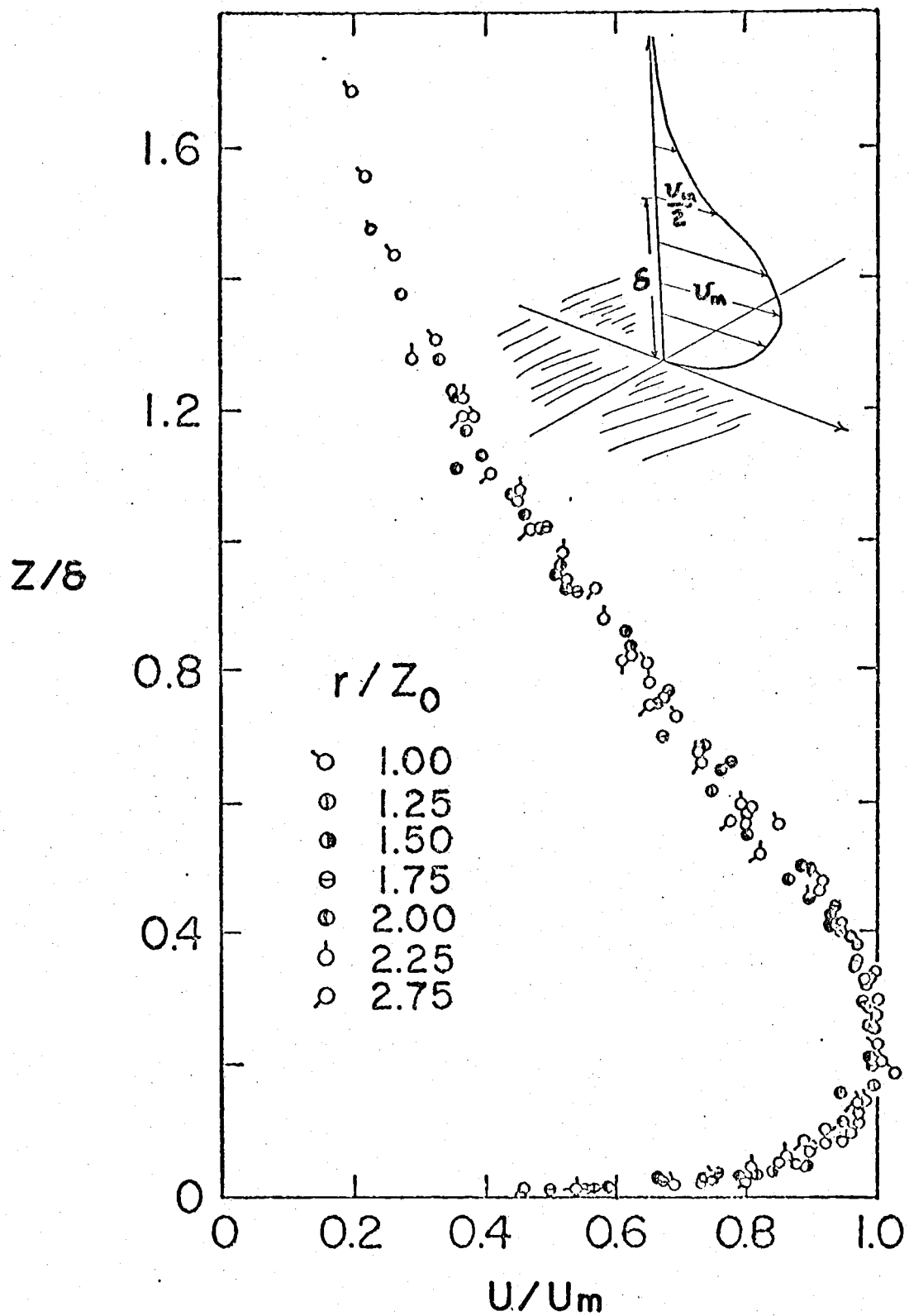


Figure II-6. Dimensionless distribution of mean radial velocities; after Bradbury (1972).

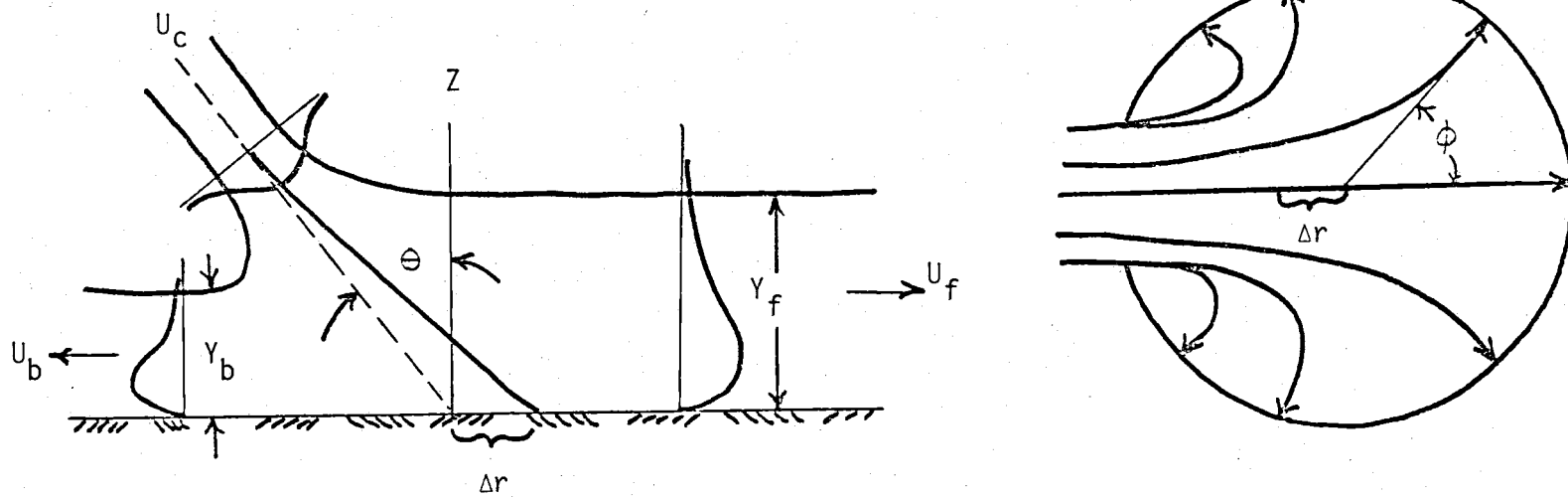


Figure II-7. Control volume for a deflected, axisymmetric round jet.

region. The flow pattern, both U_f and U_b , will have similar configurations as a wall jet. The angle θ is a measure of the angle from the principal direction of jet flow. The work of Slotta and Montes (1975) has shown that

$$\Delta r = 1.54r_{1/2}\sin\theta$$

applies for a jet striking a solid boundary. Their work has also shown that

$$\frac{U_{180^\circ \text{ max}}}{U_{0^\circ \text{ max}}} = \left(\frac{r - \Delta r}{r + \Delta r} \right)^{1.1}$$

governs the ratio of forward to backflow of a deflected jet. This relationship is important in the region very near the impingement point.

Jet flow, as applied to considerations regarding the agitation dredge, thus far has been described for various jet orientations in a static fluid. If the jet flow were issued into a uniform crossflow, a deflected jet (Figure II-8) of a different nature than previously described would be created. The transition region of the jet flow will be made up of a core and a wake, but because of the shearing action of the deflecting flow, the jet's core loses its axisymmetric shape and takes on a kidney shaped cross section. The wake is located in the downstream indent of the kidney shape and the flow has a turbulent structure. The cross flow, due to the intense shear at the edge of the jet, causes the change in shape. The edges could possibly roll into the centerline of the jet, causing the extreme case of two counter-rotating vortices proceeding down flow. This configuration will be shown to be similar to the wake of a twin propeller craft in confined water. Available literature regarding the strength of downstream vortices is extremely limited; therefore, no further discussion of

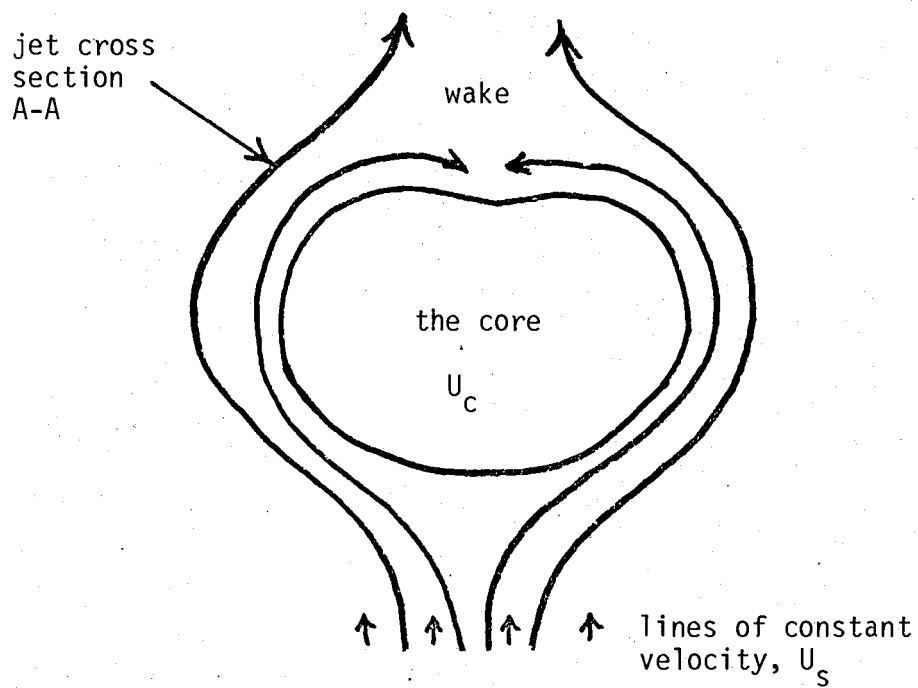
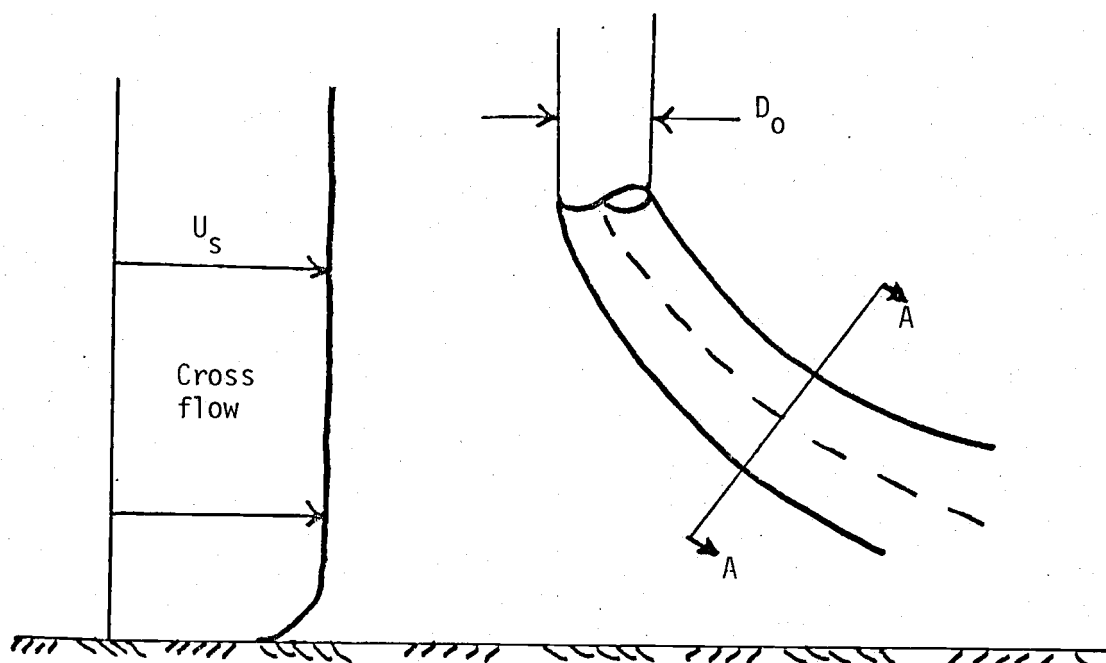


Figure II-8. Jet deflected by flow, section A-A, after Slotta and Montes (1975).

vortex-induced velocities will be attempted.

The final aspect of jet flow to be considered involves unsteady or pulsating jets or jets which have a velocity as a function of time such as:

$$U = U_0 (1 + \alpha (\sin \sigma t)).$$

Pulsating jets have been shown by Westrich (1973) to erode larger amounts of sediment than that possible with a continuous jet of the same geometry. The significant parameters regarding pulsating jets include the jet spread and decay of maximum velocity. Figure II-9 shows typical variation of jet spread $\frac{r_{1/2}}{D_0}$ and centerline velocity decay of both pulsating and stationary jet streams. Figure II-10 shows a non-dimensional energy spectrum at $r/D_0 = 0$ and $Z/D_0 = 12$ for the same case as Figure II-9 for stationary and pulsating jets. These curves would indicate that there is a more energetic mixing in the early development of the jet. The core length of the pulsating jet is reduced to less than one-half that of a stationary jet where the lateral spread is now based on the diameter of the nozzle and $U = U_{\max}/2$. The mean velocity of the pulsating jet matches well with a steady jet at even short distances from the nozzle.

Pulsating jets apparently behave like stationary jets, with the exception of their scour potential. Westrich's experiments (1974) have shown that the amplitude of the jet velocity has very little influence on the scoured volume; the frequency of pulsing flow governs the scour rate. Slotta and Montes (1975) concluded from Westrich's data that the turbulence in the collapse of the pulsating jet serves as a responsible agent in maintaining a high scour potential.

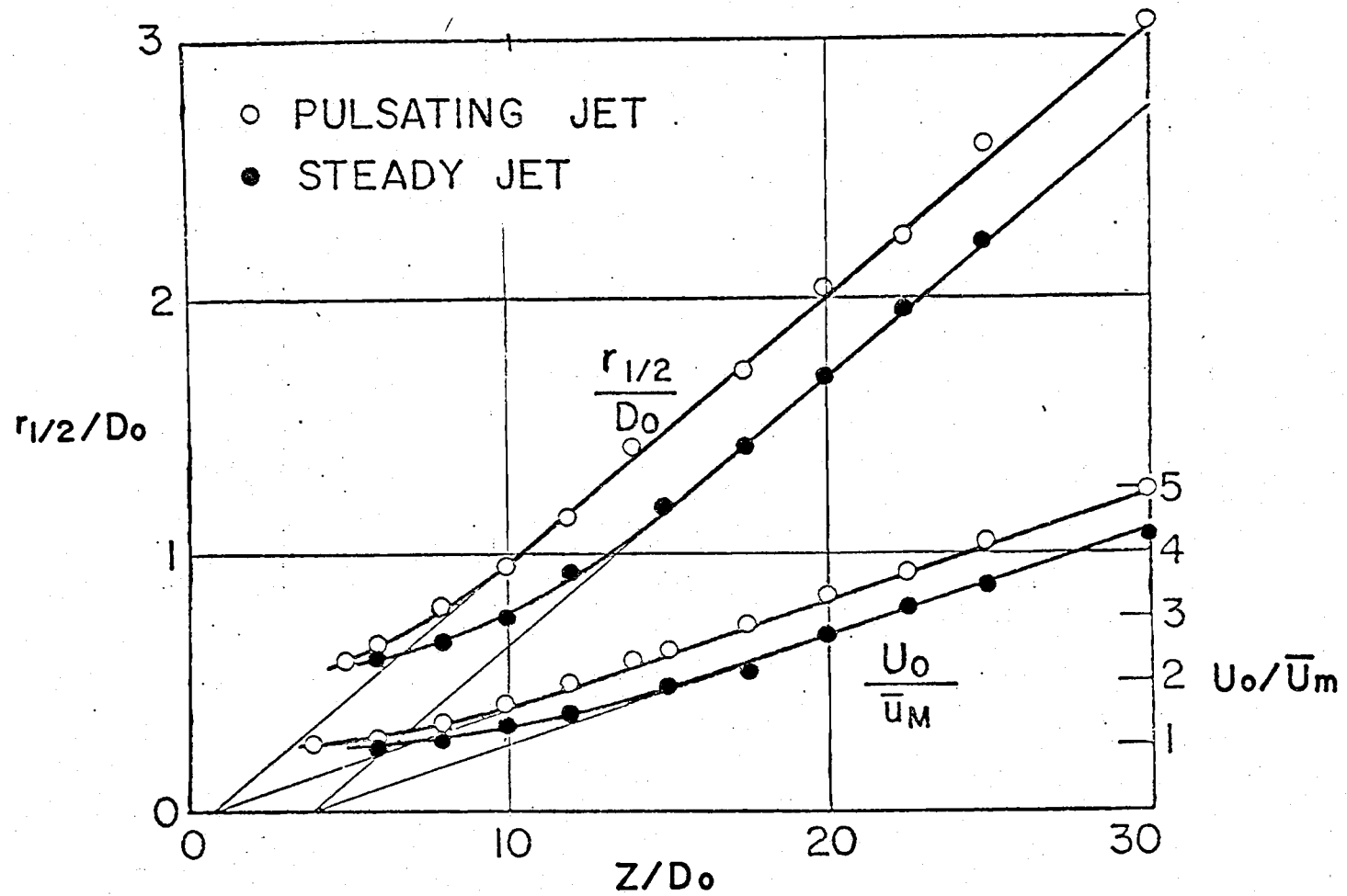


Figure II-9. Variation of jet spread $r_{1/2}/D_0$, and centerline velocity decay, from Miyake and Binder (1970).

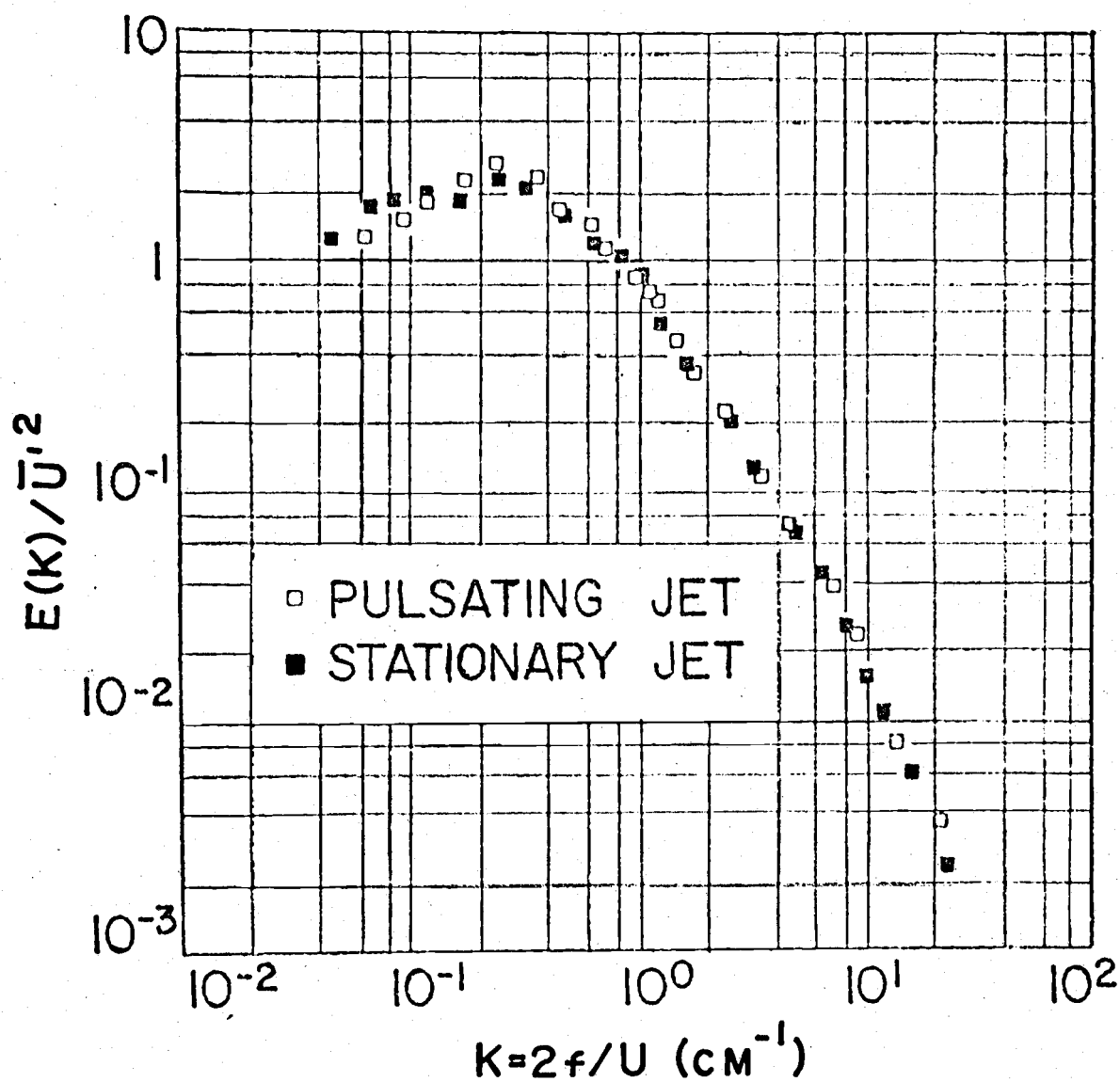


Figure II-10. Non-dimensional energy spectrum at $r/D_0 = 0$, $Z/D_0 = 12$.
After Miyake and Binder (1970).

In summary, a discussion of jet literature has been applied to characterize the propeller wash of the LCM Sandwich. The propeller wash is similar to a pulsating deflected wall jet. The non-dimensional characteristics of jet flow are used to understand the model's and prototype's operation. Next, the influence of this jet wash reacting with the bed material is discussed.

III. Sediment Processes-Scour and Settling

Theory of Bed Scour

Thus far the fluid mechanics of jets and how jet velocities are changed by the water column and striking a bottom boundary have been considered. The process by which the sediment is transported into an equilibrium condition will next be discussed. The key concept of this discussion will concern minimum velocity required for scouring, entraining and transporting submerged sediment particles.

In general, a particle on the bed will experience forces associated with the local fluid velocity. These forces are grouped as creating either skin friction on the surface of the particle or pressure forces of the velocity distribution near the particle. A particle would resist motion by its weight and inter-particle forces of both the friction type and weak chemical bond type. Since a force analysis on each particle would become overly complex, the assumption is made that the upward projection of the fluid force on the particle must exceed or equal the particle's weight for commencement of particle motion.

The jet flow striking the bed can be described as containing three flow regions:

A. Laminar zone, where, far from the jet, the viscous effects of the fluid dominate. Particles there would be shielded from turbulence by distance alone.

B. Transition zone, where turbulence and viscous stresses are of similar magnitude.

C. Turbulent zone, where turbulence and associated fluctuations govern the forces on the particle.

These flow regions are not identical to those defined for the jet as the reference frame for these regions would be upwards from the bed, not outwards from the jet. The process by which sediment particles are moved is inherently associated with turbulence; therefore, continued discussions dealing with the mechanics of transition and turbulent zones will be necessary.

Yalin (1972) correlated a relationship of a dimensionless velocity, U^2/gSd_s , with a dimensionless sediment size, d_s/h ; where d_s is the diameter of the sediment particle, h a characteristic height, and s the specific gravity. Figure III-1 shows this interrelationship for determining critical erosion or particle pickup velocities for stream flow. The stream bed for Yalin's critical velocity relationship has been assumed to be horizontal. If the bed were sloping at some angle, the force required to move the sediment downstream would be reduced by the cosine of the angle of repose multiplied by the weight. To correct for the bed slope Slotta and Montes (1975) formed a figure from previous studies of the critical angle of repose; these results are shown in Figure III-2. A slope correction of 0.92 was found satisfactory for most common sediments, since differences in threshold sediment erosion velocity data would be considerable, the slope correction would be minor.

The formation of scour holes formed by jet action will be discussed next. If the velocity of the jet impingement on the bed exceeds the threshold entrainment velocity, the sediment grain will move along with the jet flow. Since the jet has a lateral decrease in velocity with distance, transport ultimately ceases at some place downstream from the influence of the jet wake. This process continues until an equilibrium scour hole is developed having either stationary or cyclic form.

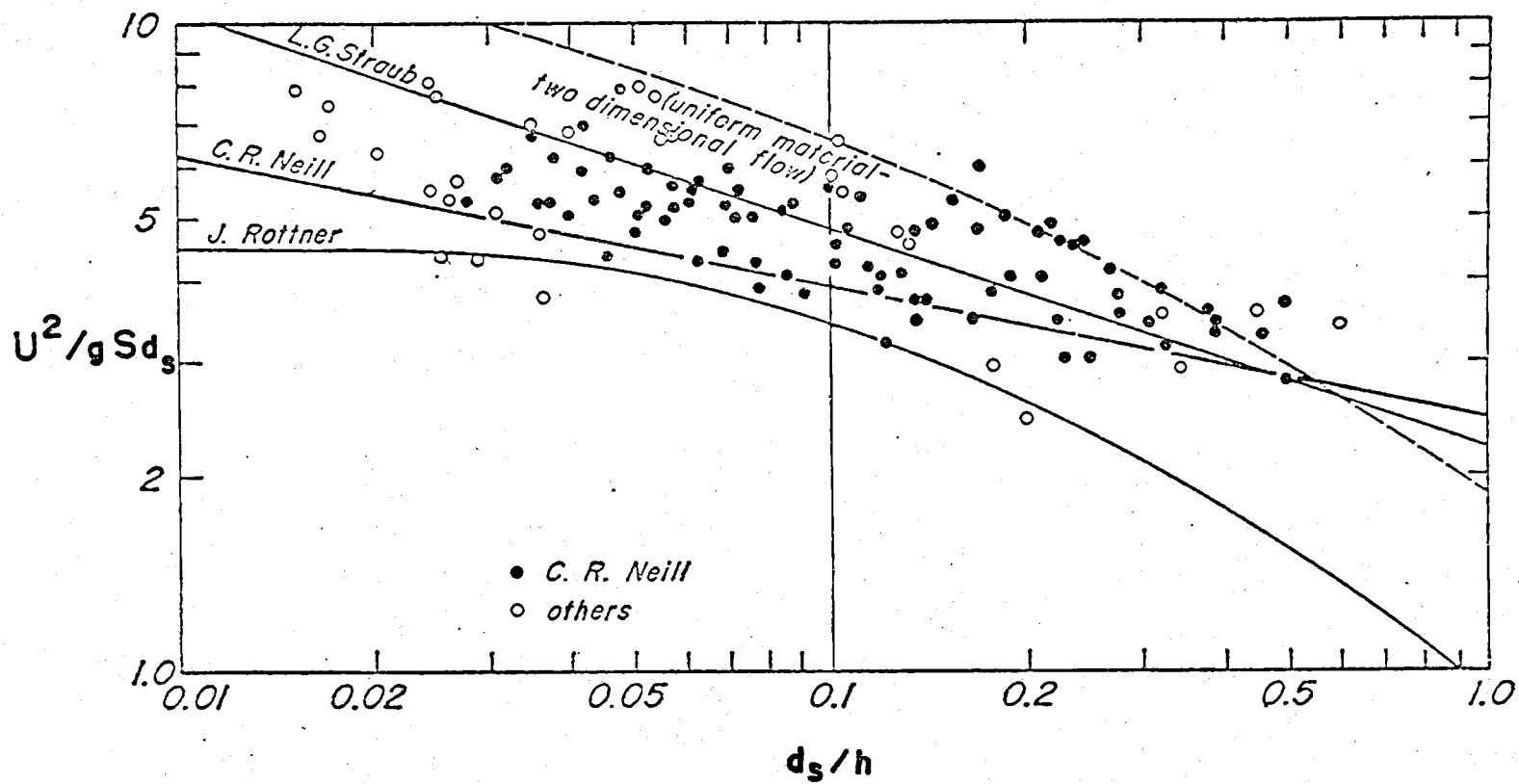


Figure III-1. Comparison of critical erosion velocity relationships, from Yalin (1972).

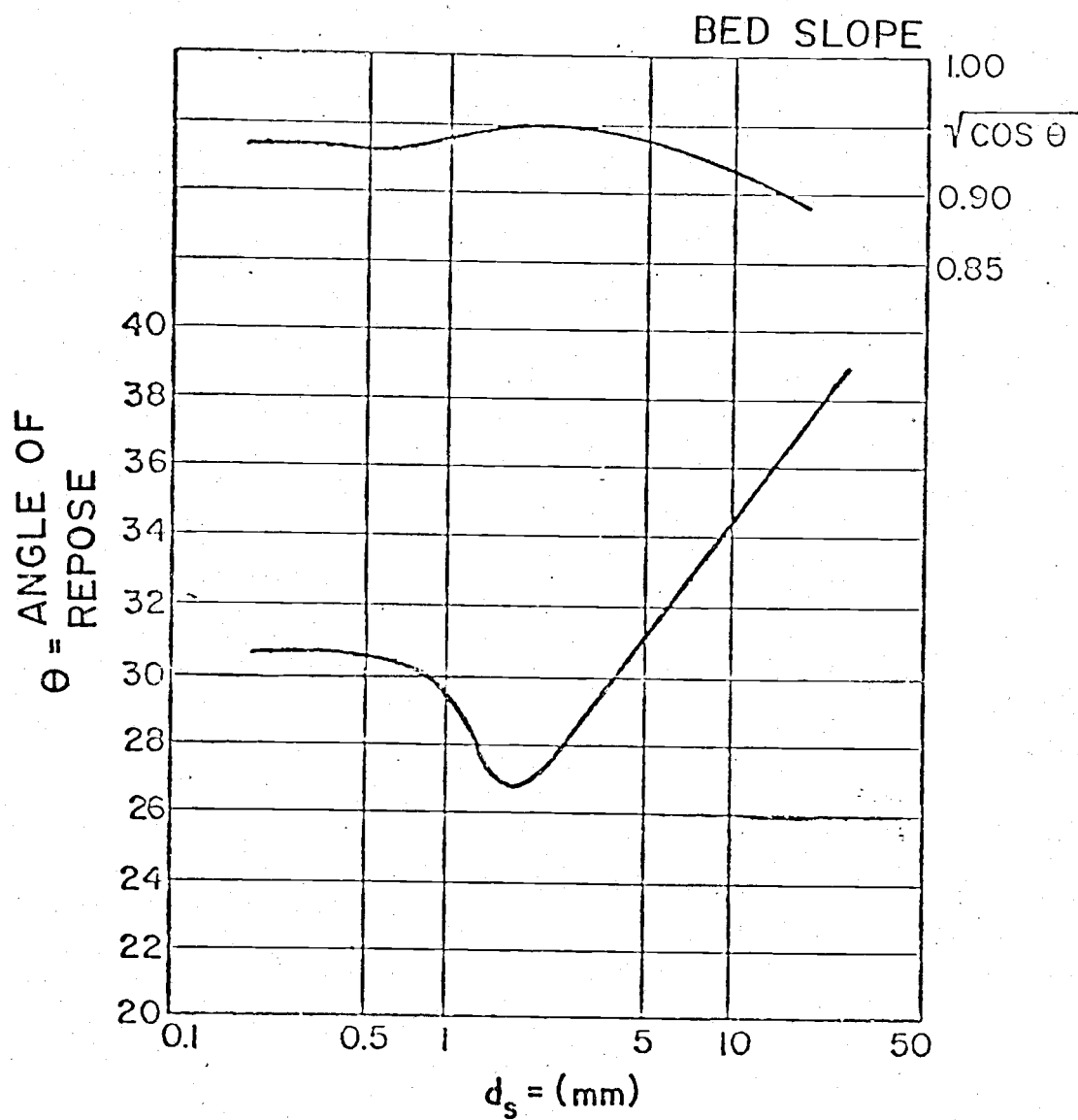


Figure III-2. Angle of repose and bed slope for moderately angular sand grains from Slotta and Montes (1975).

Westrich (1974) found that the scour hole can be self-similar, with time, for the axisymmetric round jet. Figure II-2 showed an example of these patterns which are used in the comparison of scale model and prototype measurements. When the jet is pulsed the results are similar and scour hole patterns remain self-similar. The volume scoured is larger for a pulsed jet, but the scour hole pattern, when normalized by the maximum hole radius, remains self-similar to the patterns of Westrich (1974).

When the jet is not round, but planar in character, the scour mechanism is similar. When the hole radius of maximum value is used as a normalizing parameter, Altinbilek (1973) found the scoured holes also to be self-similar (Figure III-3). This figure compares well with that of Westrich's data, Figure II-2. From Figure III-3 the maximum depth of scour was found to be

$$Z_{\max} = 30.5 D_o (U_o/w_s)^3 (d_s/D_o)/(Z/D_o)^{1/2} (U/(gD_o))^{1/2},$$

with w_s as the fall velocity of the sediment particle. The volume scoured per unit width of jet can be calculated to be

$$\Psi = 1581 B D_o^2 U_o^2 g d_s^2 / \tan \theta w^4 Z_o.$$

Altinbilek's empirical results compare favorably with Westrich's (1974).

The behavior of a pulsating jet, as would be observed in prototype conditions, and its turbulent structure will next be discussed.

A few diameters from the source of a pulsating jet, the flow appears as that of a steady jet. This anomaly, suggested by Slotta and Montes (1975), is a result of a pressure pulse at some frequency, delaying the point where entrainment stops. A critical observation of this process was made by O'Loughlin, et al. (1970). "... The most relevant observation concerns the extraordinary sensitivity of the

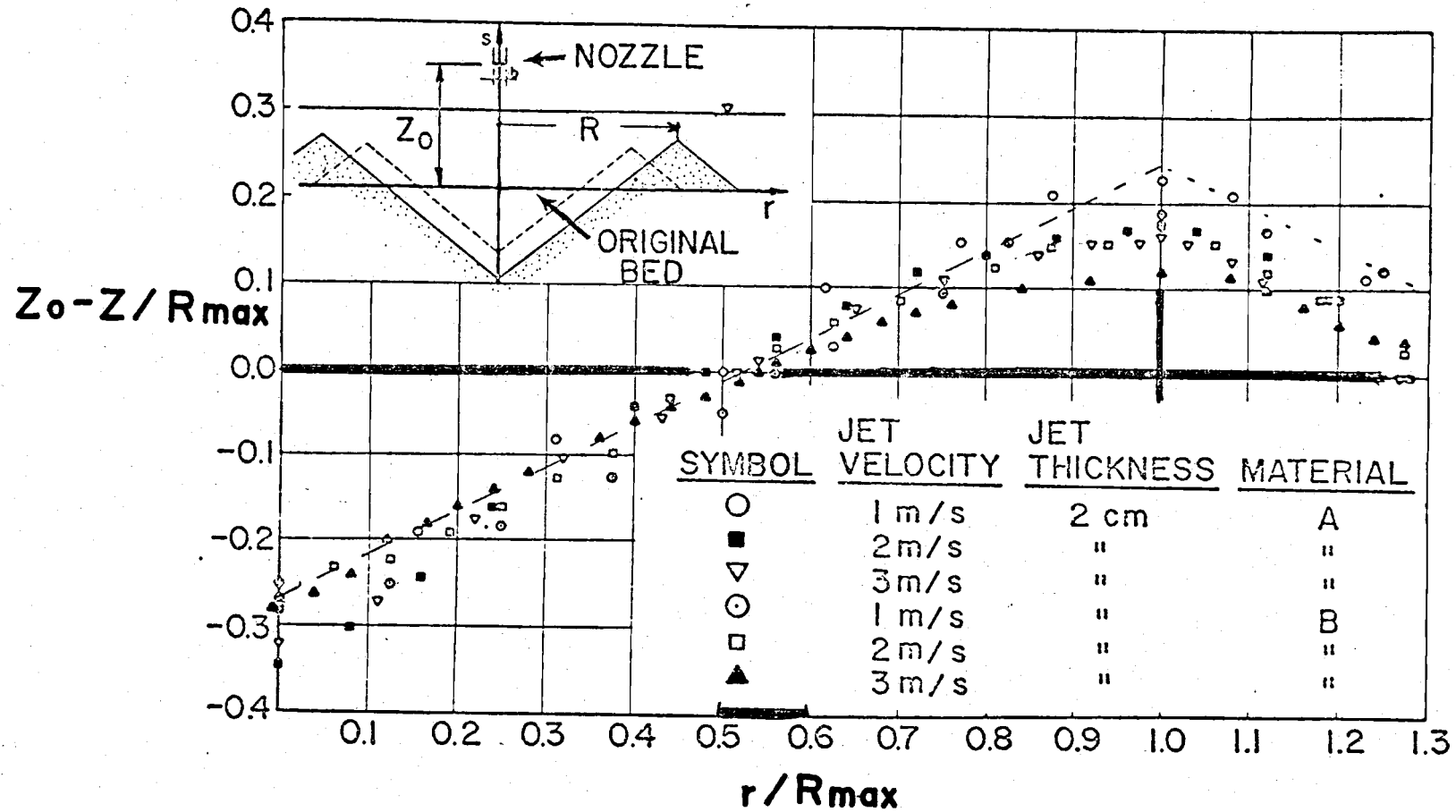


Figure III-3. Self-similar scour hole for a plain jet, from Altinbilek, et al. (1973).

scour rate to temporal or spatial perturbations in the incoming flow."

O'Loughlin, et al. found the rate of increased scour was logarithmic with time in Figure III-4, by using the square root of the mean weight scoured, $\sqrt{\bar{w}}$. Thus the scale of turbulence (e.g. presence of screens) is noted to be a very critical factor in Figure III-4 and would be considered very important as affecting any sediment scour process.

Wheelwash dredging would form a self-similar scour hole with time. The pulsating nature of a propeller wash can scour more bed material than a stationary jet. The turbulent structure of the wash is unique in the geometry and is a critical factor in the scour volume. The material moving as bed load in the model will have conservative predictions when applied to the prototype.

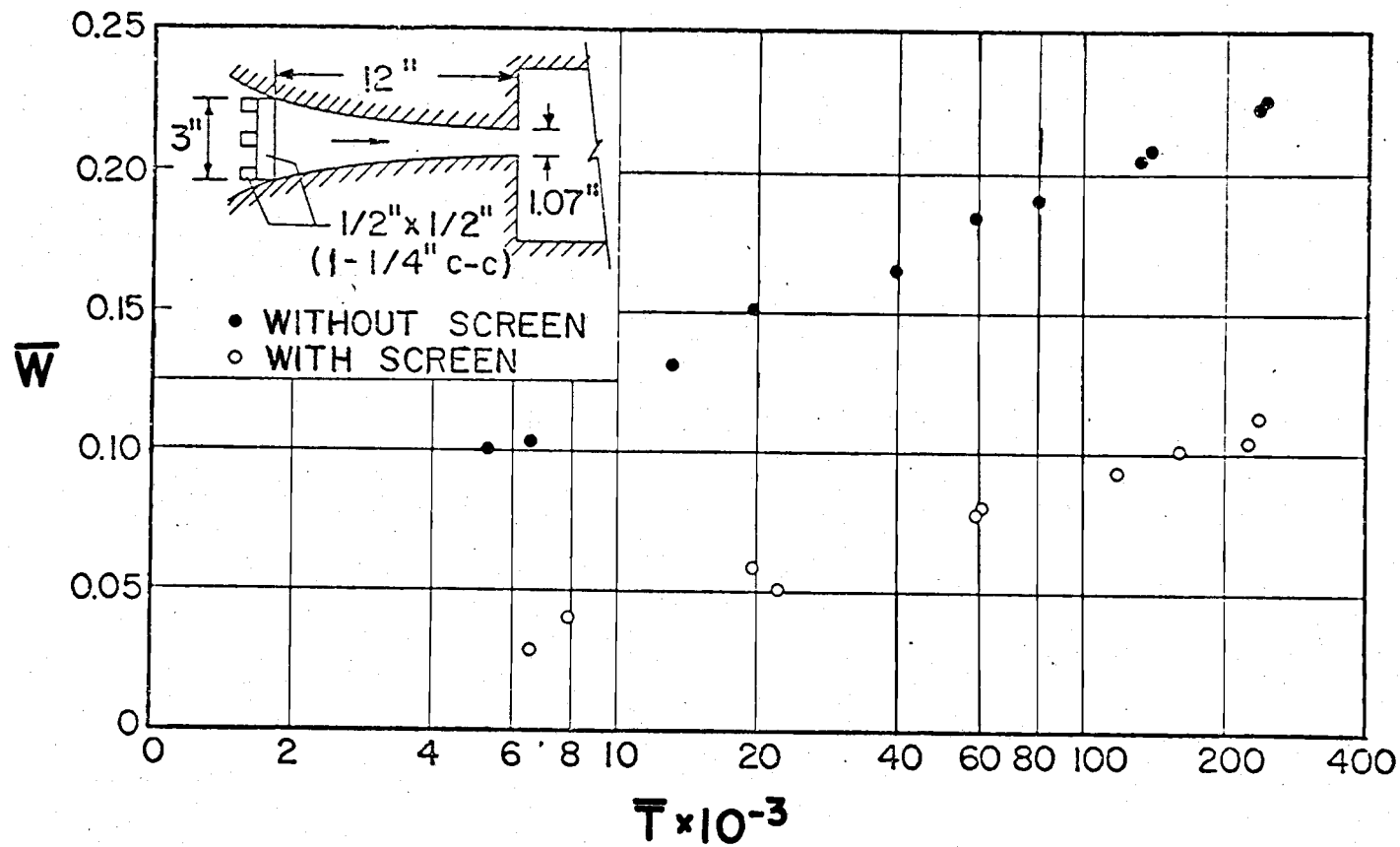


Figure III-4. Effect of screen presence on normalized depth of scour, $d = 4$ mm, $\bar{F} = 2.53$, $\bar{R} = 2550$, from O'Loughlin (1970) of horizontal flow from a fixed bed contraction across an expansion having a sediment bed.

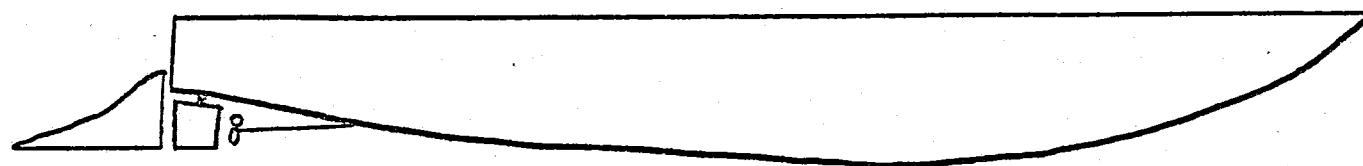
IV. Model Study

Background

Model studies were conducted to allow a varying range of parameters impossible to investigate regarding shoal removal by the LCM Sandwick in the field. Models of two scales, 1:40 and 1:12, were built, tested, and used to observe the flow around the deflector door which directed the propeller wash toward the bed and to observe the scoured bed material patterns.

The basic shape of a LCM-8 landing craft is shown in Figure IV-1 with the deflector door of the Sandwick added; geometrically similar models were tested. Appendix 1 presents details of the Sandwick's design and deflector door specifications. Table IV-1 lists the prototype and the scaled parameters. Both models were built of wood and coated with a polyester resin to ensure water integrity. Due to the wooden construction the models were appropriately ballasted to attain the water line of the prototype. The water line used was determined from photographs and verified by observation in the field while the LCM Sandwick operated on site. A hinged deflector door was modeled to match the deflector door of the prototype.

In both models, the twin propellers were powered by electric motors which were controlled by an electric circuit to measure their rate of revolution and to synchronize their speed. Figure IV-2 shows the circuit schematic indicating the means by which the motors were synchronized by the repeated breaking of a light beam to count the rpm's of both motors. For both models the propellers used were constructed of brass stock in the Oregon State University Ocean Engineering shop. The propellers matched the prototype's in pitch and scaled diameter.



42.2m prototype scale

0.3048m 1:40 scale

0.152m 1:12 scale

Figure IV-1. Sketch of model hull used in tests.

Table IV-1
Modeled Parameters

	<u>1:40 model</u>	<u>1:12 model</u>
Length	$L_r = 1:40$	$L_r = 1:12$
Area	$A_r = L_r^2 = 1:1600$	$A_r = 1:144$
Volume	$V_r = L_r^3 = 1:64,000$	$V_r = 1:1728$
Time	$T_r = L_r^{1/2} = 1:6.3$	$T_r = 1:3.46$
Velocity	$V_r = L_r^{1/2} = 1:6.3$	$V_r = 1:3.46$
Unit pressure	$P_r = L_r \gamma_r = 1:40$	$P_r = 1:12$
Force	$F_r = L_r^3 \gamma_r = 1:64,000$	$F_r = 1:1728$
Weight	$W_r = L_r^3 \gamma_r = 1:64,000$	$W_r = 1:1728$

Note: Liquid specific weight scale 1:1 = γ_r

	<u>Prototype</u>	<u>1:40 model</u>	<u>1:12 model</u>
Length	22.55 m	56 cm	1.8 m
Beam	6.4 m	16 cm	0.53 m
Draft	1.8 m	4.5 cm	.15 m
Propeller			
Diameter	0.86 m	2.2 cm	7.2 cm
Blades	3	3	3
Pitch	0.5 m	1.25 cm	4.2 cm
rpm	1500	5000	1500
Sediment	0.25 mm	0.5 mm (used) (needed 6 microns)	0.5 mm (used) (needed .021 mm)
Wake velocity maximum 6 m/sec		25 cm/sec (needed 95 cm/sec)	1.4 to 1.5 m/sec (needed 1.734 m/sec)

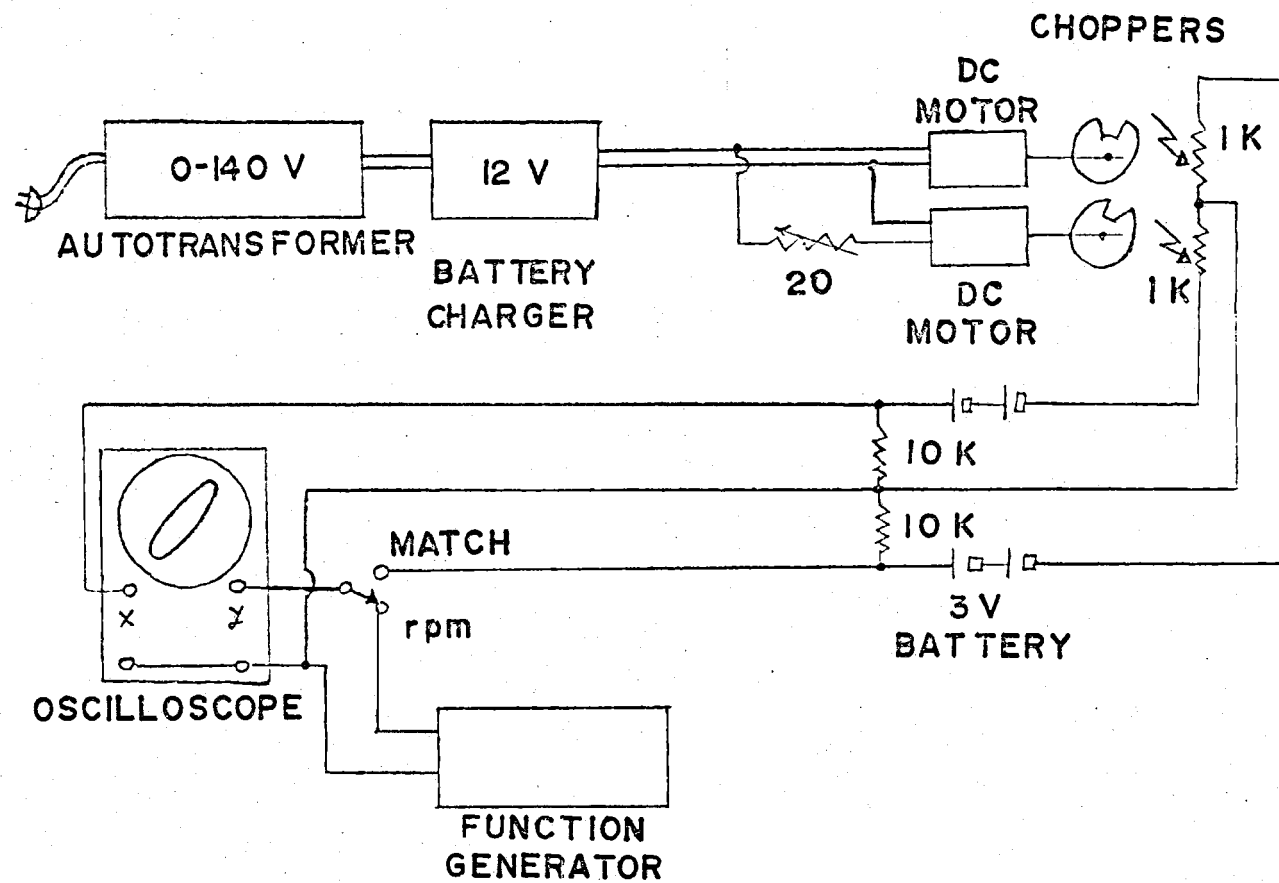


Figure IV-2. Model test circuit schematic.

The synchronizing circuit and the scaled propellers allowed the models to generate a wake having similar characteristics as observed on the prototype.

Model Similitude

In general, dimensional analysis is a method of applying a partial knowledge of a problem to secure information on important details. This has the advantage of requiring the application of only a limited knowledge of variables that govern the problem. The technique requires an analysis of the dimensionless form of the governing equations which can be used to fullest advantage in obtaining a general solution to a problem having numerous variables.

The pertinent variables of the jet flow problem are listed in Table IV-2. These are combined and are written as a function of discharge, Q :

$$Q = f(D_0, \mu, g, U_0, \rho, \omega, r).$$

In a non-dimensional form the variables can be combined to show that the flow is a function of the Froude number, the Reynolds number, a scaling ratio and a normalized velocity. These are also listed in Table IV-2. Since an attempt will be made to apply the principles of dimensional analysis to a model of the LCM Sandwich for studying shoal removal and geometric similarity, important dynamic forces must be matched.

In the LCM studies, the model was limited to use in water, as was the prototype. The associated flows are fully turbulent so that Reynolds similarity is assured; however, the Froude scale ratio must be matched. Matching of model and prototype Froude numbers is critical if the flows are to be dynamically similar. The

Table IV-2

Pertinent Variables of Jet Discharge

Discharge	Q
Jet diameter	r
Pulsation rate	ω
Density of the fluid	ρ
Velocity at exit	U_0
Gravitational force	g
Viscosity of fluid	μ
Nozzle diameter	D_0

Froude number: $\frac{\text{inertial forces}}{\text{gravitational forces}} = \frac{U_0}{gD_0}$

Reynolds number: $\frac{\text{inertial forces}}{\text{viscous forces}} = \frac{U_0 D_0 \rho}{\mu}$

Scaling ratio: $\frac{\text{jet diameter}}{\text{nozzle diameter}} = \frac{r}{D_0}$

Normalized velocity: $\frac{\text{pulsed velocity}}{\text{discharge velocity}} = \frac{\omega D_0}{U_0}$

actual scaling of the model is completed in the model section.

Scaling of Sediments

The problem of scaling sediment transport has been examined by many authors, Graf (1967), Donaldson (1971), and Westrich (1974), and most conclude that any sediment transport models, mostly from necessity, have some limitations. Pertinent variables important in scour and sediment transport are listed in Table IV-3. These variables involve both jet dimensions h_1 , the jet's height, and \bar{y} , mean jet width, and sediment properties. With similitude arguments used for the jet discharge, the weight of scoured bed material can be written

$$\bar{W} = g(w, d_s, \gamma_s, \mu, \rho, h_1, \bar{y}).$$

Three important similitude numbers from these variables are also listed: the Reynolds number, $R = \frac{U d_s}{\mu / \rho}$, the Froude number, $F = \frac{U^2 d_s}{\gamma / \rho}$, non-dimensional time, $t^* = \frac{tU}{w_s}$. O'Loughlin, et al. (1970) observations on the scour process included:

- 1) In geometrically similar models, small, systematic differences in scour depths are observable.
- 2) If a minimum Reynolds number is reached, little difference is found from model to model and most scale effects are minimal.
- 3) Similar internal flow geometry will lead to similar scour behavior.

The free surface conditions for the model test dictated that Froude scaling would best apply for the study. The actual scaling used in the modeling is included in Table IV-1. The trade offs in this modeling technique are discussed later in the data analysis section.

Table IV-3

Pertinent Variables to Scour

Weight of material scoured up to time t	W
Particle diameter, D_{50}	d
Specific weight of bed particles	γ_s
Specific weight of the fluid	γ
Dynamic viscosity of the fluid	μ
Mass density of the fluid	ρ
Width of entry jet	h_1
Specific weight ratios, γ_s/γ	$\bar{\gamma}$
Dimensionless weight of scoured material	\bar{W}
Volume scoured	∇
Reynolds number, $Ud\rho/\mu$,	R
Froude number, $U \sqrt{d(\gamma_s - \gamma)/\rho}$,	F
Non-dimensional time, U/h_1	\bar{T}
$W/\nabla \gamma_s$	\bar{W}

The test flume for the 1:40 scale test was 2 meters long, .75 meters wide and .75 meters deep. A larger flume was used for the 1:12 scale test; it was 10.5 meters long, 1.5 meters wide and 1.5 meters deep. In both tanks the water level could be changed to simulate different depths. The water used in the tests was Corvallis city water at room temperature, 17°C. The recirculated water was dosed with bleach to inhibit algae growth. Each flume contained sand only over a limited reach; a well graded sand having a uniform $d_{50} = 0.5$ mm grain size was used for propeller wash scour experiments.

Test Procedure

Reference for depth and velocity measurements was taken at the rim of the flume. Sites for these measurements were located with a point gauge suspended from a beam spanning the flume. The model vessel was free floating; however, forward motion was restricted by a block of styrofoam floating on the water. Tests were conducted by running the model's motors either continuously for the velocity measurements, or for one minute intervals for the scour testing.

The motors were checked throughout the tests to verify they were still matched in rpm's and phase synchronization. Very little fine tuning was needed once the system was started for a day of testing. The bed would be leveled prior to each scour test and checked with a straight edge and point gauge at five sites, until the bed was level within 3 mm. The model craft would then be placed in position, freely floating at its ballasted trim.

The model tests were broken into two sections: measuring the jet velocity behind the model and measuring the volume of displaced or

scoured material. Velocity mapping for different door settings and propeller settings was conducted first without sand in the test flume and, subsequently, the sediment scour tests followed.

Parameters Measured

Model velocity mapping was conducted on the 1:40 model to observe the flow characteristics of the jet generated by the propeller wash. Dye was used, as were floating particles, to determine the extent of entrained flow and the general phenomena of wheelwash dredging. Attempts to measure the flow on this small model were not completed due to transducer limitations. The stationary model propeller wash included large vortices shed at irregular intervals, the size of which were on the order of the propeller diameter. This intermittent phenomena was later observed in the field tests of the LCM Sandwich. Equipment was unavailable at the time to measure the velocity from such a small model to determine the scale of turbulence produced.

The model, like the vessel, was allowed to move about in response to the propeller forces, making an absolute frame of measure difficult. Much was learned from the initial tests of a qualitative nature. The deflected propeller wake behaves quite like a wall jet having little reverse flow upon striking the bed. This was due to the shallow angle of the wash approaching the bed. The propeller wash of the twin propellers was indistinct from one another at a distance of four door lengths from the vessel. The rotation orientation of the propeller was found to be very important in the wake configuration. Two left-handed propellers were once used; a strong continuous vortex formed, and the resulting flow had a very large rotational component which

was not present with counter rotating propellers. Also, for the co-rotating case, the deflected wake pattern was no longer symmetric with the axis of the vessel and was skewed.

With the larger 1:12 scale model, a small 10 mm Ott current meter was used to measure propeller wash wake velocity; three isovel plots for different deflector door angles are presented in Figure IV-3 through IV-5. The measurements were taken over a one minute period. The velocities were normalized based on the maximum velocity directly behind the deflector door and taken for a one minute average. The pattern for a ten degree deflector door angle appears most similar to a decaying deflected jet. The extent of the deflected prop wash jet was found to be very limited behind the vessel.

The central axis of the propeller wake was selected to normalize its decay. Figure IV-6 shows the decay of maximum centerline velocity along the central plane. Observed values were plotted in addition to the curve of Rajaratnam and Pani (1973) for the decay of maximum velocity. The normalization area used for the model test data was that area enclosing the twin propellers. This approach seems to be conservative as some observed values were below Pani's theoretical and experimental findings; data for the ten degree deflector door seems to match satisfactorily. Prediction of the velocity decay from similar curves and data would be useful for comparing propeller wash of various vessels that are being scale tested in other laboratories.

The lateral velocity distribution of the model LCM Sandwich's wake creates a three dimensional wall jet as shown in Figures IV-7 and IV-8. These plots are superposed on the curves of Rajaratnam and Pani (1973) for comparison of the wash with observations of three dimensional

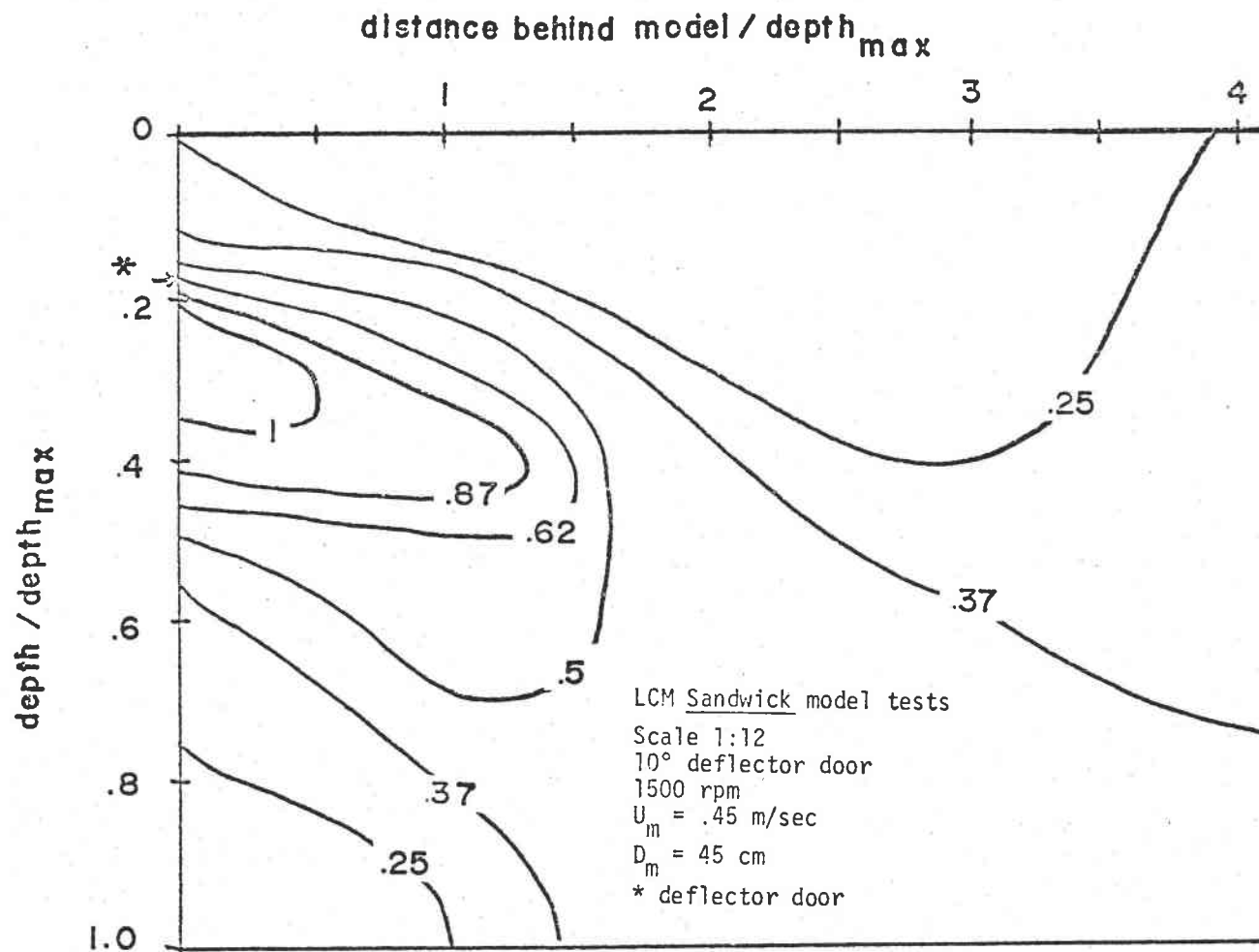


Figure IV-3. Plot of U/U_{max} for LCM Sandwich model deflector door at 10°.

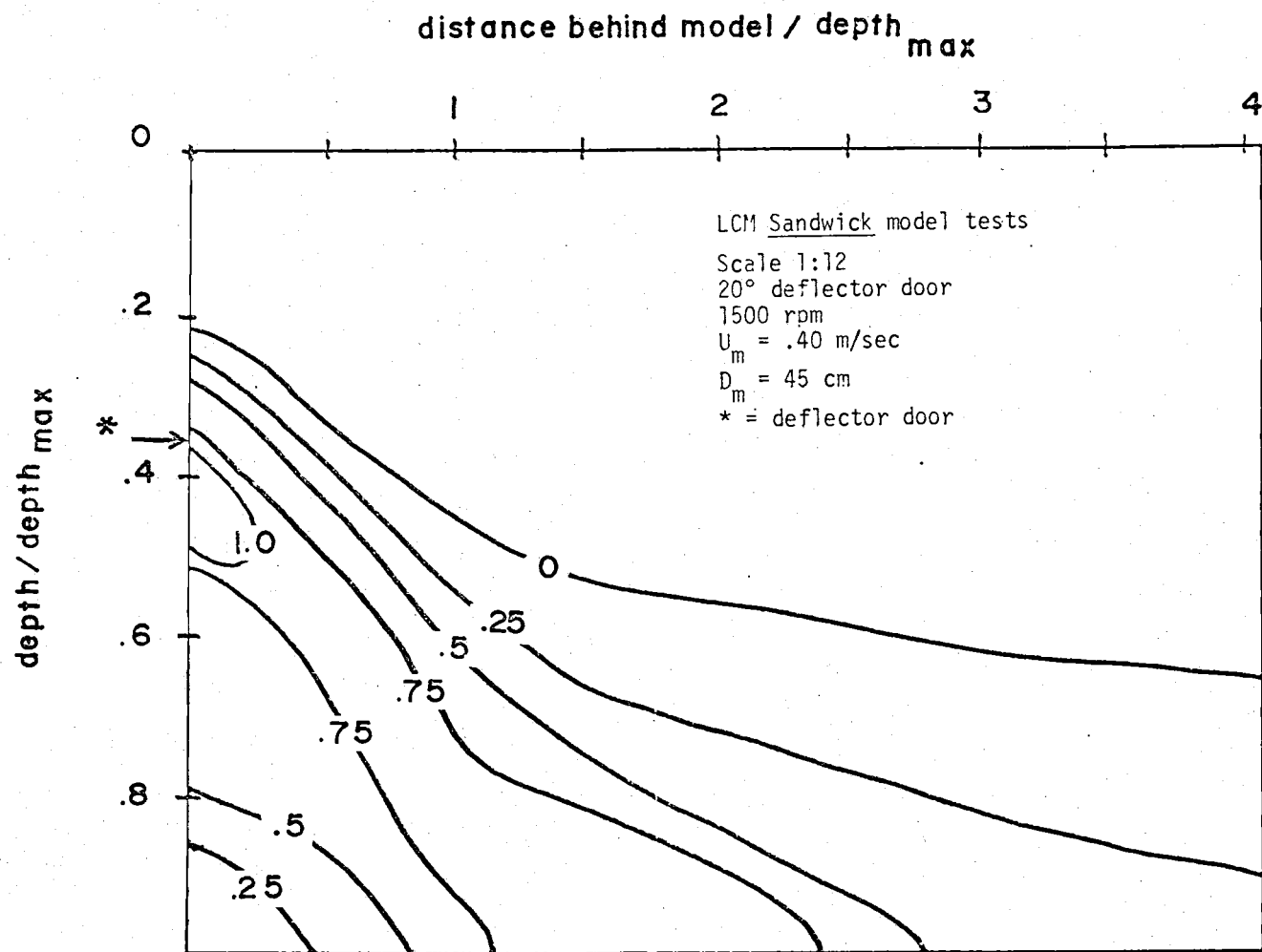


Figure IV-4. Plot of U/U_{max} for LCM Sandwich model deflector door at 20°.

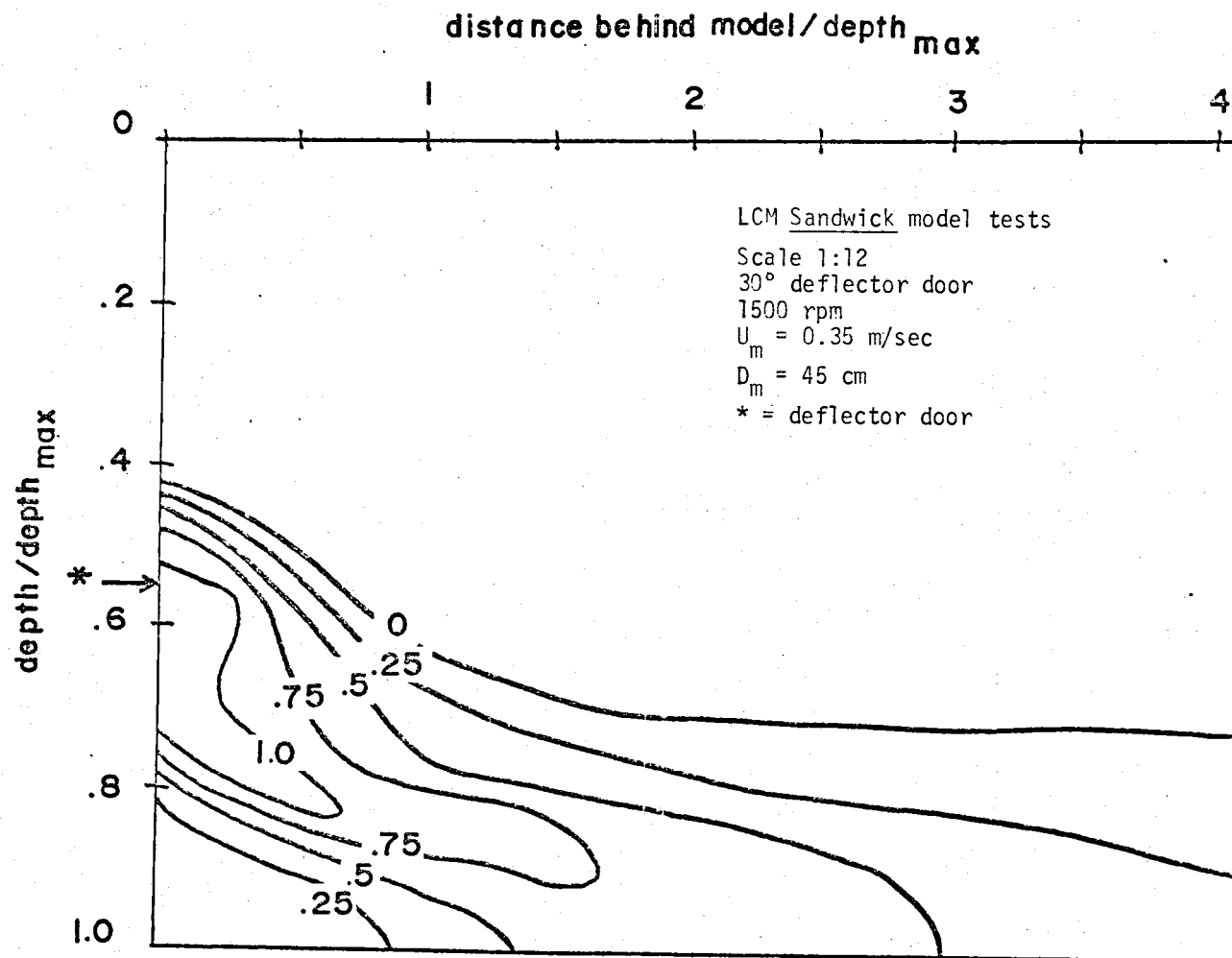


Figure IV-5. Plot of U/U_{max} for LCM Sandwich model deflector door angle of 30°.

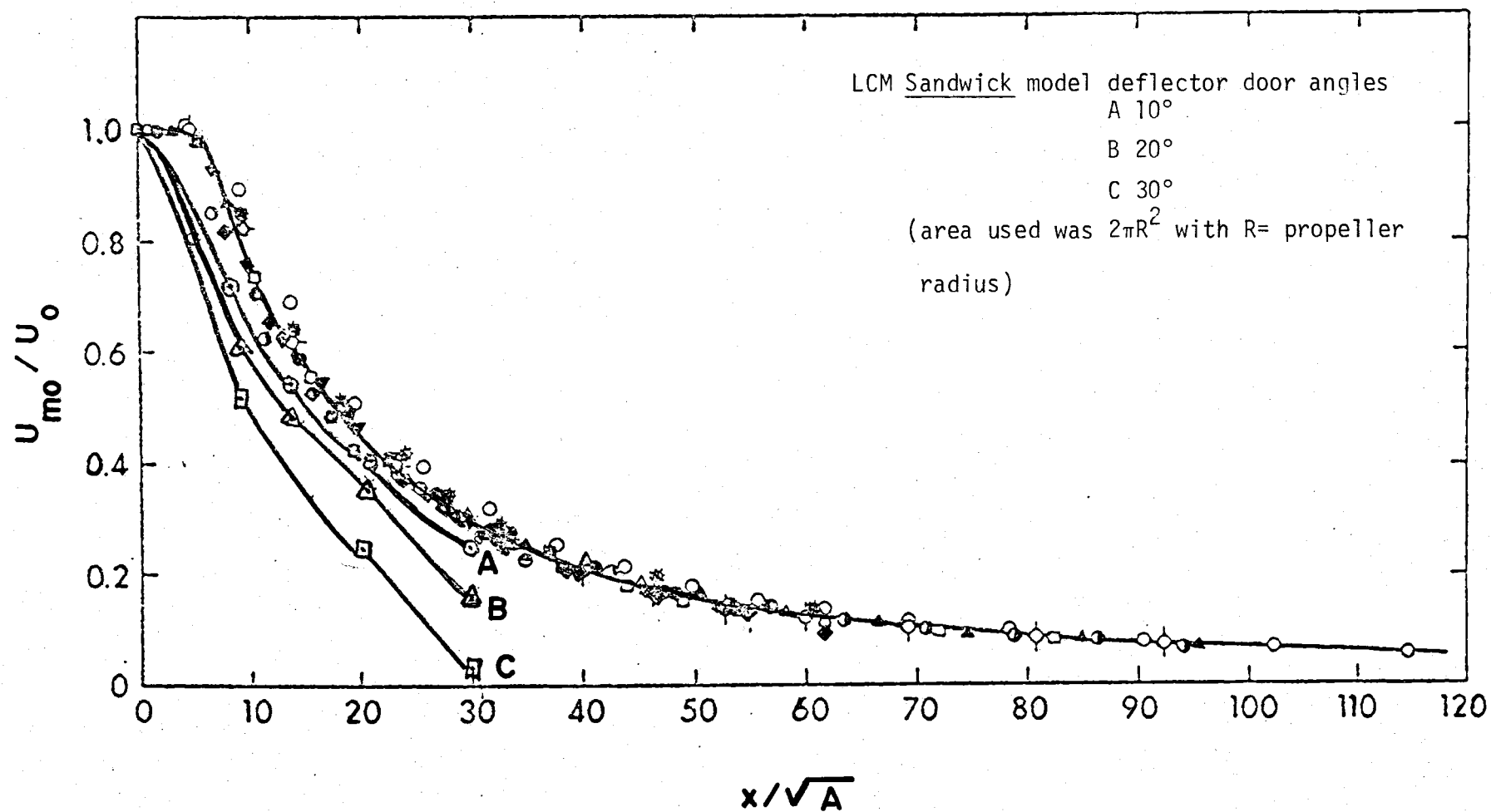


Figure IV-6. Decay of maximum velocity along center plane with square root of nozzle area, after Rajaratnam and Pani (1973).

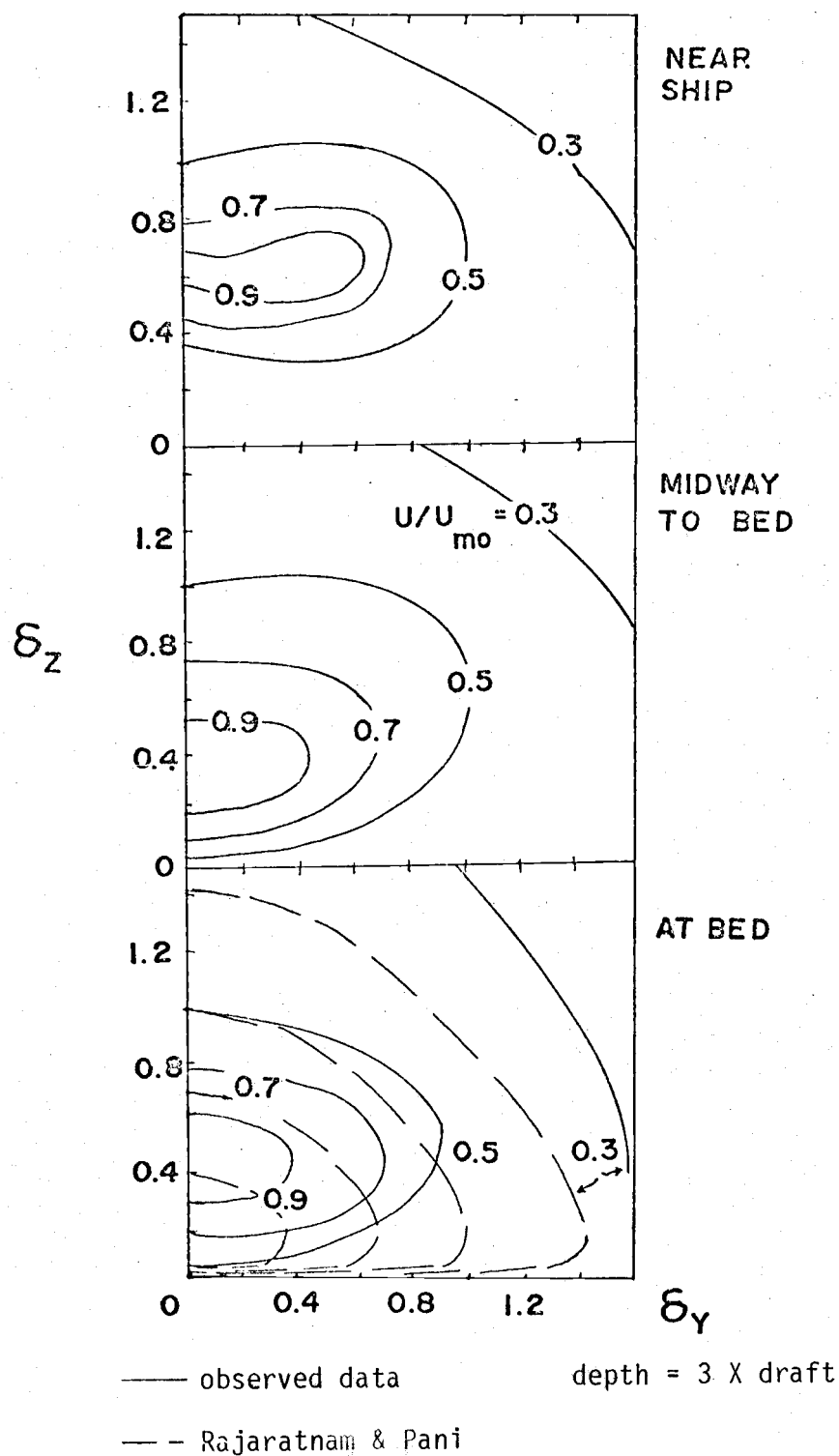


Figure IV-7. Isovets for 10° deflector door. The Sandwich 1:12 scale model, after Rajaratnam & Pani (1973).

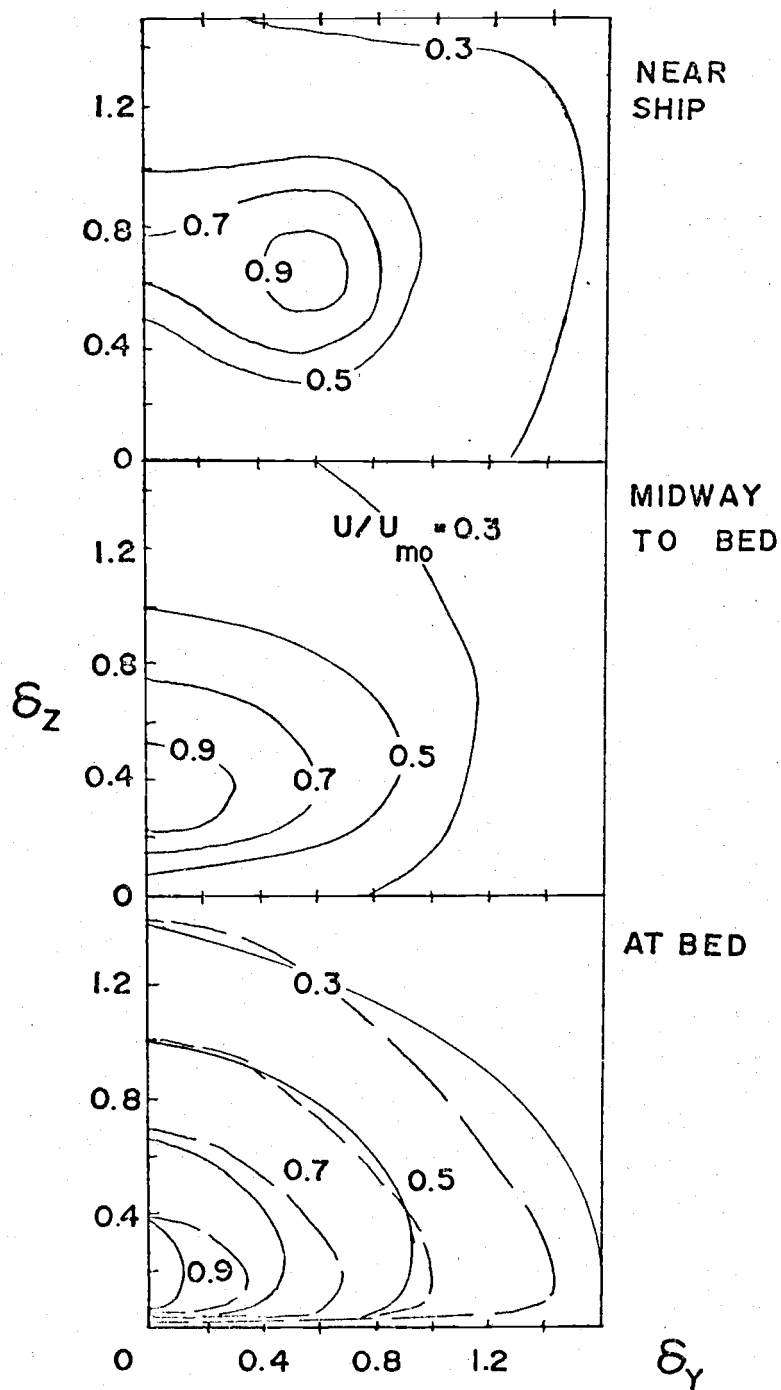


Figure IV-8. Isovels for 20° deflector door. The Sandwich 1:12 scale model, after Rajaratnam & Pani (1973).

turbulent wall jets. The comparison is considered satisfactory, as the measurements shown were taken when the velocity first struck the sediment bed. The individual flow features of the propellers were observed to homogenize with distance, as would be expected.

The grain size selected for both model tests and prototype tests, .25 to .50 mm in diameter, is shown in Graf's settling velocity curve (Figure IV-9) for comparison with the natural Tillamook sediments' settling velocity. Sieving analysis of the Tillamook sediments is contained in Appendix 2. The settling velocity of 7 mm/second for the model tests is two to three times faster than the settling velocity of Tillamook sediments. The erosion-deposition criteria for the model and field studies are shown in Figure IV-10, also from Graf. The velocity which must exist to scour and deposit the sediment particles in each case can be found. The erosion velocity of 20 cm/second for the two test sediments and the transportation velocity of 1.8 cm/second for Tillamook sediment is lower than the 2.8 cm/second required for the model sediment. The angle of repose for both sediment types is also of interest and Slotta and Montes' (1975) graph of angle of repose is shown again in Figure IV-11 with the two sediment sizes plotted. The behavior of the two sizes is again very similar and the curve indicates a constant value of angle of repose for the range of most sand-sized particles. In summary, the sand in the model tests had similar mechanical characteristics when compared to Tillamook sediments, not fall velocities.

Tests were carried out for determining the scour action on the bed material by the modified LCM. The test flumes were drained and large containers (.3 m by .7 m for the 1:40 model and 1.3 m by 2.6 m for the 1:12 model) were located on the flume bottom and filled with sand.

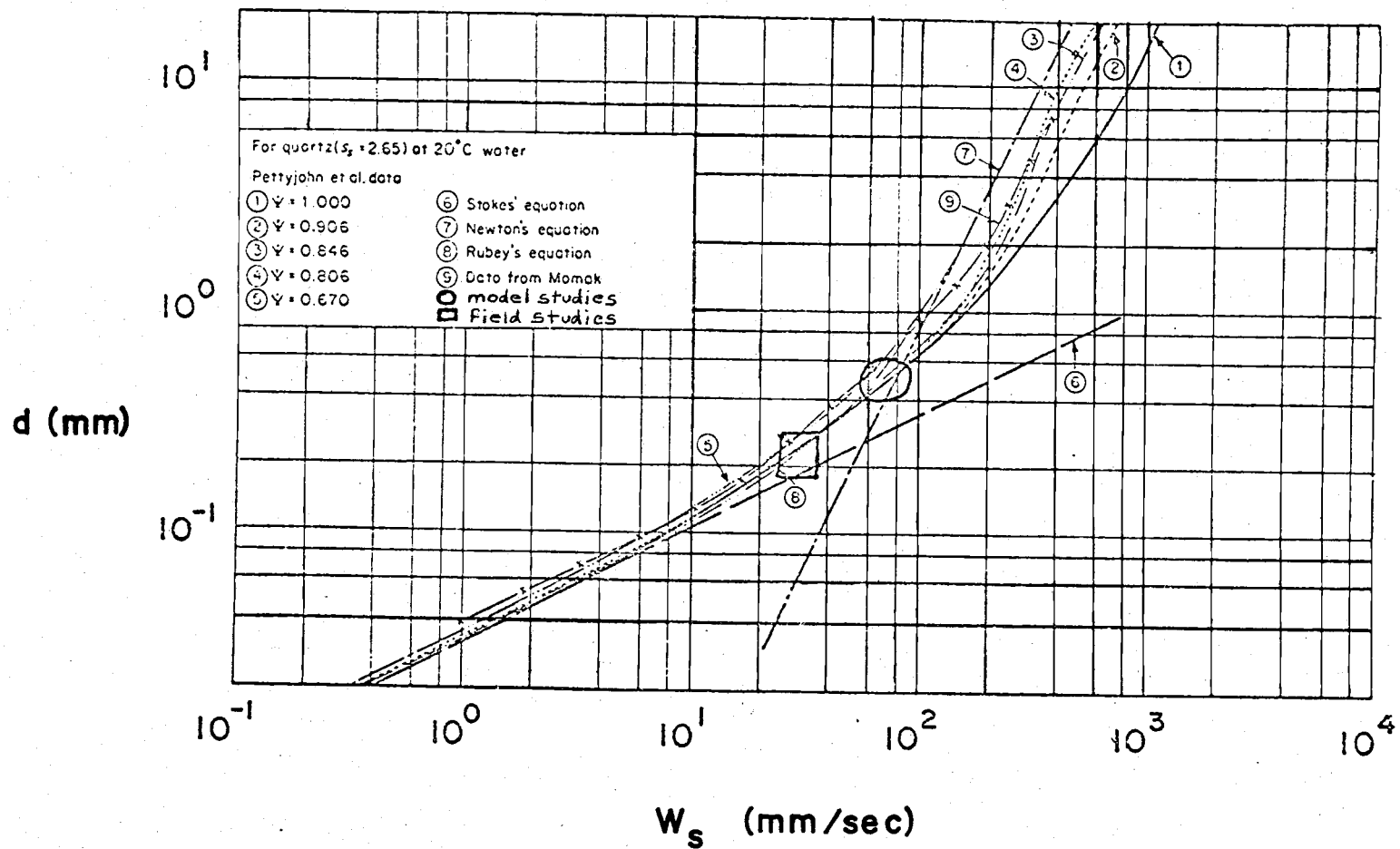


Figure IV-9. Settling velocity vs. particle diameter, after Graf (1966).

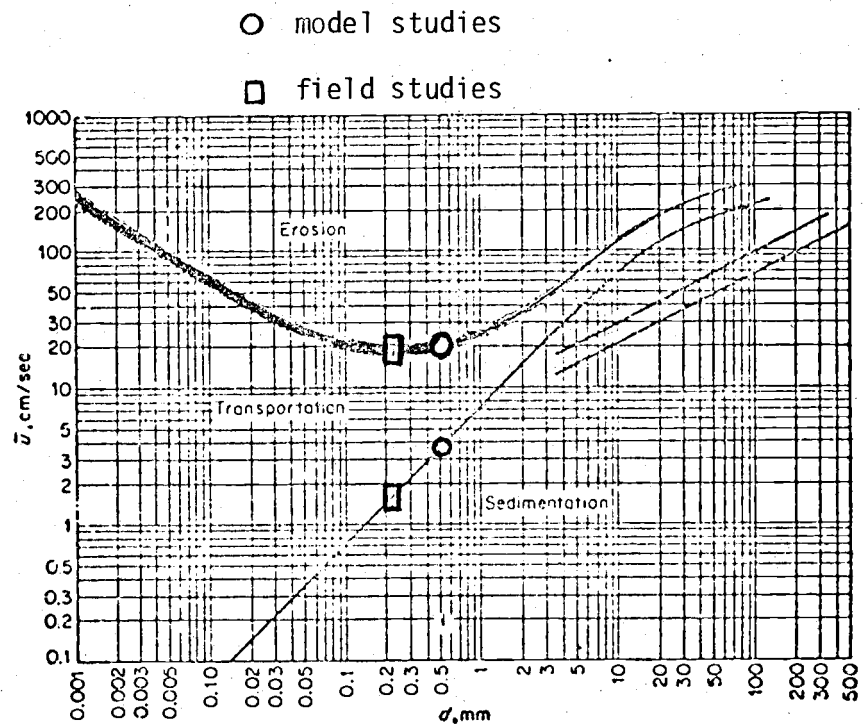


Figure IV-10. Erosion-deposition criteria for uniform particles. [After HJULSTRÖM (1935).]
After Graf (1966).

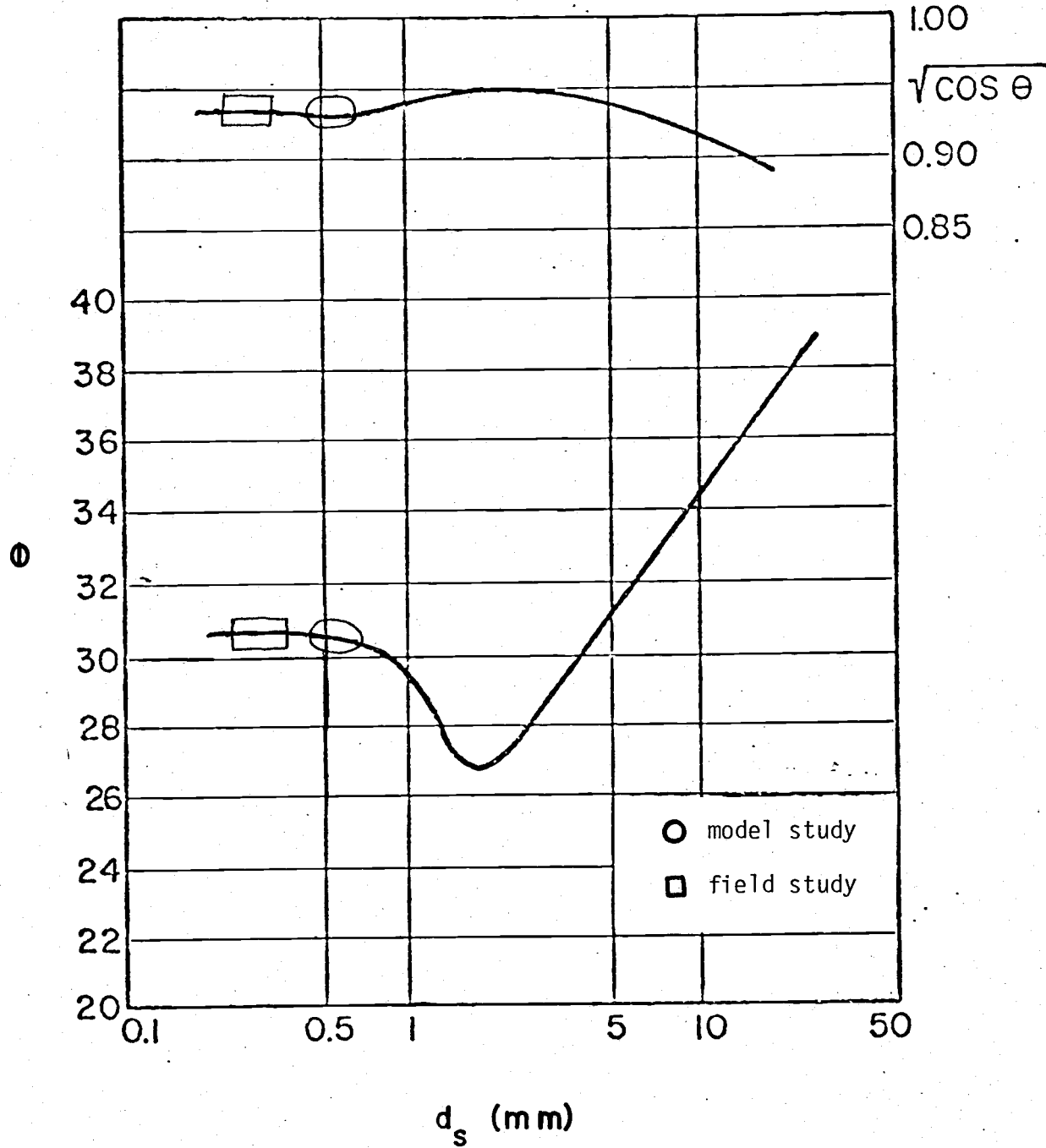


Figure IV-11. Angle of repose for sand grains, from Slotta and Montes (1975).

Washed quartz sand, $d_{50} = 0.5$ mm, having similar characteristics to the field sediment, was selected. Sand also permitted sidewall and vertical photography in data collection without having to contend with turbid suspensions. Modeling of cohesive sediments with a non-cohesive sediment, like sand, would lead to incorrect estimates of transport, thus field measurements would be necessary for calibrating and/or verifying predictions extrapolated from the model.

During the scouring process, characteristic outlines of the scour holes in plan view were observed. The four forms observed in this study appear in Figure IV-12A, B, C, D, and examples can be found in Appendix 3. The four forms occur as extreme cases of the model and bed configuration. Form A occurs when the water is deep and the propeller wash must travel a long distance through the water before striking the bed. In this case, the effects of each propeller are blended together as a single source jet. Form B is a result of scour in shallow water with the deflector door near the bed. This form shows that each propeller acts independently in moving bed materials. Form C shows the scour form when the propellers are reversed from the normal rotation found on the LCM Sandwick. For this situation, the propellers were interchanged and the electric motors operated in reverse rotation. The scour pattern is seen to be wider and the propeller wakes cause interference. Form D shows the bed form when the propellers rotate in the same direction. The singular scour pattern is the result of a strong vortex being formed behind the model. The bed was found to react differently if a strong rotational wake component is present than from counter rotating propellers. The vortex-type wake keeps its character much longer than the normal

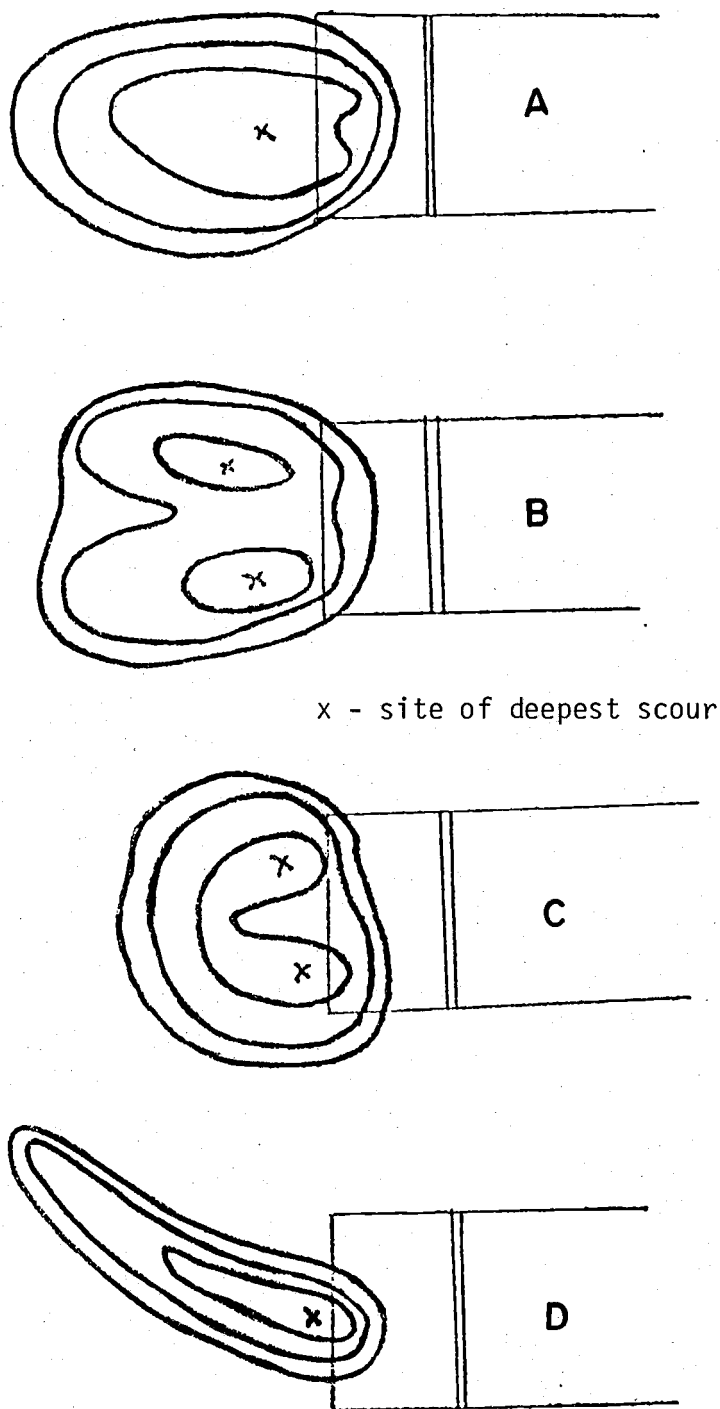


Figure IV-12. The four basic scour forms observed for the 1:40 model.

propeller wash. The patterns represented in Figure IV-12 were observed with the 1:40 scale model showing flow and scour potential of a dredge can be altered in many ways by changing only the propeller configuration. The patterns created with the 1:40 scale model were of a weak jet form and only with shallow water depth was the pattern of a strong jet.

Westrich's (1974) scour depth predictions of the scour hole shape and cross section, were found to be self-similar; such predictions will be compared for the LCM Sandwick models and prototype scouring operations. A plot of the extreme cases observed for scour tests using the 1:12 scale model of the LCM Sandwick is given in Figure IV-13. The scour hole cross section extremes are given only for the 20° deflector door and 1500 rpm's of the electric motors; however, 18 tests were conducted. The scour pattern has a configuration more closely related to Form II of Westrich's turbulent jet. The depths and distances were obtained from photographs taken of bed contours. Selected photographs are found in Appendix 3. While the tests were conducted, the sand particles were observed to be transported in sheets at frequent, irregular intervals. Between these mass movements out of the scour area, the grains moved very slowly; a few at a time, parallel to the induced flow. The grain size resulted in the sediment being transported as bed load, along the bed, rather than as a suspended load in the water column. These model results of bed form movement would thus give conservative prediction of prototype scour ability.

The depth of maximum scour for the depth of water is of interest in the application of this scour method. The 1:12 scale model was carried through a series of tests to determine the influence of deflector door

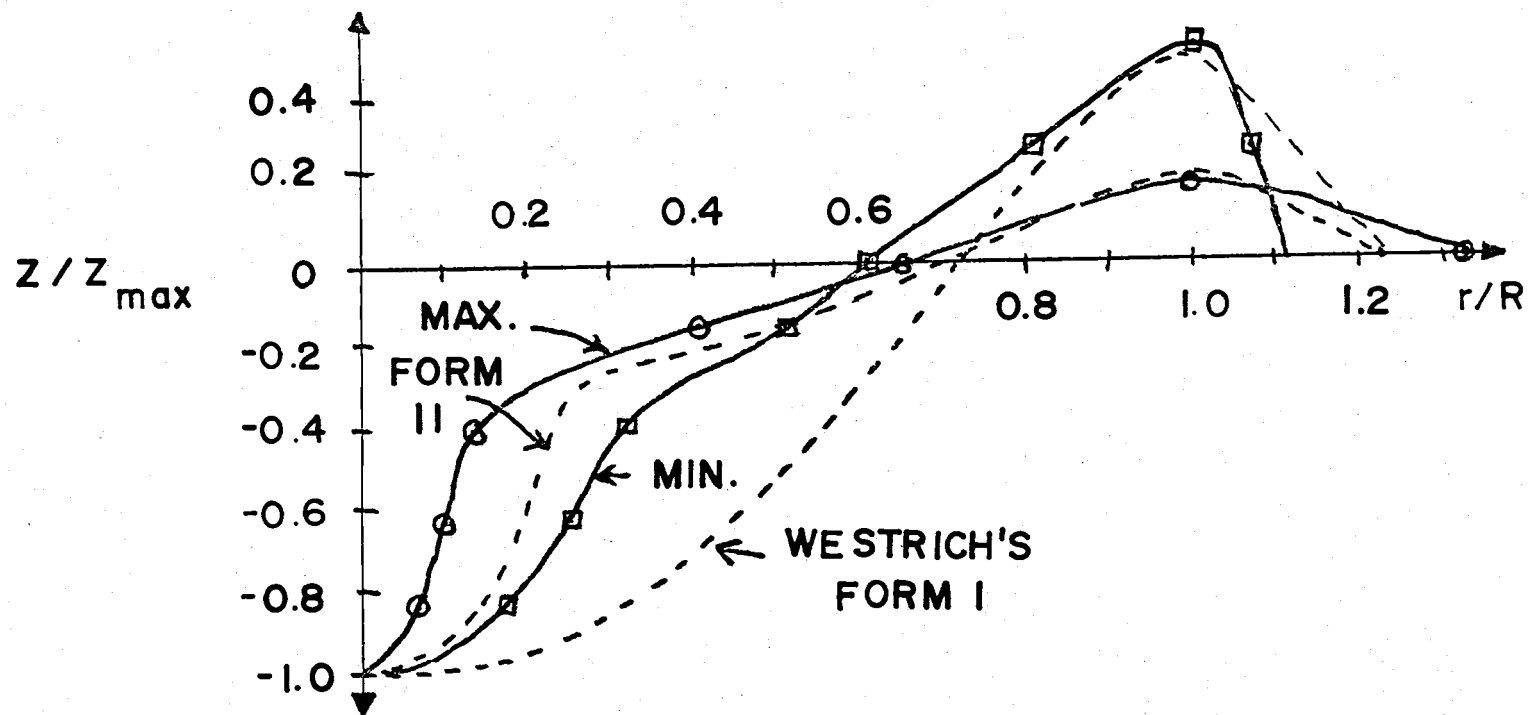


Figure IV-13. Self-similar scour holes, the extremes observed, on the LCM Sandwich 1:12 model having a 20° deflector door angle,

angle and the depth of maximum scour. Figure IV-14 illustrates typical information obtained from these tests. The deflector door limits were the physical restraints of the model in addition to the resulting bed configuration. As indicated on Figure IV-14, at depths of 1.5 drafts, deeper scour is only obtained by lowering the deflector door. The depth of scour is observed to be similar for the shallower depths. In no case was the scour observed to be deeper than the draft of the model. Similar information was obtained for the 1:40 scale model. From Figure IV-15, one observes that a depth of four drafts might be the maximum depth for erosion with the present LCM configuration.

The depth of scour or shoal removal versus time is important, for the LCM wheelwash operator should realize the speed for moving his vessel in order to have optimum scour. The volume of material scoured versus time is also a measure of the scour process. Figure IV-16 of the normalized volume scoured by the two different size models is plotted versus a time normalized with the fall velocity of the sediment. This figure shows the volumes obtained for one particular water depth and the standard 1500 rpm propeller speed for the 1:12 scale model and 5000 rpm for the 1:40 model by refilling the scoured hole with a known volume of wet sand. The 1:12 model scour volume was determined by reducing photographs taken of a contoured bed. Example photographs are shown in Appendix 3. Figure IV-16 indicates the scour pattern is in an equilibrium configuration at 600 t^* units.

In conclusion the model tests have allowed determination of the velocity distribution in the wake behind a model of the LCM Sandwick. The model's wash behaved as a deflected wall jet. The presence of large, turbulent fluctuations were observed which tended to increase

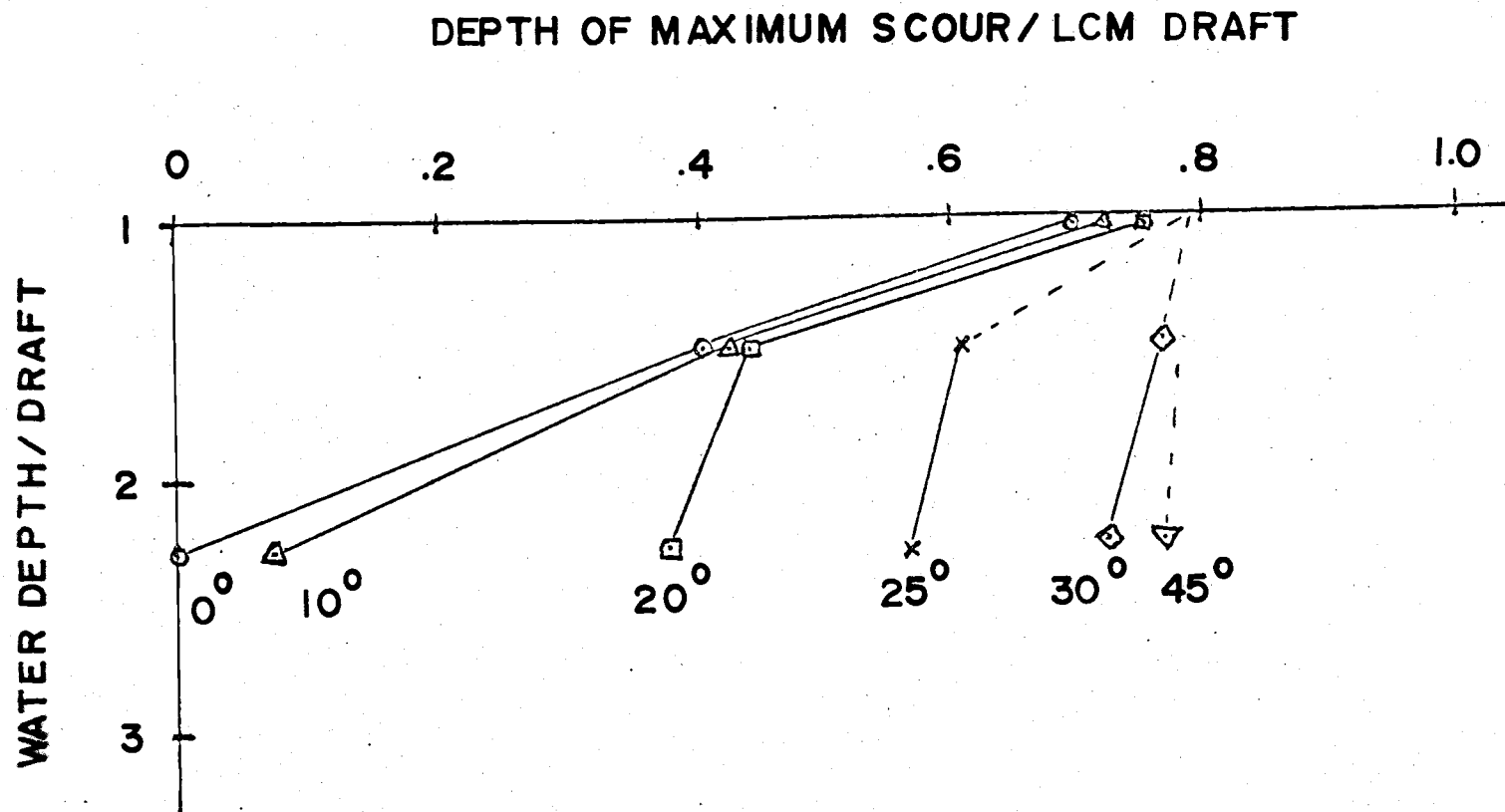
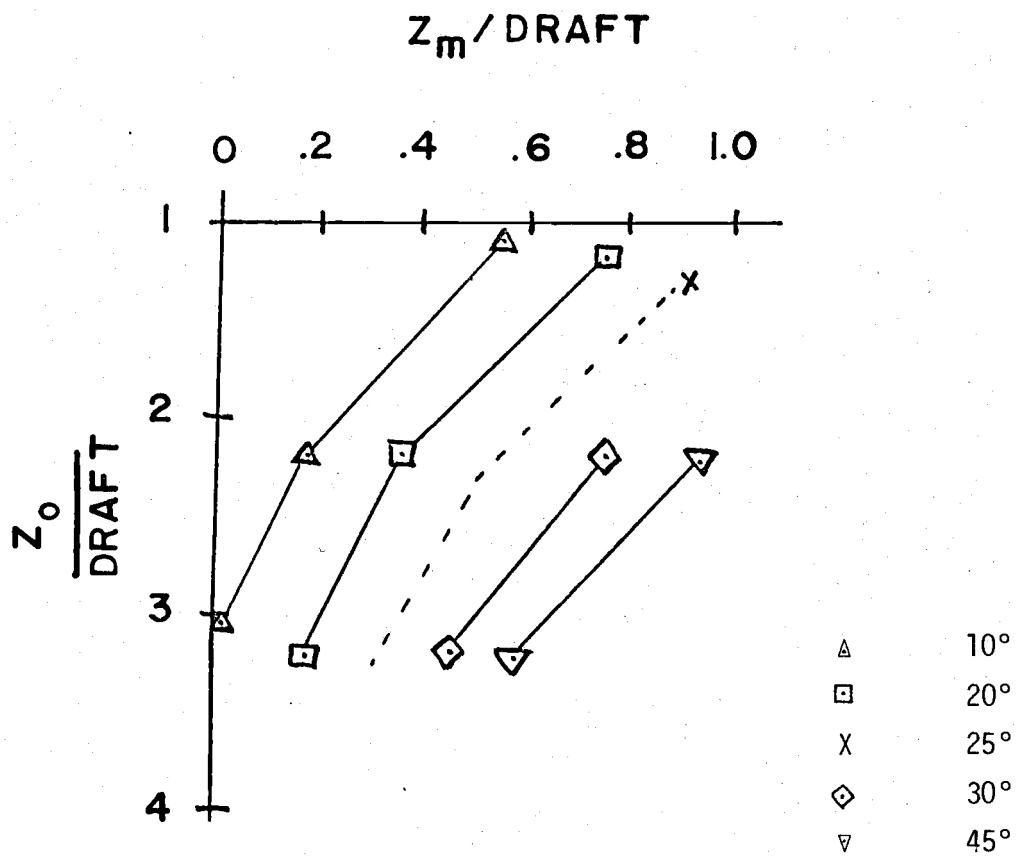


Figure IV-14. Depth of scour for different LCM deflector door angles, 1:12 scale.



model operated for 10 minutes
at 5000 rpm with 3.8 cm draft

Figure IV-15. Depth of maximum scour for different deflector door angles. 1:40 scale.

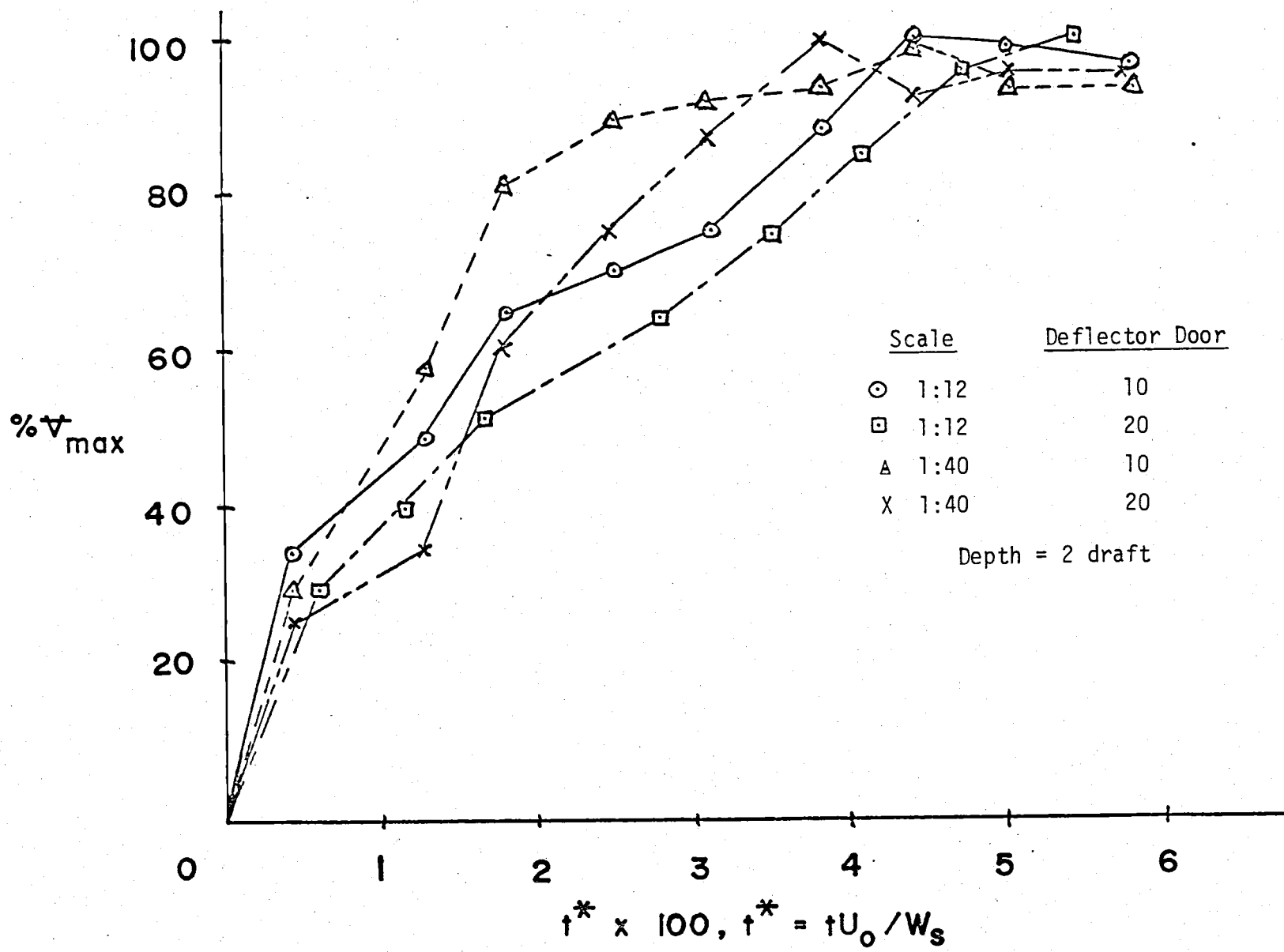


Figure IV-16. Normalized volume scoured vs. normalized time.

the scour over that found for a stationary jet. The depth of scour versus water depth was observed for two models and plotted to relate the maximum depth of scour available for a specific model configuration. The volume of material scoured with time has been found for model configurations similar to the scaled operating depths of the LCM Sandwich.

V. Field Study

Background

The operations of the LCM Sandwick were studied at two sites, one in Tillamook Bay and another in Coos Bay, to determine the velocity distribution behind the dredge and the rate and volume of sediment scour. The purpose of these measurements was to document the actual deflected propeller wash for comparison to the measured scale model results along with the published information on jets. The scour measurements were made to determine the gross efficiency and the resulting scour and shoal removal bed form configurations with the LCM Sandwick in natural sediments.

The two sites have different characteristics; velocity mapping and scour rates were determined in the shallower water of Tillamook Bay only. The Coos Bay site was selected for observing the propeller wash in conditions of a distant sediment bed. These measurements were conducted in conjunction with a study of impacts of this dredging method on estuaries reported in Effects Of Shoal Removal By Propeller Wash, December 1973, Tillamook Bay, Oregon by Slotta, Hancock, Williamson, Sollitt, et al. (1974).

Methods

The conditions of the testing program are summarized in Table V-1. The LCM Sandwick anchored on site by a four point anchoring system. Flow measurements were taken by locating a catamaran (a support vessel) in the wash of the LCM Sandwick and extending a current meter mounted on a rigid pipe below water. The catamaran was held in location by one anchor and two marked lines attached to the LCM

Table V-1
Test Summary

<u>Date</u>	<u>Purpose</u>
12 December 1973	Current measurements. 20°, full extension of, deflector door.
13 December 1973 a.m.	Current measurements. 10°, half extension of, deflector door.
13 December 1973 p.m.	Hole was scoured on the western edge of the tidal flat.
19 December 1973	Three holes were scoured in a more central region of the tidal flat.
6 May 1974	Coos Bay deep water current tests.

Sandwich's stern. The shallow water velocity measurements at Tillamook used a bi-vane current meter to indicate the vector direction of the current and its velocity. The shallow water tests gave few satisfactory velocity measurements as the current meters incurred damage from scoured bed material containing large pieces of wood and limbs. The direction of flow was obtained with certainty. The deep water tests at Coos Bay used a 2-axis Marsh-McBirney current meter mounted at right angles to the rigid support pipe; this mounting allowed the observer to aim the meter to find the maximum velocity and its vector orientation. The Marsh-McBirney current meter used in Coos Bay performed well and allowed a closer look into the detail of flow had the catamaran proved a more stable craft. The observed velocities were recorded as one minute time averages of the meter's output. The turbulence in the flow could not be separated from the motion of the boat or a slight swing in the 4 meter long support pipe from which the current meter was extended. Large vortices, observed often to be 2 meters in diameter, were shed by the LCM Sandwich at irregular intervals during the tests.

To obtain the scour measurements, the LCM Sandwich was operated over submerged tidal flats on the extreme high tides in Tillamook Bay on 13 and 19 December 1973. The tidal flats were subsequently exposed on the following low tides; then, surveying parties were able to determine the bathymetry and approximate shape of the scour holes. This measurement procedure was applied to the four scoured holes created by operating the LCM Sandwich for different time periods. No scour hole observations were made during the Coos Bay measurements as the tides were unfavorable for exposing the dredged bed.

Parameters

Field measurements of streamlines and velocity in the wake of the LCM Sandwich are shown in Figures V-1 through V-4. From these plots, it can be generalized that the fully extended deflector performs similarly to the model's, in that the wash is better directed toward the bed than the partially extended deflector. Both the streamline pattern and velocity pattern show improved confinement of the propeller wash when the deflector door is fully extended. The flow's added confinement increased the water velocity striking the bed. Since field velocity measurements could not be extended below 4 meters, the velocity below that depth could not be quantified.

Determining the scale of the turbulence would be untenable without an array of sensors in a fixed reference frame. However, the turbulence was observed on two time scales during measurements. Turbulence of a one minute period and twice the reported velocity was observed. Less frequent turbulent fluctuations of 3 meters/second velocity occurred every 15 to 20 minutes. The less frequent turbulence was most likely due to vortices being shed from the starboard side of the LCM Sandwich. The values plotted on the Figures V-1 through V-4 represent the averages of three steady-condition readings. The scour processes behind the LCM Sandwich are dynamic and transient; the few measurements which were obtained are a gross estimation of what takes place in the wake of this craft.

Both bathymetry and shape of the prototype scoured holes were determined by direct measurement by surveying parties at low tide. The sites of the four scour holes are indicated on Figure V-5. The resulting profiles, both longitudinal and transverse contour charts, are presented

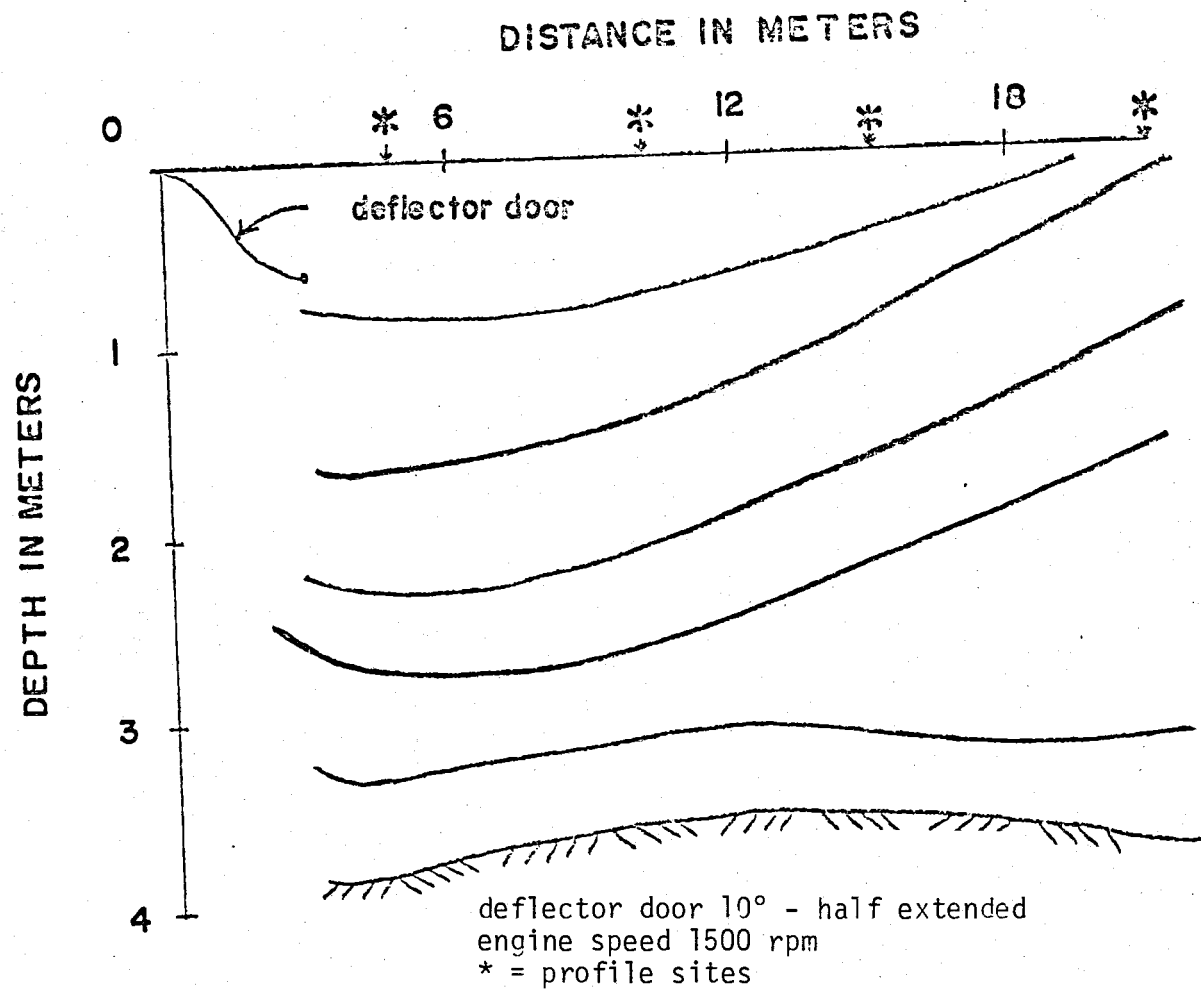


Figure V-1. Streamlines behind the Sandwich with a 10° deflector door.

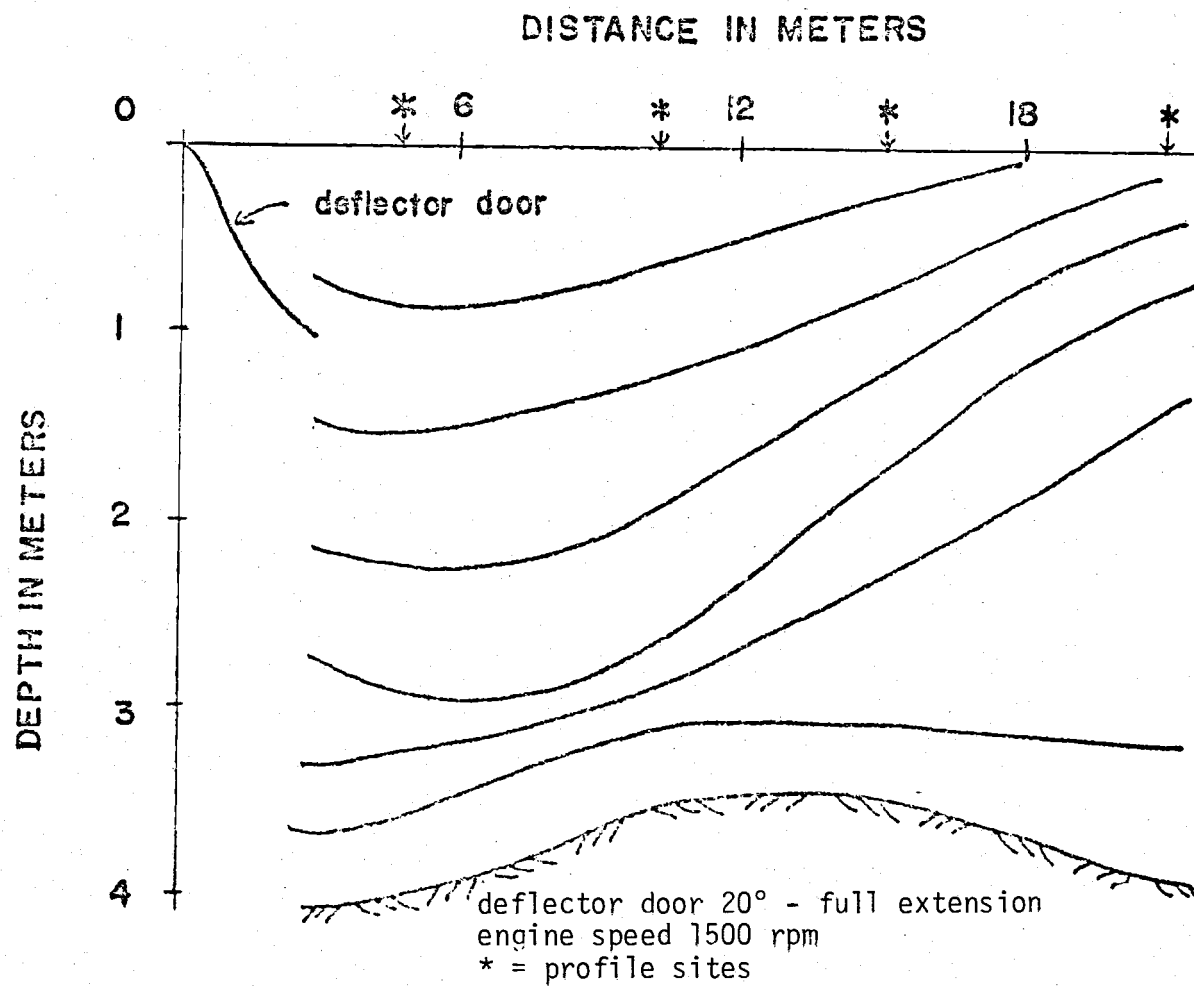


Figure V-2. Streamlines behind the Sandwich with a 20° deflector door.

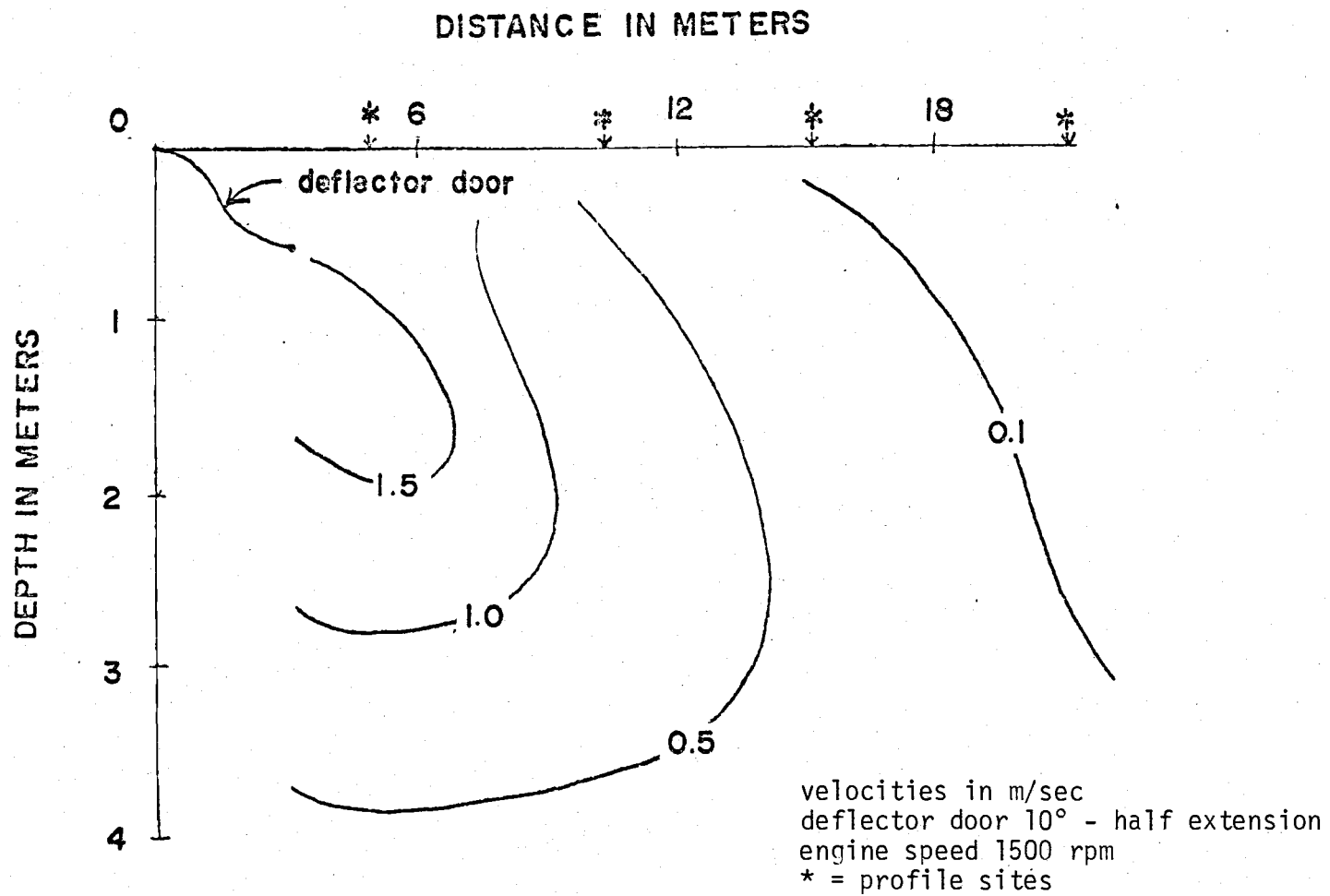


Figure V-3. Velocity profile behind the Sandwich with a 10° deflector door.

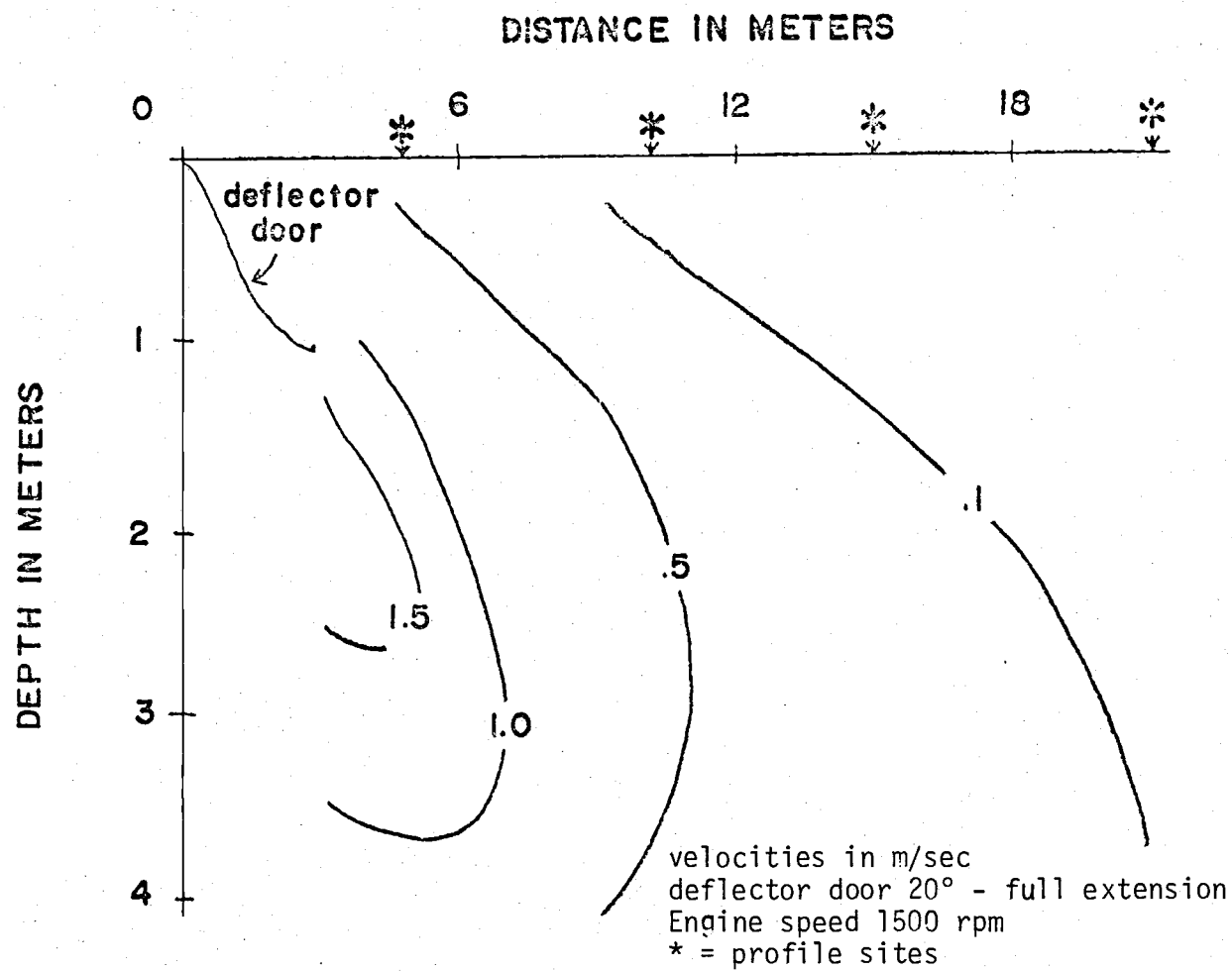


Figure V-4. Velocity profile behind the Sandwich with a 20° deflector door.

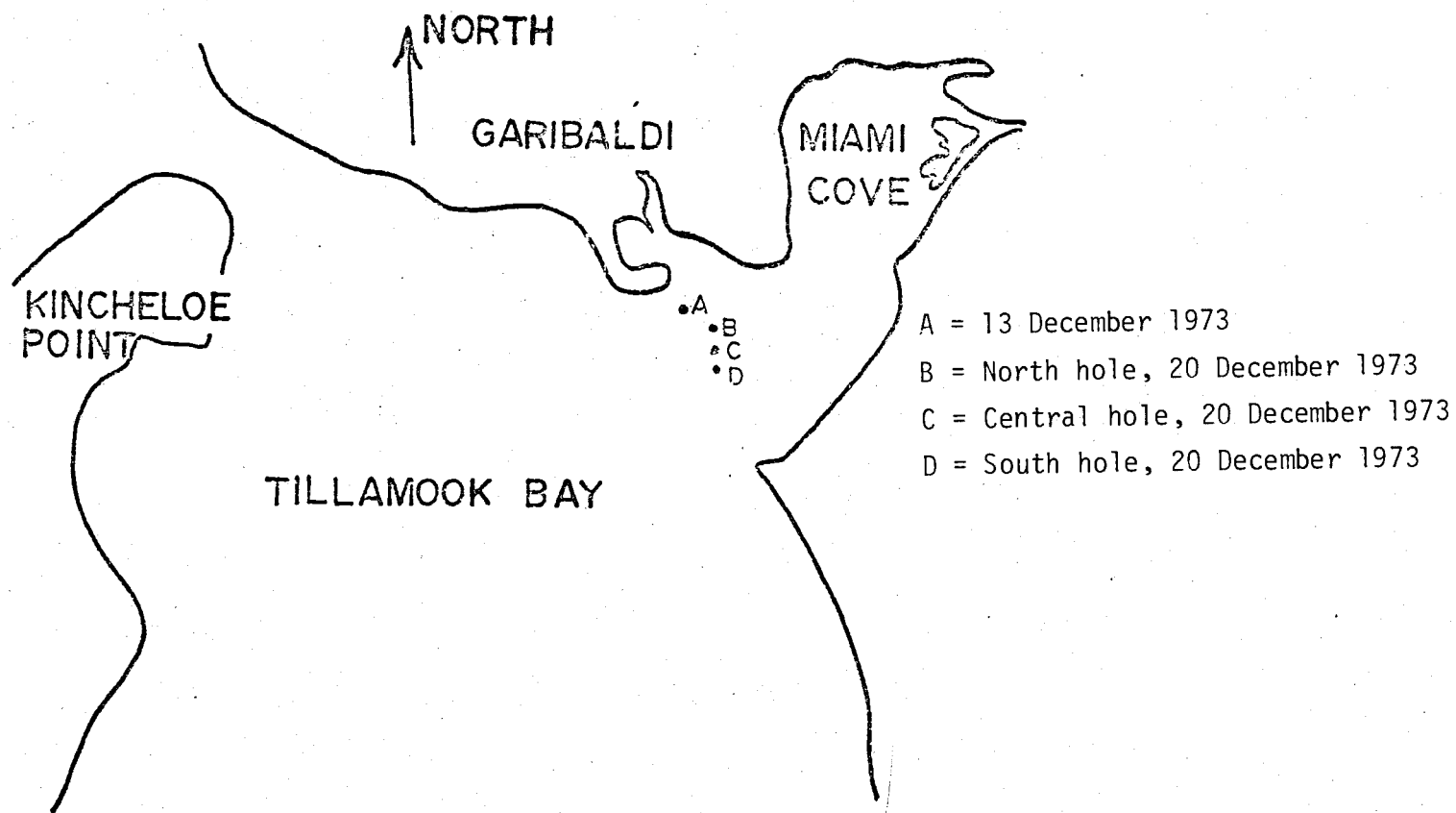


Figure V-5. Location of scour holes, from C and GS, #6112, 29th ed. (1971).

in Figures V-6 through V-8. The initial scour was found to have two basic patterns. The twin propellers acted as one to form a simple single scour hole in the north hole as opposed to the situation when the propeller acted independently by formation of a lobe of slow sediment movement along the center line in the central and south holes. The shapes of the scour holes were found to fit Westrich's Form I shown in Figures V-9 through V-11. The lack of a high rim is very noticeable in these non-dimensional plots. The operating conditions of these tests are summarized in Table V-2 along with the corresponding excavation expressed in both dimensional and non-dimensional form.

The rate of excavation is an important measure of the efficiency of the LCM Sandwich agitation dredging; Figure V-12 indicates the rate of excavation for the December 1973 dredging field tests. The scour rate proceeds linearly from 2,440 m³/hr (3,300 yd³/hr) at the beginning of excavation, then tapers off in an asymptotic manner in 6 minutes to an equilibrium configuration.

The slope stability and fill-in rates of the scoured holes is of interest in that the side slope is a governing criterion in the volume which can be scoured by agitation or wheel wash dredging. The three scour hole sites were revisited on 6 February and 20 May 1974 (the 13 December 1973 hole was disturbed by the dredge on 14 December 1973). Side slope measurements were difficult to make due to erosional forces that had occurred in the interim on the exposed bed by waves at low tide. Measurements of submerged side slopes were projected to the actual top of the hole. The contour charts found in Figures V-13 through V-18 were found by direct soundings in the field.

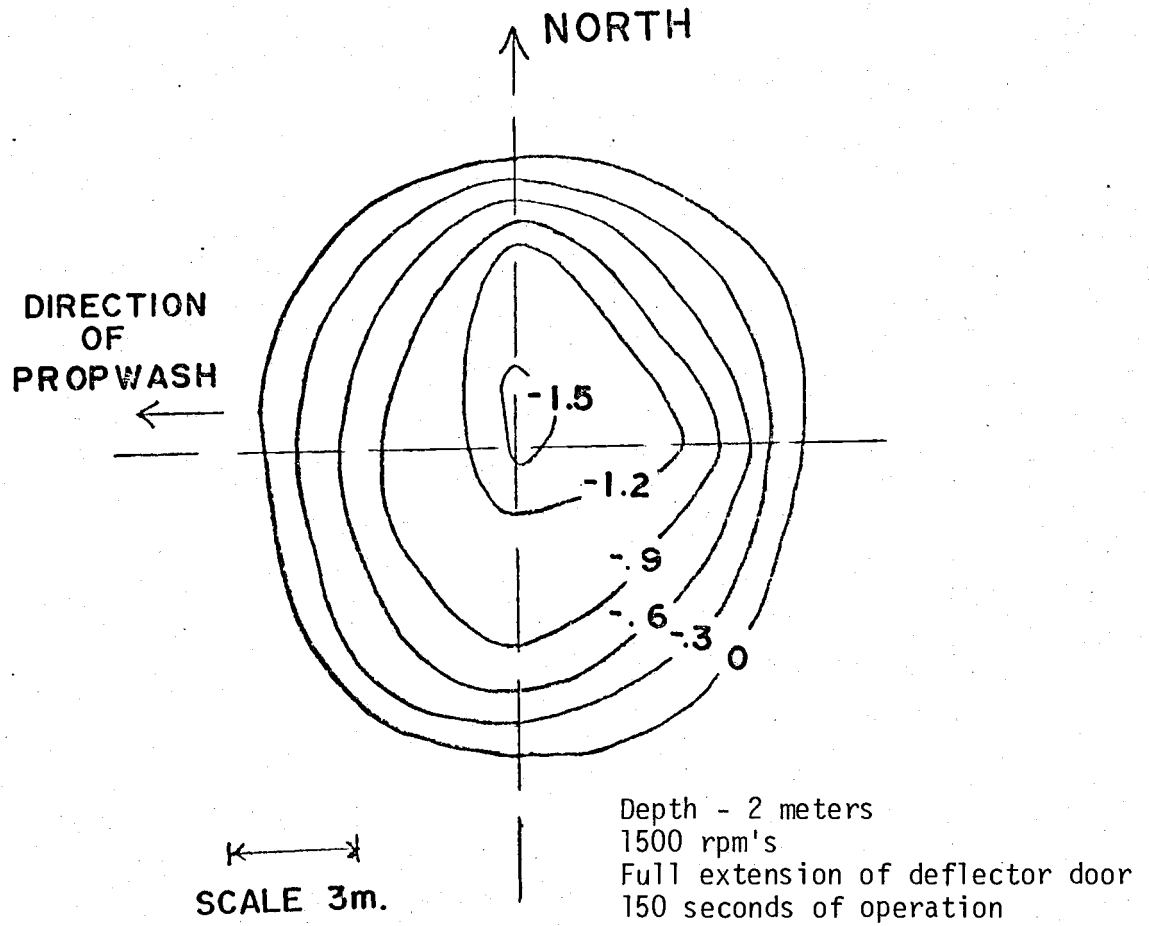


Figure V-6. North hole, 20 December 1973, labeled as B in Figure V-5, Tillamook Bay, Oregon.

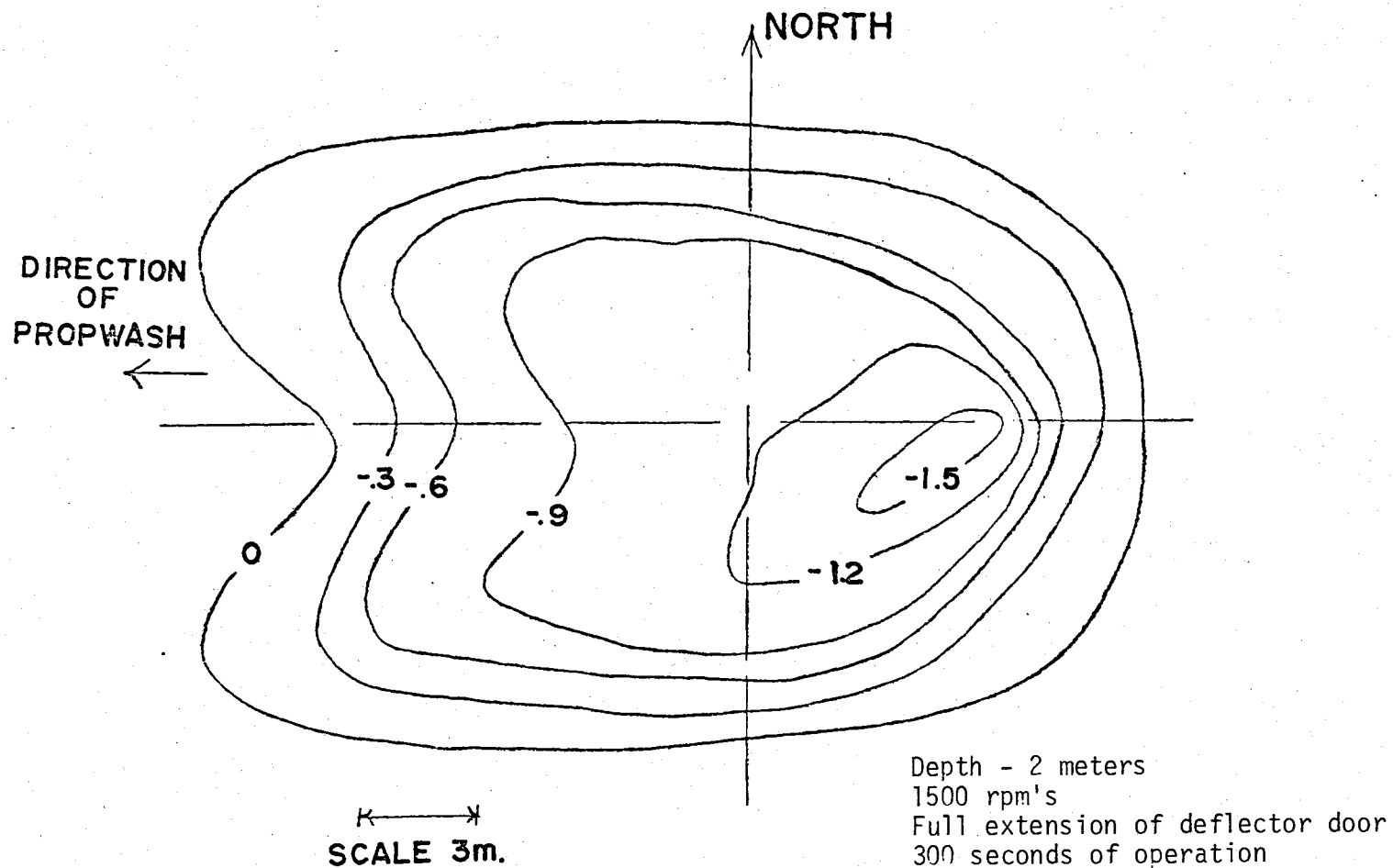


Figure V-7. Central hole, 20 December 1973, labeled as C in Figure V-5, Tillamook Bay, Oregon.

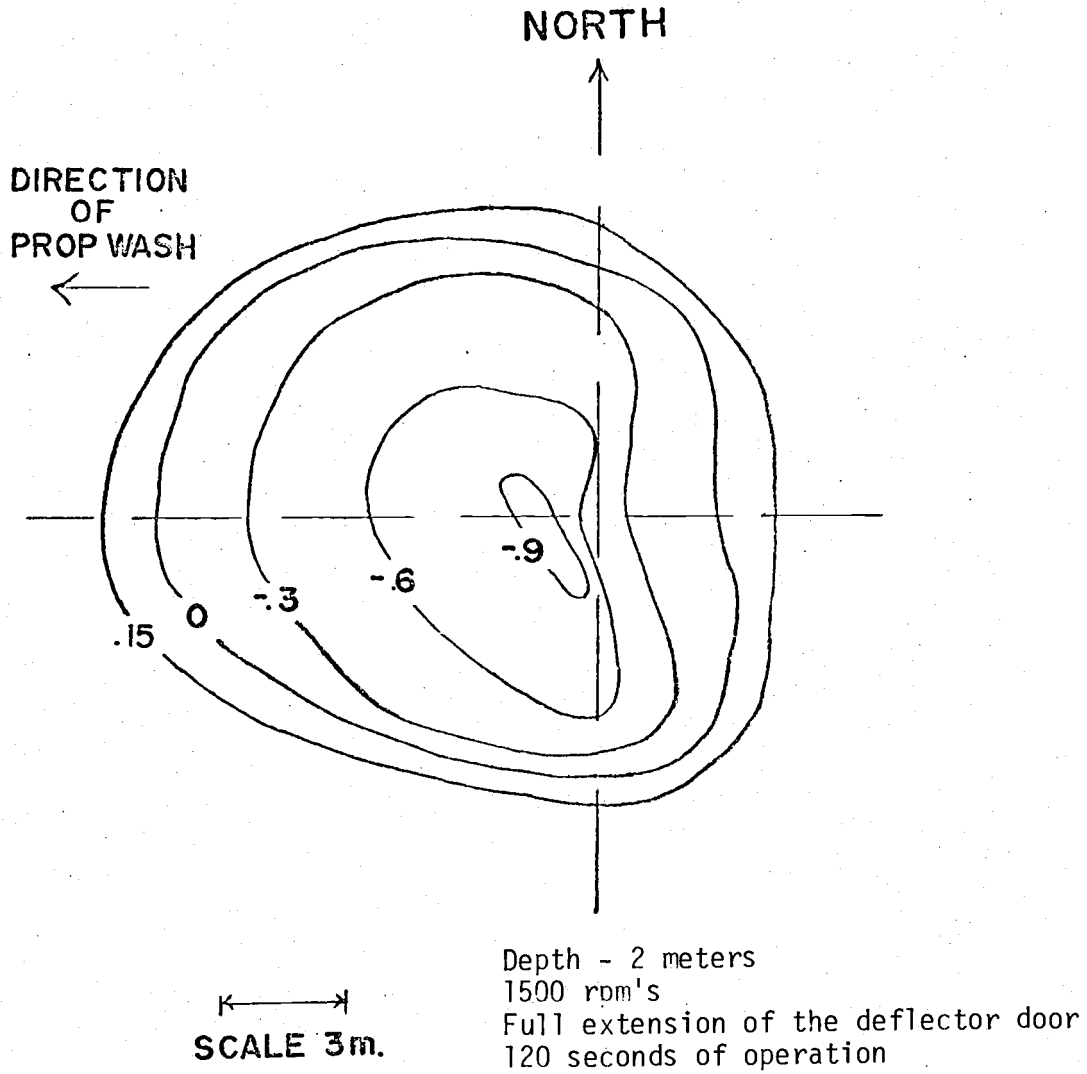
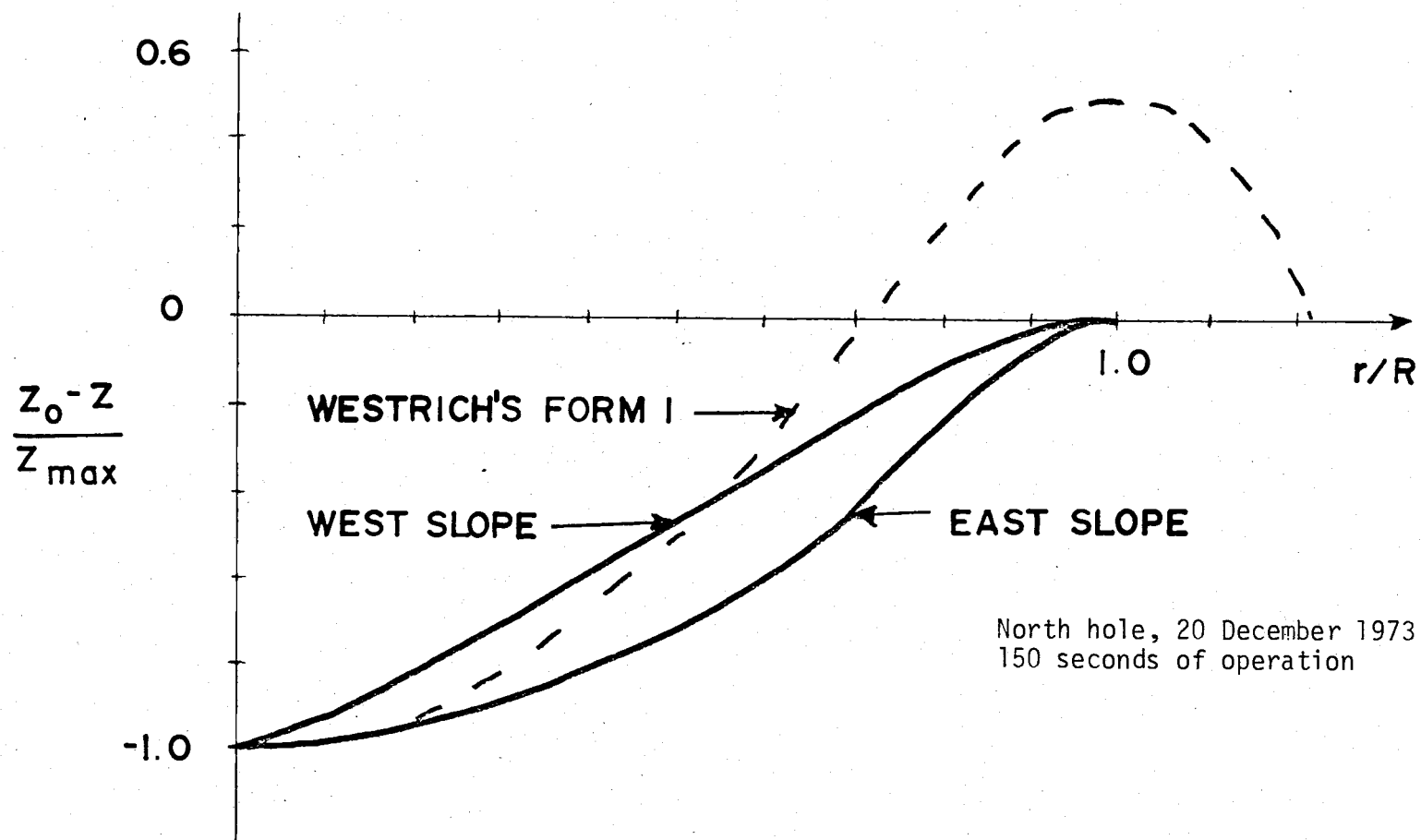
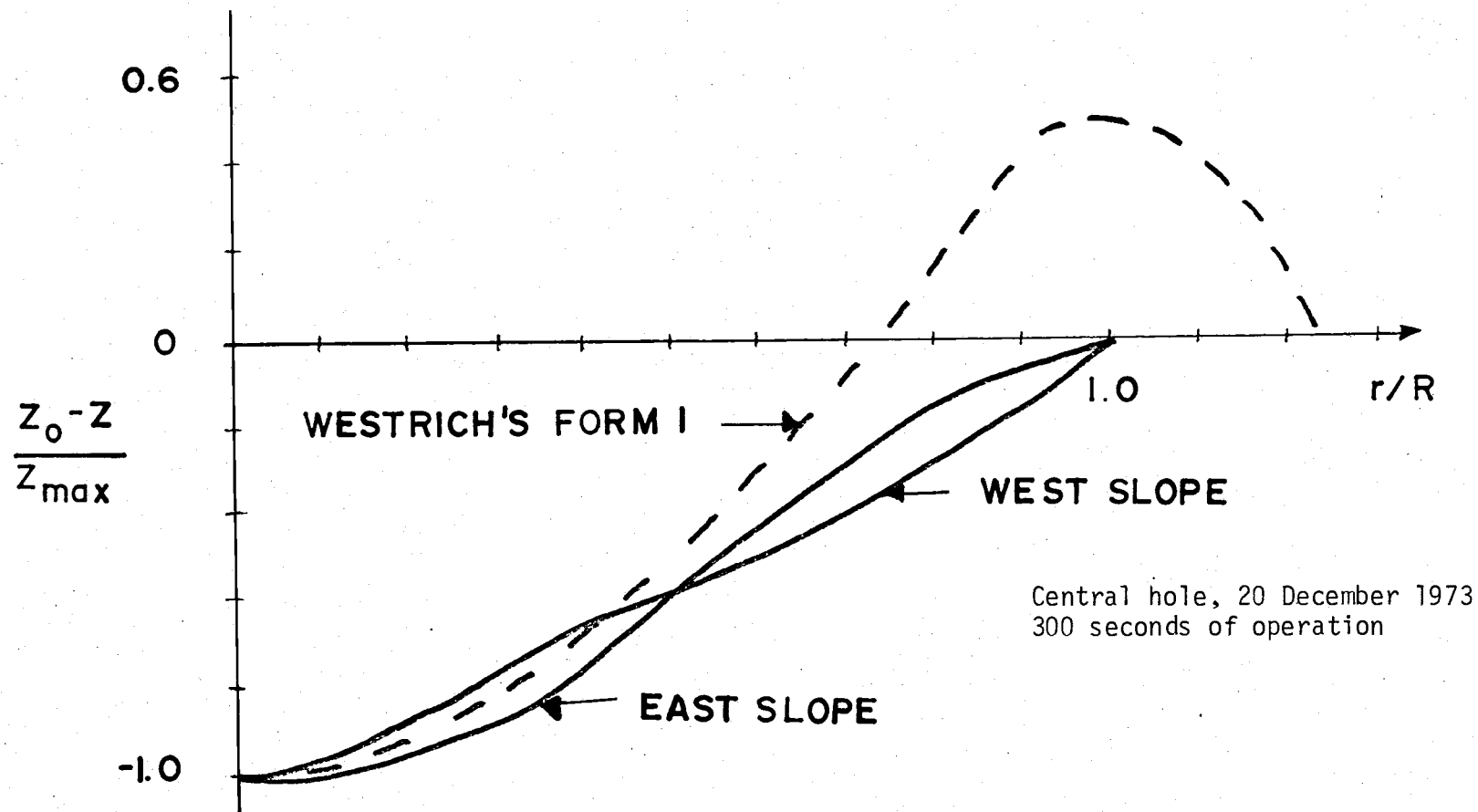


Figure V-8. South hole, 20 December 1973, labeled as D in Figure V-5, Tillamook Bay, Oregon.



North hole, 20 December 1973
150 seconds of operation

Figure V-9. North hole, slope comparisons in non-dimensional form to Westrich's (1974) scour patterns, labeled B in Figure V-5, Tillamook Bay, Oregon.



Central hole, 20 December 1973
300 seconds of operation

Figure V-10. Central hole, slope comparisons in non-dimensional form to Westrich's (1974) scour patterns, labeled C in Figure V-5, Tillamook Bay, Oregon.

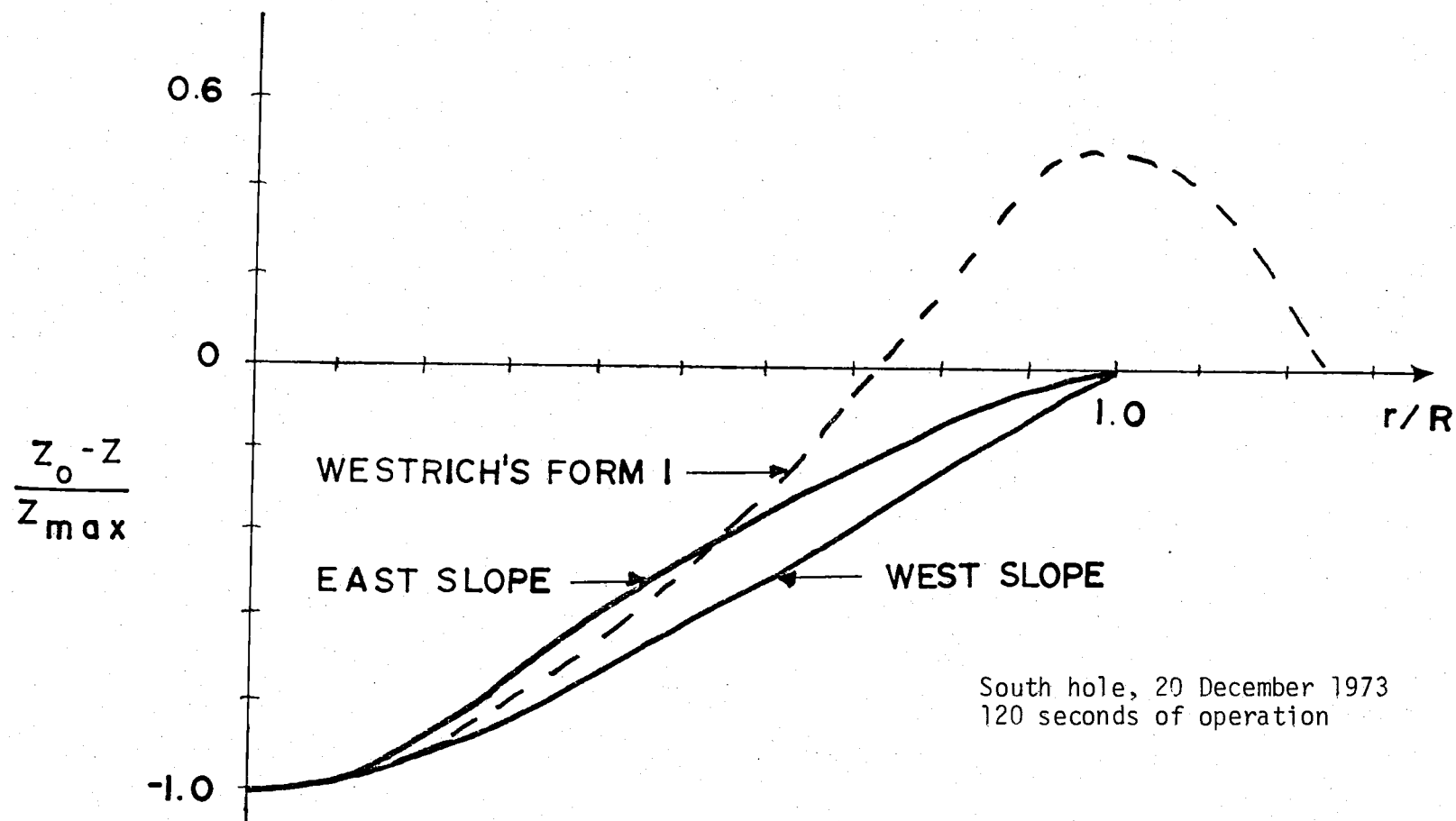


Figure V-11. South hole, slope comparisons in non-dimensional form to Westrich's (1974) scour patterns, labeled D in Figure V-5, Tillamook Bay, Oregon.

Table V-2

Volumes Excavated for Various Test Conditions

<u>Date</u>	<u>Duration (seconds)</u>	<u>t*</u>	<u>Volume (m³) Excavated</u>	<u>ψ*</u>	<u>Location</u>
13 Dec 1973	495	1.80	182	.467	West
19 Dec 1973	150	0.55	109	.281	North hole
19 Dec 1973	300	1.09	187	.479	Central hole
19 Dec 1973	120	0.45	65	.169	South hole

Depth = 3 meters

Engine rpm = 1500

Deflector door fully extended (20° below horizontal)

$$t^* = W_s t / Z_0 = 10 \text{ mm/sec } t \text{ 2743 mm}$$

$$\psi^* = V / Z_0^3 \times 6.28 \times 10^3 = V / 4580$$

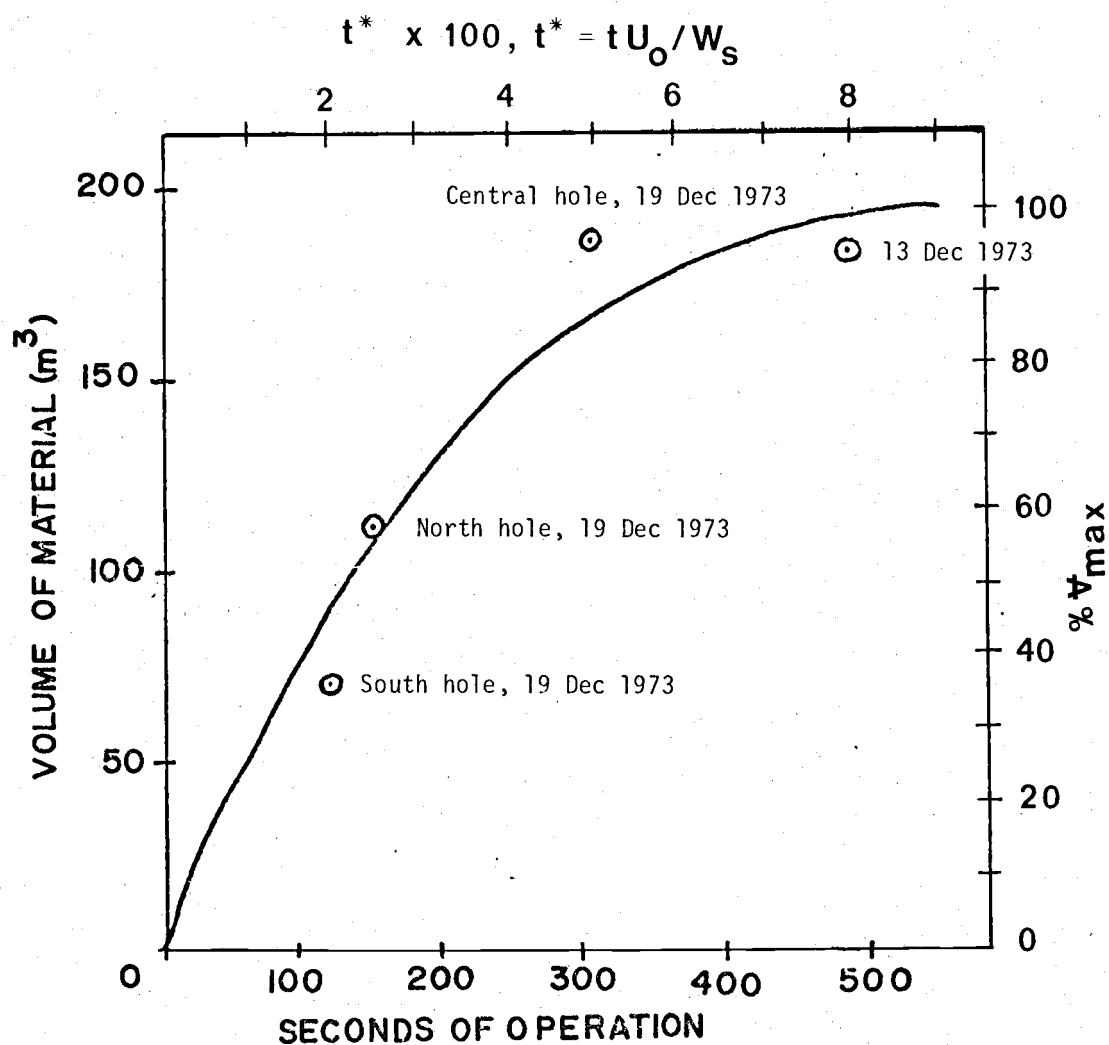


Figure V-12. Volume of material removed vs. time of operation.

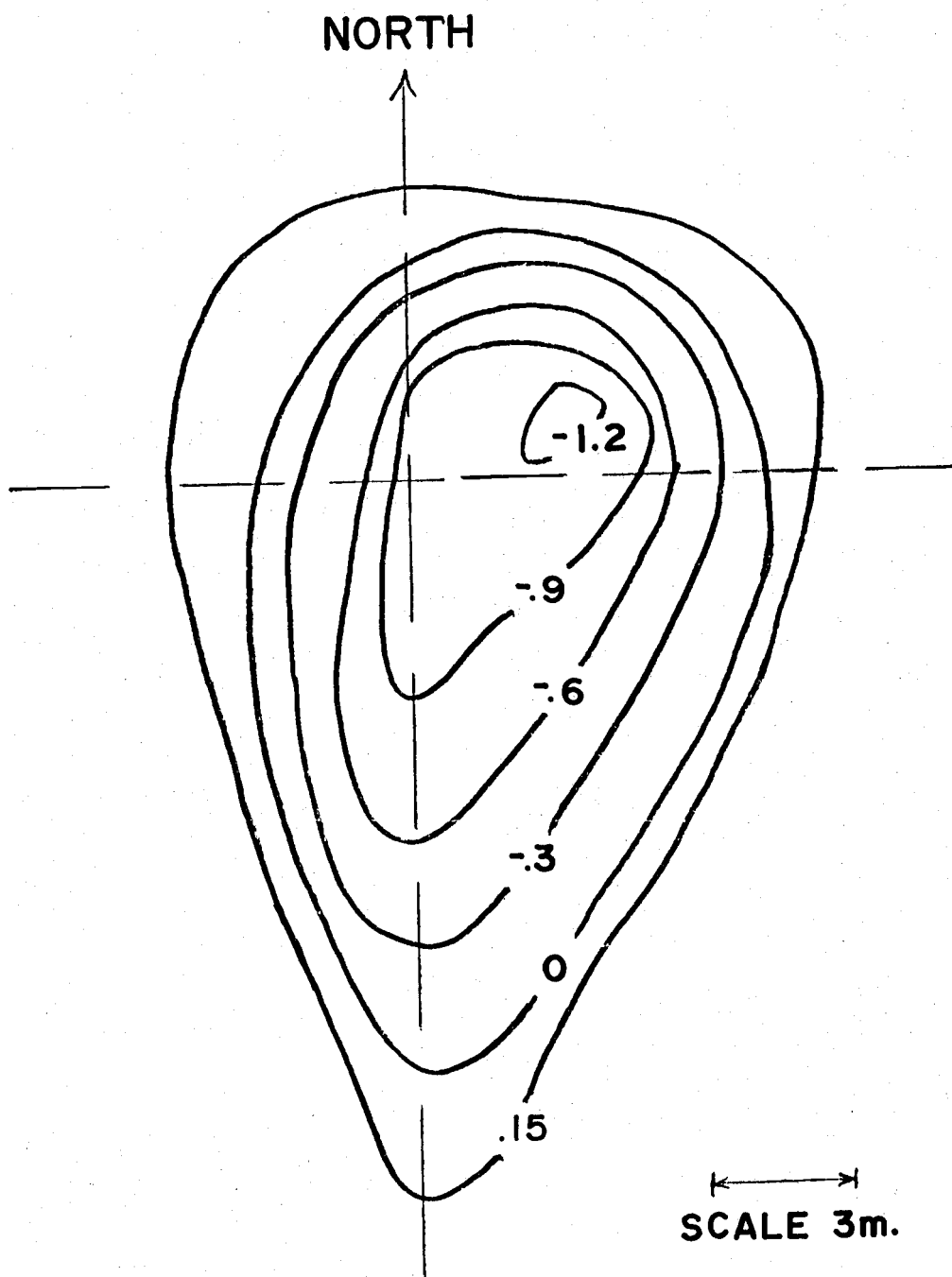


Figure V-13. North hole, 6 February 1974, labeled as B in Figure V-5, Tillamook Bay, Oregon.

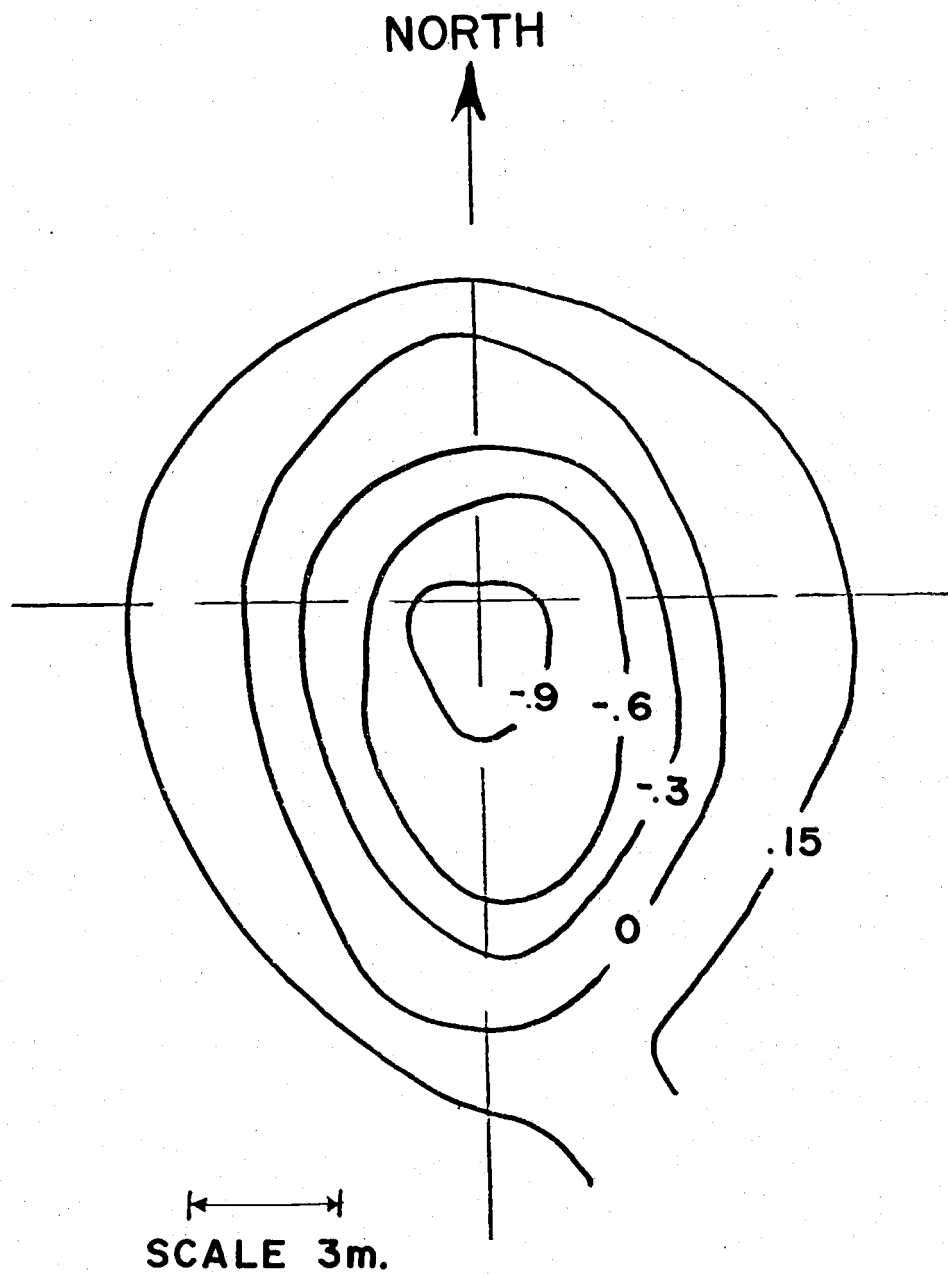


Figure V-14. North hole, 23 May 1974, labeled as B in Figure V-5, Tillamook Bay, Oregon.

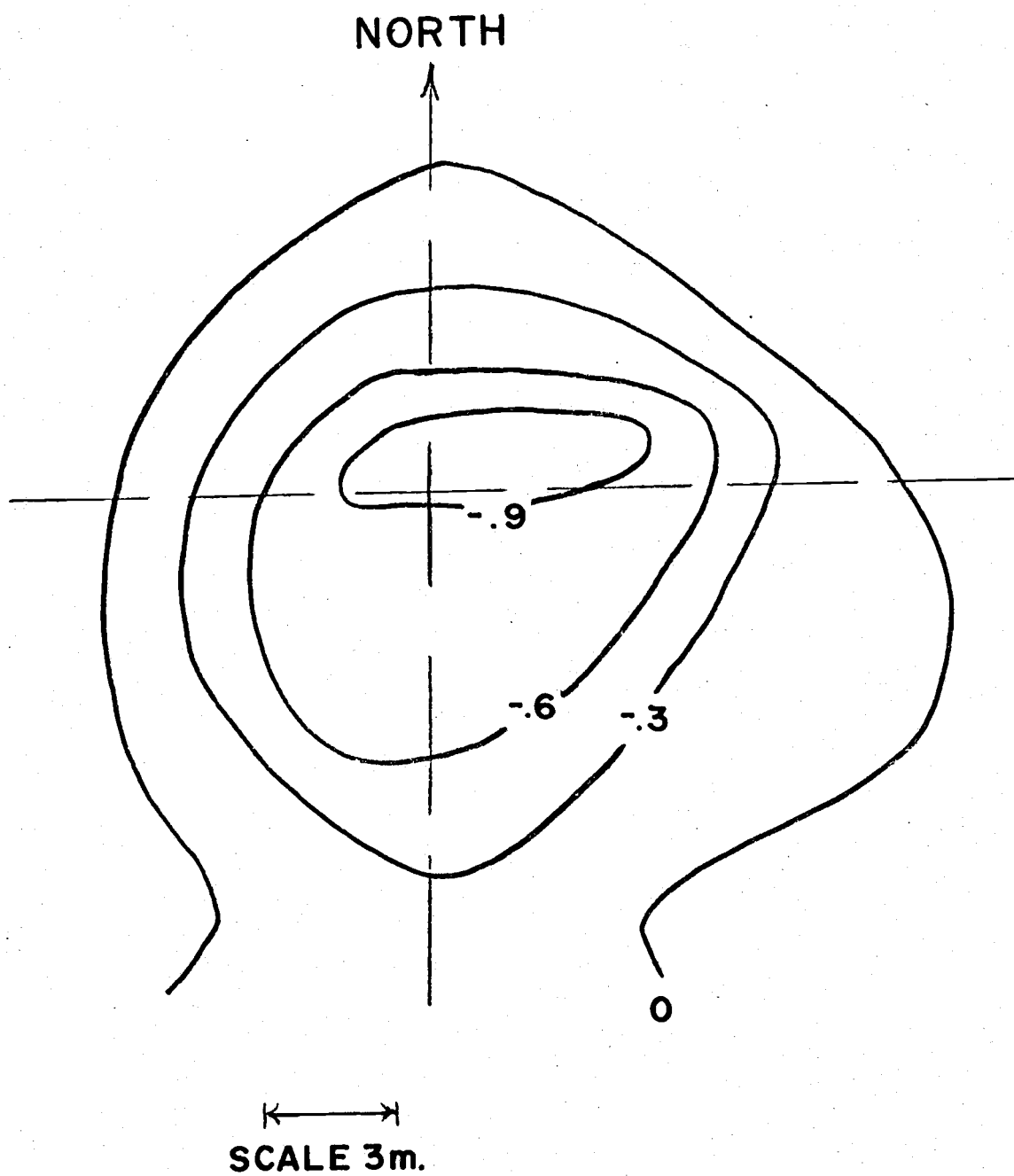


Figure V-15. Central hole, 6 February 1974, labeled as C in Figure V-5, Tillamook Bay, Oregon.

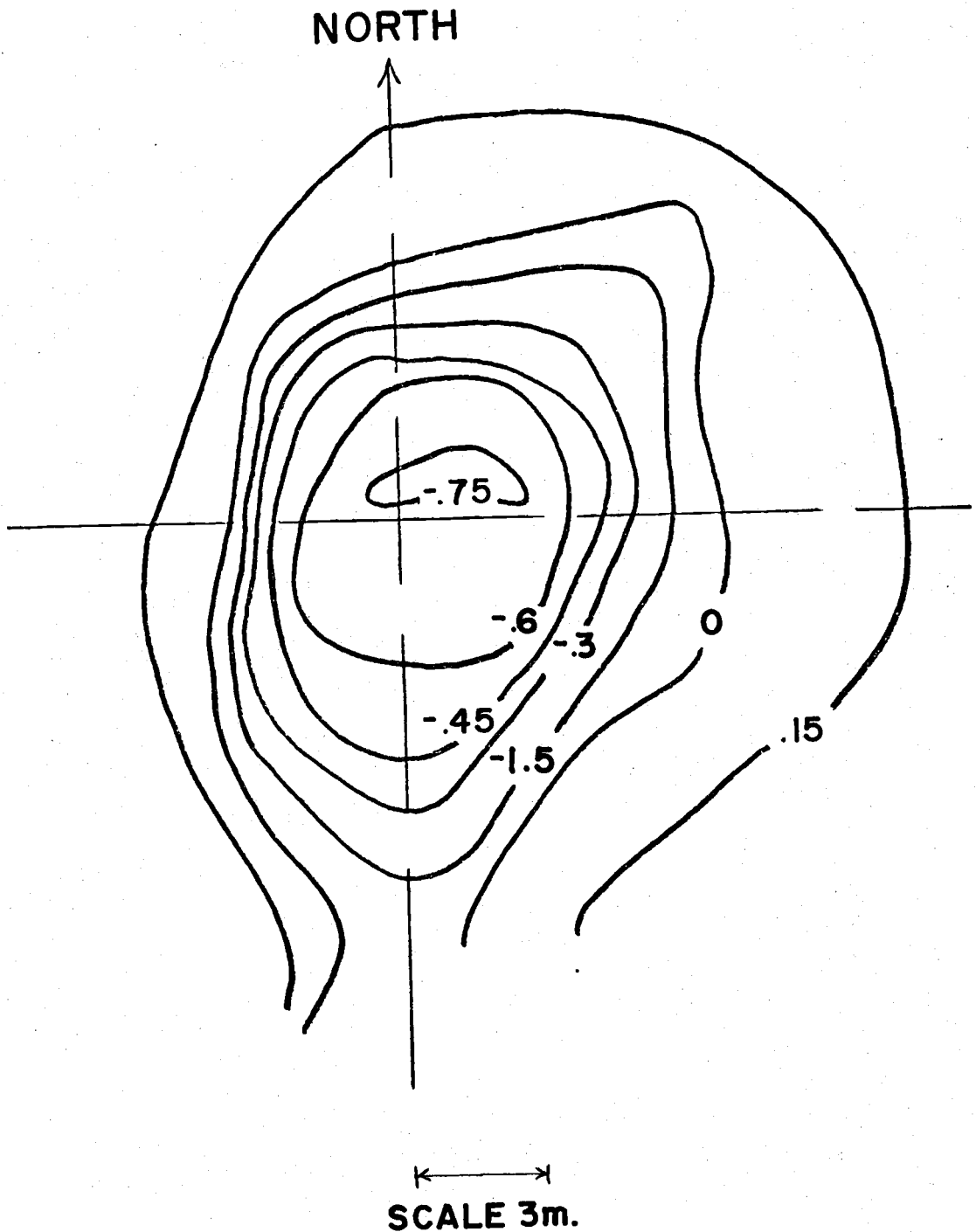


Figure V-16. Central hole, 23 May 1974, labeled as C in Figure V-5, Tillamook Bay, Oregon.

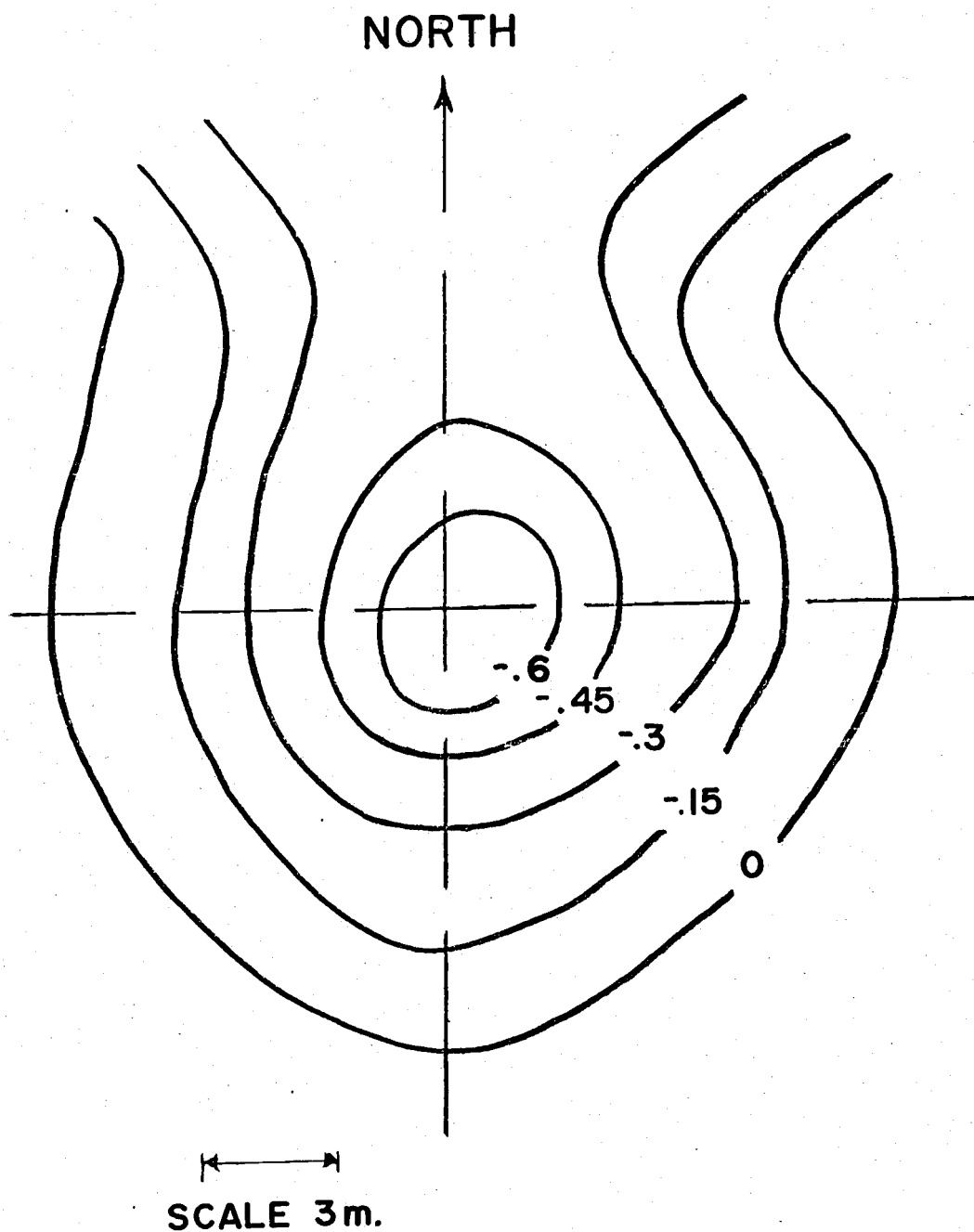


Figure V-17. South hole, 6 February 1974, labeled as D in Figure V-5, Tillamook Bay, Oregon.

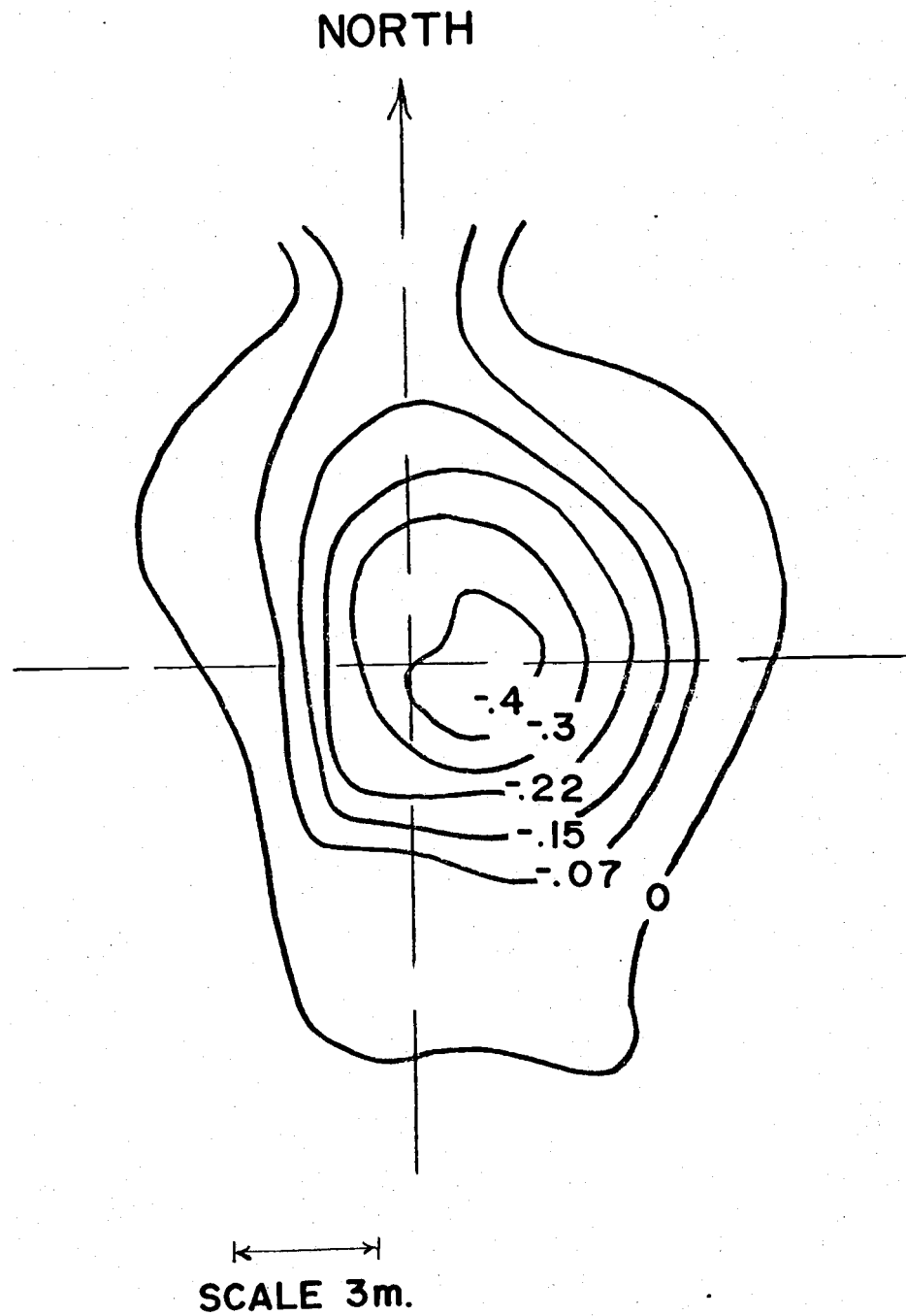


Figure V-18. South hole, 23 May 1974, labeled as D in Figure V-5, Tillamook Bay, Oregon.

The fill-in rates for the sites are shown in Table V-3 and have been plotted in Figure V-19. Any conclusion drawn from these measurements will be conservative as tidal erosion could have contributed to an increased fill-in rate by natural processes. The material found inside the scour hole was finer in size than material on the rim or tidal flat. The filling-in of the scour holes is observed to be nearly linear as seen in Figure V-19, although the rate of fill-in was found dependent on the site depth and location; the central and north holes were slower to fill in than the south hole. This would suggest the initial disturbance conditions, geometry and local soil conditions are as important as sedimentation conditions. The side slopes of the dredged holes are tabulated in Table V-4. These values have a wide range with the steepest slope observed of 47° , with many initial slopes less than the predicted angle of repose near 30° . This suggests that the predictions of side slope based solely on sand grain dimensions will be steeper than side slopes in the actual dredging process. A stable deposition slope over time was reached at nearly 5° in the southern end of the tidal flat and 17° in the northern region. The southern end of the tidal flat would be a more active region for wave erosion. The northern end may contain more sediment in suspension from Miami Cove and the local streams.

Soil Property Measurements

The LCM Sandwick field operation results may be normalized for correlation with those obtained with measurements of the sand and sediment properties of the dredge area. The grain size distribution being the most important measurement along with the specific gravity

Table V-3

Dredge Hole Accretion

<u>Location</u>	<u>Date</u>	<u>Days Elapsed</u>	<u>Absolute Volume (m³)</u>	<u>ΔV (m³)</u>	<u>% Change</u>
North	20 Dec 1973	0.5	112		
	06 Feb 1974	48	103	- 9	8%
	23 May 1974	106	89	-23	21%
Central	20 Dec 1973	0.5	187		
	06 Feb 1974	48	142	-45	24%
	23 May 1974	106	94	-93	50%
South	20 Dec 1973	0.5	62		
	06 Feb 1974	48	59	- 3	5%
	23 May 1974	106	39	-23	37%

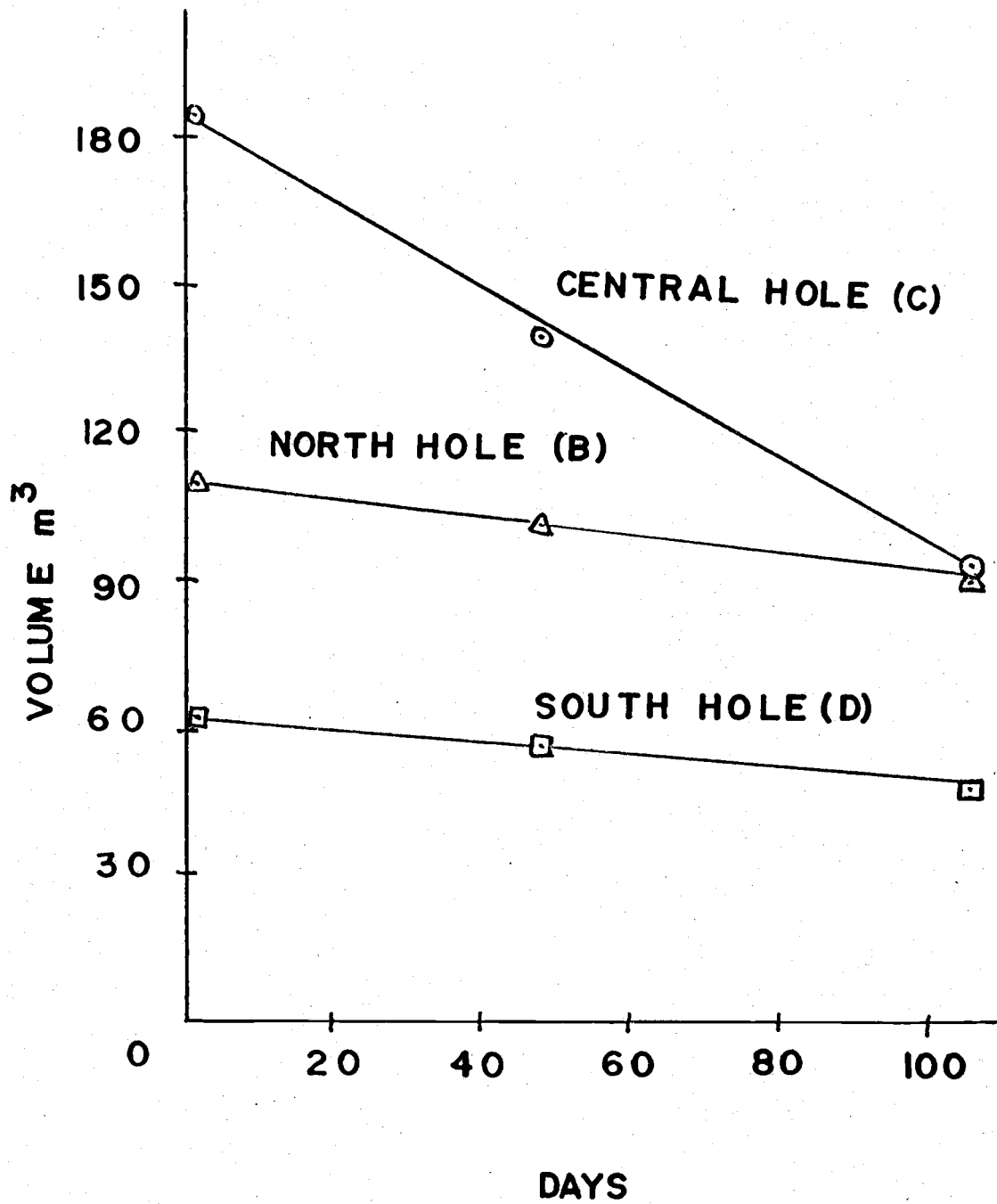


Figure V-19. Fill-in vs. time for three scour holes, Tillamook Bay, Oregon.

Table V-4
Slope Measurements

<u>Location</u> <u>Direction</u>		<u>20 Dec 1973</u> <u>(.5 days)</u>	<u>Slopes</u> <u>06 Feb 1974</u> <u>(48 days)</u>	<u>23 May 1974</u> <u>(106 days)</u>
North				
	North	33°	18°	18°
	South	20	8	15
	East	20	26	16
	West	16	15	19
Central				
	North	18°	12°	12°
	South	20	--	7
	East	47	13	8
	West	12	12	11
South				
	North	16°	4°	3°
	South	23	7	7
	East	18	6	6
	West	5	6	14

of the sediment. The native Tillamook sediment had a specific gravity of 2.68 and the grain size distribution is plotted in Appendix 2. The D_{50} value for the sample was found to be .19 mm.

VI. Conclusions and Recommendations

The characteristics of the LCM Sandwick's deflector door configuration have been formulated in non-dimensional charts. These charts can be applied to improve the operation of the prototype vessel. To this end, the efficiency of the deflector door in directing the propeller wash toward the bed has been shown in the form of velocity contours. The energy lost in redirecting the flow was noted to be a 10% reduction in velocity of the centerline from 39 to 35 cm/sec with a 10° to 30° deflector door change in the 1:12 model. Turbulence fluctuations superposed in the average velocity made this reduction untenable in the field studies. Determination of the actual propeller power required for field shoal removal to compare with model situations was not undertaken; however, this would be necessary for a complete efficiency study.

The scour process in both model and field studies has been described using non-dimensional plots of volume scoured, bed configuration, and maximum depth of scour. Comparison of theoretically predicted and model scour depth patterns to prototype data was favorable. However, data from field observations showed a lack of higher depositional rim. The use of self-similar plots shows that the relative turbulence in the model tests is greater than the field tests. Westrich's (1974) Form I, for less energetic flow, was found to match the field data; while Form II, for strong flow, matched the model data. In the field it was observed that sediment transport occurs primarily due to suspended load. The bed material had considerable fines and would have been classified as a cohesive sediment. The angles of the scoured hole bank steepness found in the field tests were not as close to the angle of repose as data obtained in the model tests.

The depth at which the redirected prototype propeller wash scour takes place is approximately three times the vessel's draft, with the present deflector door. If the deflector door were lowered five more degrees below the horizontal, scour could be affected even more deeply. To achieve maximum scour the vessel must operate in water less than draft depth. Other deflector door geometries were not tried after the different scour holes were formed by rotation changes of the propellers.

Since the deflector door-ship match is a system which should be tuned, it is recommended that extensive model testing be conducted before a deflector door is added to regular craft.

The rate at which sediment was scoured was observed to follow a nearly linear rate at the beginning of the scour process. This was observed in both the model and field studies. This linear rate followed Westrich's (1974) prediction in that equilibrium was reached in $600 t^*$ units ($t^* = tU_o/W_s$). The fill-in rate of the field scour holes was observed to correlate with the scour holes' stability. The fill-in rates were also linear with time, but the rate was observed to be a function of each location and other factors as depth and wave orientation. The field data results on fill-in rates may be better than first anticipated because the material in the scoured holes was finer than that scoured.

Future laboratory and field efforts should examine the scale of turbulence generated by the LCM Sandwick. The turbulence frequency is in the low audio range and might be studied with acoustic methods as well as velocity measurements. Changes in scour volume, by means of pulsing the wash, as with changes in the rudder settings or disturbing the flow in other ways, could prove an interesting study.

VII. References

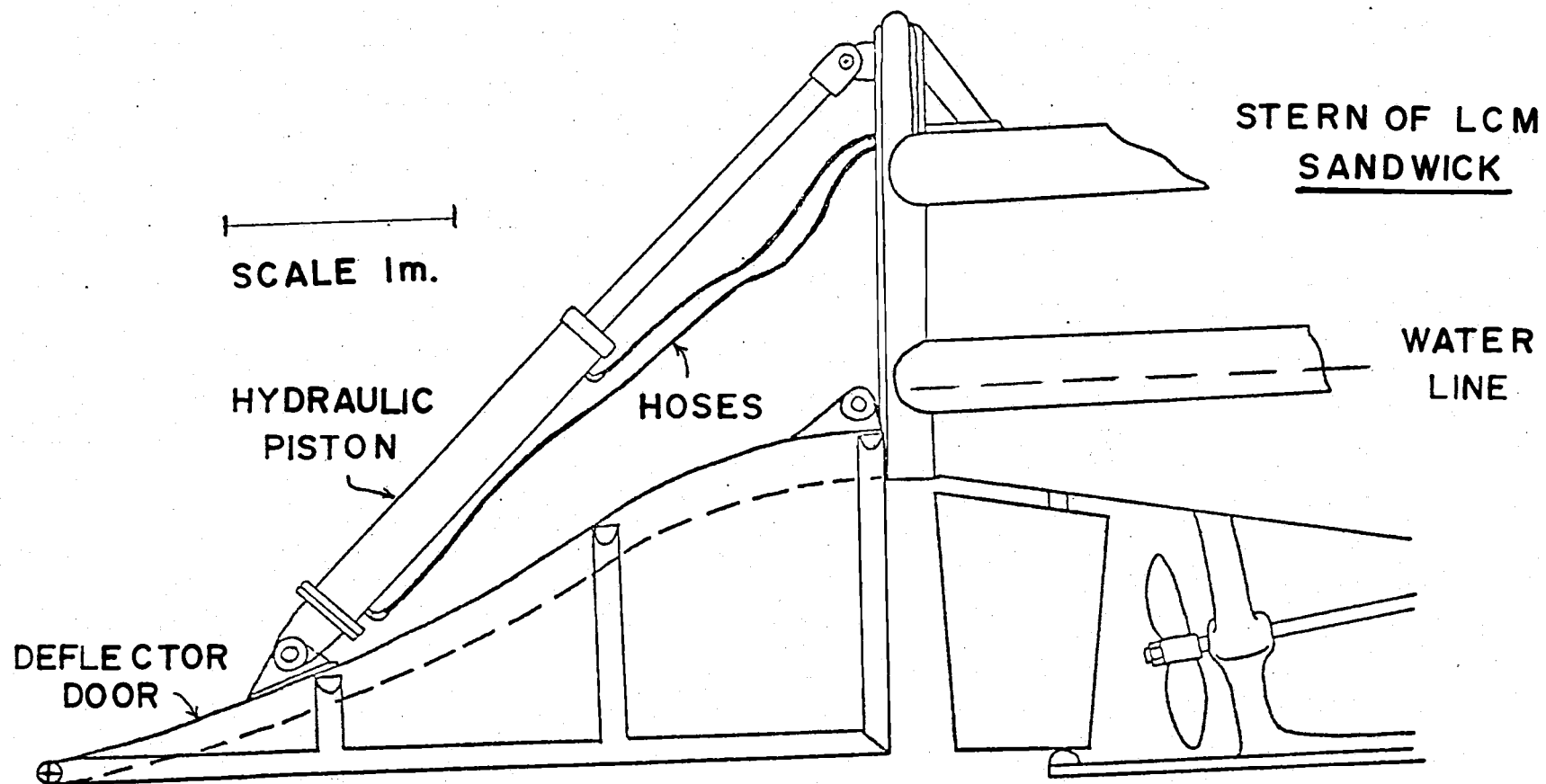
- Altinbilek, H.D. and Okyay, S. Localized Scour in a Horizontal Sand Bed Under Vertical Jets, IAHR Istanbul, A-14, pp. 99-106, 1973.
- Bechley, J. 'Sandwick' Gives Nature a Boost on Shoal Removal, World Dredging, September 1975.
- Bradbury, L.J.S. The Impact of an Axisymmetric Jet onto Normal Ground, The Aeronautical Quarterly, 23, pp. 141-147, 1972.
- Comstock, J.P., Editor. Principles of Naval Architecture, The Society of Naval Architects and Marine Engineers, N.Y., New York, 1967.
- Corps of Engineers, Portland Districts, U.S. Army. Operation of the Sandwick: A New Development in Critical Shoal Removal, 1973.
- Donaldson, C. dup. and Snedeker, J. A Study of Free Jet Impingement, Part I, Mean Properties of Free and Impinging Jets, Journal of Fluid Mechanics, pp. 2, 45, 281-319, 1971.
- Graf, W.H. Hydraulics of Sediment Transport, McGraw-Hill Book Co., 1967.
- Harsha, P.T. Free Turbulent Mixing, A Critical Evaluation of Theory and Experiment, Arnold Engineering Development Center, Arnold Air Force Station, Ten., AD 718956, February 1971.
- O'Loughlin, E.M.; Mehrotra, S.L.; Chang, Y.C.; and John F. Kennedy. Scale Effects in Hydraulic Model Test of Rock Protected Structures, Iowa Institute of Hydraulic Reserach, University of Iowa, February 1970.
- Rajaratnam, N. and Pani, B.S. Three Dimensional Turbulent Wall Jets, Journal of Hydraulics ASCE HY1, pp. 69-83, January 1973.
- Slotta, L.S.; Hancock, D.R.; Williamson, K.J.; Sollit, C.K. et al. Effects of Shoal Removal by Propeller Wash, December 1973, Tillamook Bay, Oregon, submitted to the Department of the Army, Portland District Corps of Engineers, Contract No. 57-74-C-0087, July 1974.
- Slotta, L.S. and Montes, J.S. Dredging by Means of Water Jets, 1975, Oregon State University, unpublished.
- Westrich, B. and Kobus H. Erosion of a Uniform Sand Bed by Continuous and Pulsating Jets, IAHR Istanbul, A-13, 1973.
- Westrich, B. Erosion Eines Gleich Formiges Sandbettes durch Stationare und Pulsierende Strahlen, Doctorial Dissertation, University of Karlsruhe, 1973.
- Yalin, M.S. Mechanics of Sediment Transport, Pergamon, 1972.

APPENDIX 1

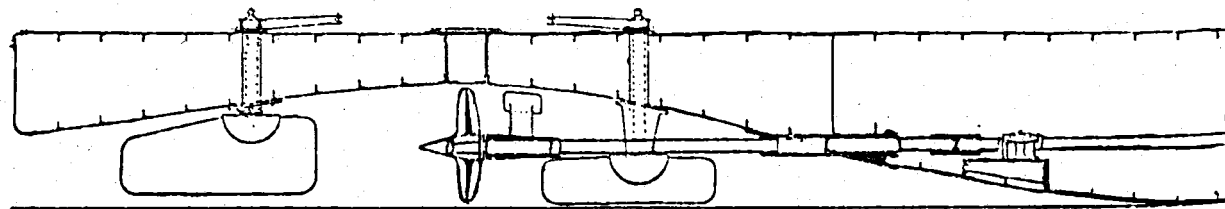
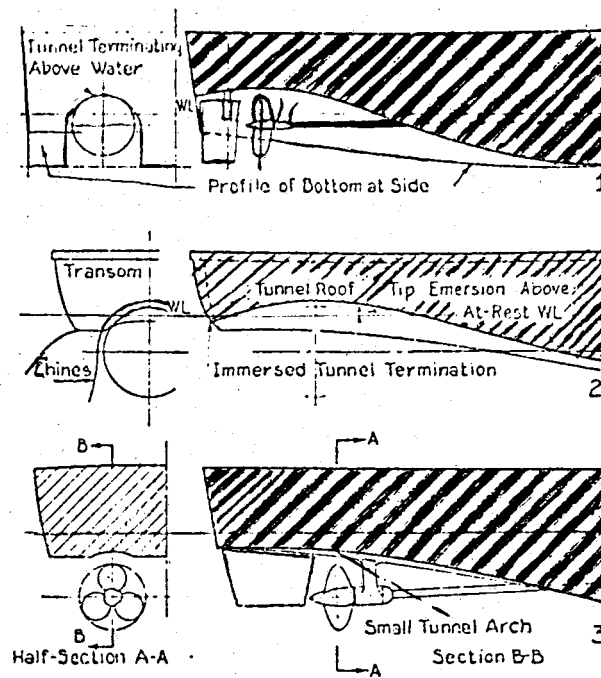
The design of the LCM Sandwich is important in the hydrodynamics of the jet formed. The LCM Sandwich employs a tunnel stern which is shown in Appendix Figure 1-1. The major components of the system are represented. A tunnel stern consists of a flap covering and extending behind the propeller. A tunnel stern has been used in the past to allow the use of a large, and more efficient, propeller in a shallow water craft. The tunnel stern has the added effect of completely submerging the propeller if it is larger than the draft of the vessel. This concept originated in England in 1856 and has been included in the design of famous crafts such as the Monitor, circa 1860. Appendix Figure 1-2 displays a few examples of this design.

The LCM Sandwich is modeled after the working tug, Salvage Chief which is owned and operated by the Fred DeVine Diving and Salvage Company of Portland, Oregon. The Salvage Chief has a patented "under-water trenching device" which deflects the wash of its propellers downward to remove bottom material. The Portland District U.S. Army Corps of Engineers obtained permission to modify an existing LCM-8, landing craft, owned by the District, with a deflector door of 5.5 m wide and 3.7 m long. The deflector door would direct the power of the twin 0.86 m propellers with a 0.5 m pitch and 330 horse power per drive shaft toward the bed.

The propellers rotate such that the port one rotates counter-clockwise and the starboard one clockwise. The propellers have three blades and rotate at 1500 rpm's which would pulse the water at 75 Hz. The propellers are separated by 2.9 m and are symmetric with respect to the ship's centerline.



Appendix Figure 1-1. Detail of deflector door of the LCM Sandwick.



Appendix Figure 1-2. Forms of tunnel sterns, from Comstock (1967).

The LCM Sandwick operates as follows. The vessel locates itself over a shoal and places four anchors or a harrow, a single stern anchor, to stay in location. The deflector door is lowered to 20°, which is the lowest extent of the three hydraulic pistons. The throttles are opened on the main engines until 1500 rpm are attained on both shafts. The propeller wash directed toward the bed causes shoaled material to be agitated and carried away down stream several hundred meters before the shoal is complete. The exact method of field operation employed depends on the currents, the tidal changes and the presence of ship traffic. The operation of the LCM Sandwick is a means of duplicating nature in shoal removal during times of flood. The operation of the vessel is determined by the season and each location's particular problems.

APPENDIX 2

The material used in the model tests was washed Ottawa sand and crushed quartz. This material was selected as it would be conservative in the scour process and clarity of the water was necessary for measurements and photographs. The volume of sand needed restricted the use of exotic materials as the 1:12 model would have required a ton of sand to fill the test region in the tank. The use of a non-cohesive bed material was selected so the bed would have dependable properties for all the tests. Appendix Figure 2-1 shows the test results.

The material for the field tests were the natural sediments of the Tillamook Bay area. No attempt was made to select a site on any sediment criteria except that the area was representative and samples were taken. The results of these tests are found in Appendix Figure 2-2.

The fall velocity was found by applying the curve in Graf (1967) as the samples were dried and organics removed prior to sieve analysis.

Appendix Figure 2-1

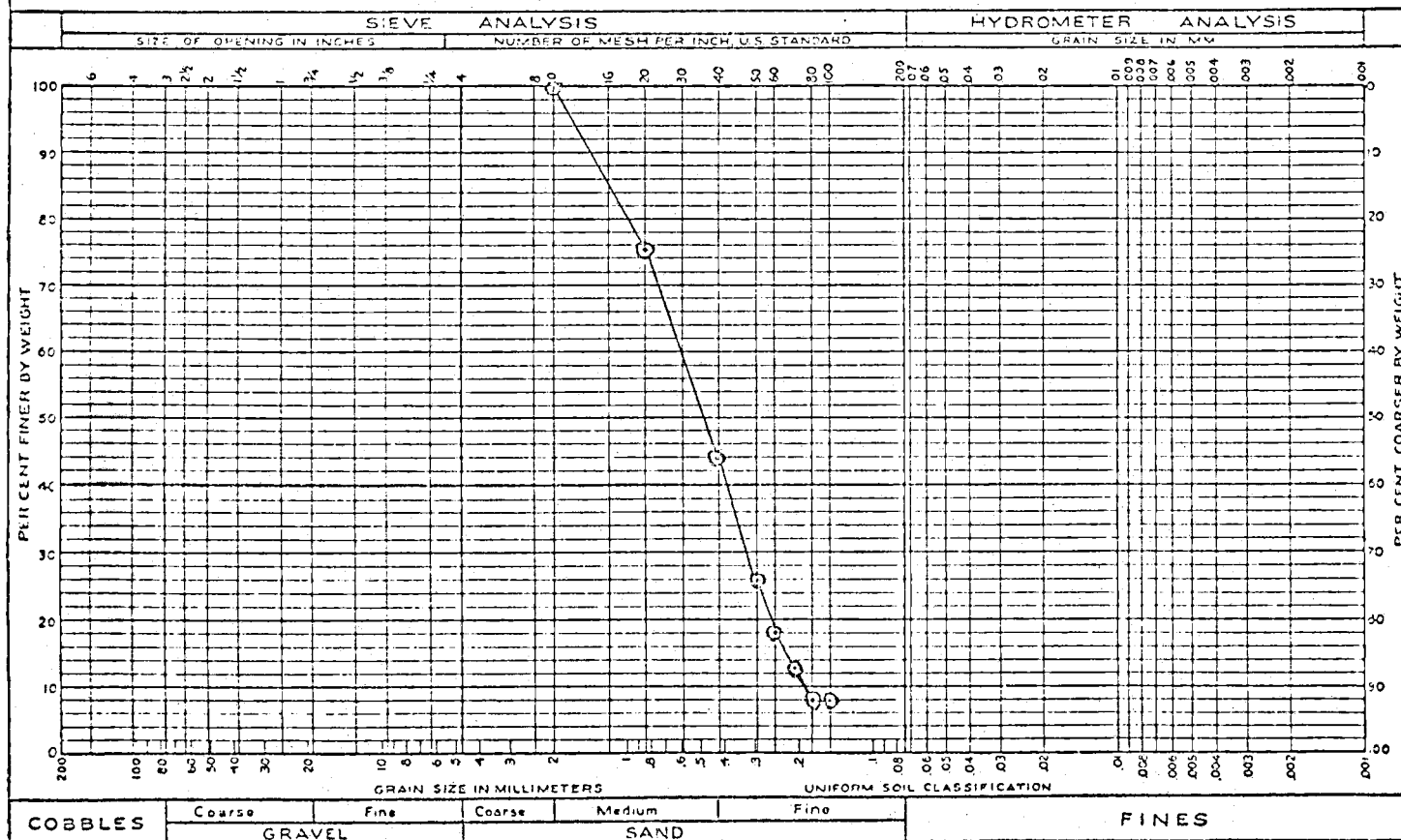
GRAIN SIZE ANALYSIS

TEST FOR "Sandwick" model sand

TEST BY Bruce Higgins

DATE 1 July 1974

SAMPLE DESCRIPTION



Appendix Figure 2-2

GRAIN SIZE ANALYSIS

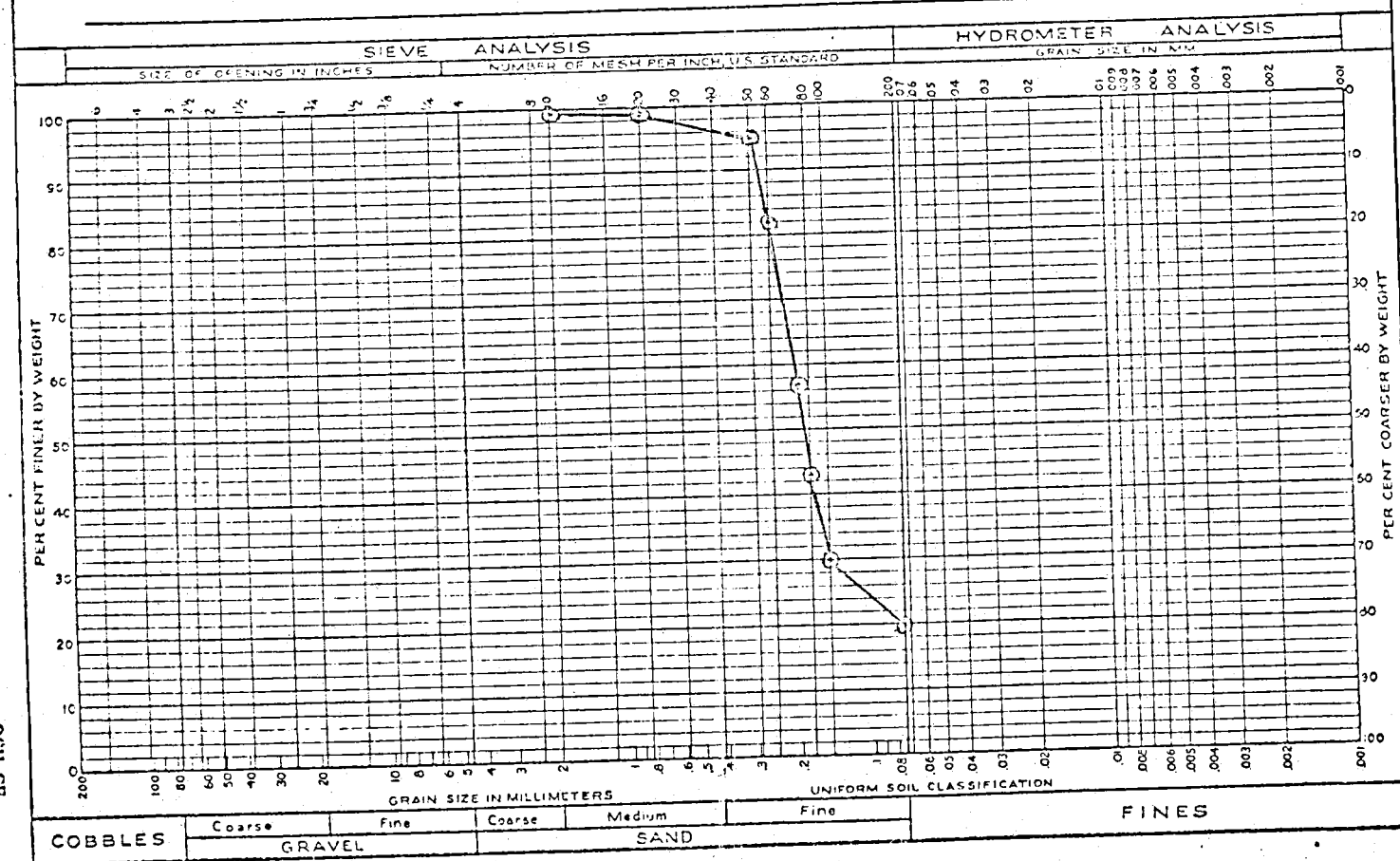
SHEET OF

TEST FOR Oven Dried Tillamook Sand

TEST BY J.P. Leshuk

DATE 09 October 1973

SAMPLE DESCRIPTION _____



APPENDIX 3

The photographs of the 1:40 scale model in the test flume and during a sample test are included on the following pages. Flow would be from right to left, unless otherwise noted. The motors were run at 5000 rpm's and propellers are rotating as in the prototype. The bed material was washed sand.

Appendix Figure 3-1. Deflector door in 20° lowered position, depth nearly the vessel's draft, 1:40 scale model of LCM Sandwich (Side panels removed for photographs).

Appendix Figure 3-2. Initial test conditions, as above; 1:40 scale model.

Appendix Figure 3-3. Scour pattern after one minute of operation, as above. Shape follows Westrich's (1974) Form I.

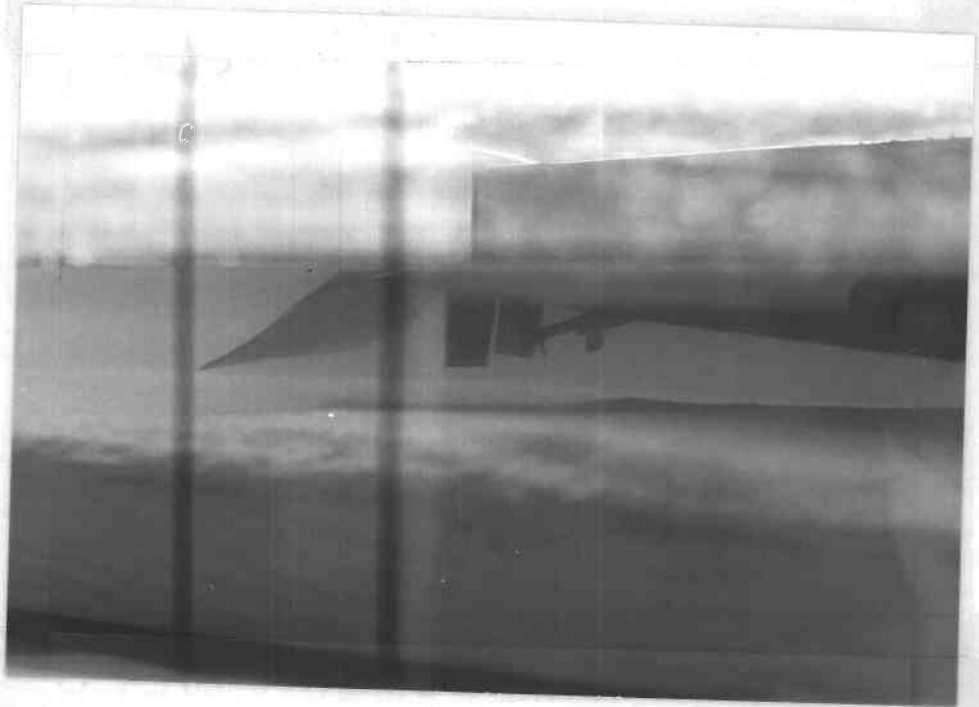
Appendix Figure 3-4. Scour pattern after two minutes of operation, as above. Scour hole is larger.

Appendix Figure 3-5. Scour pattern after three minutes of operation, conditions as above. Note that the angle of repose has been reached for the sand.

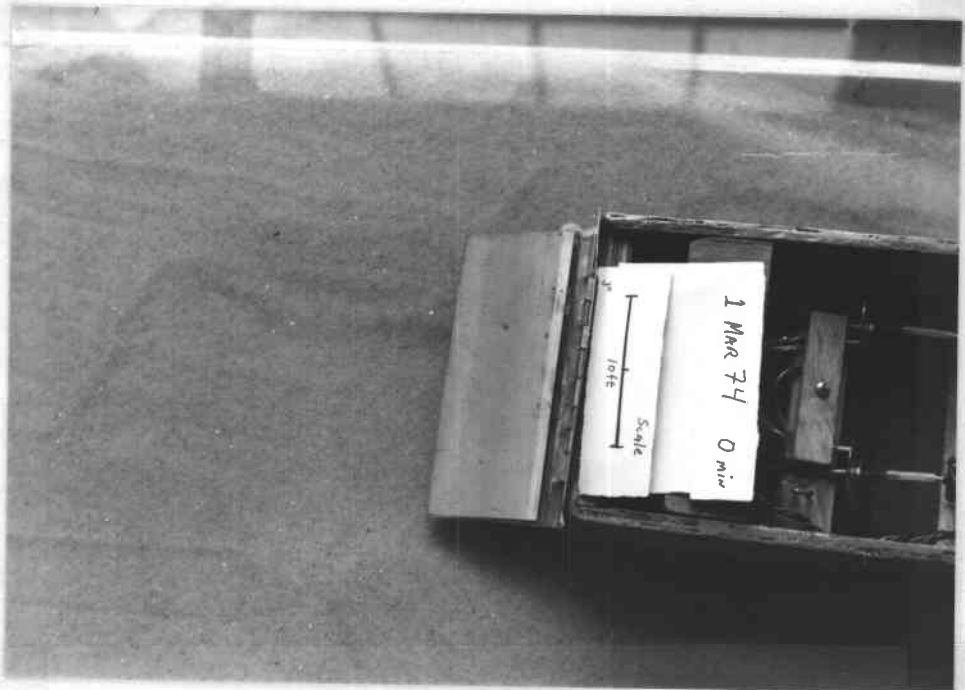
Appendix Figure 3-6. Scour pattern after four minutes of operation, conditions as above. Note that the ridge now has a flat top.

Appendix Figure 3-7. Scour pattern with motors running at five and one-half minutes of operation, conditions as above. Note little surface water disturbance.

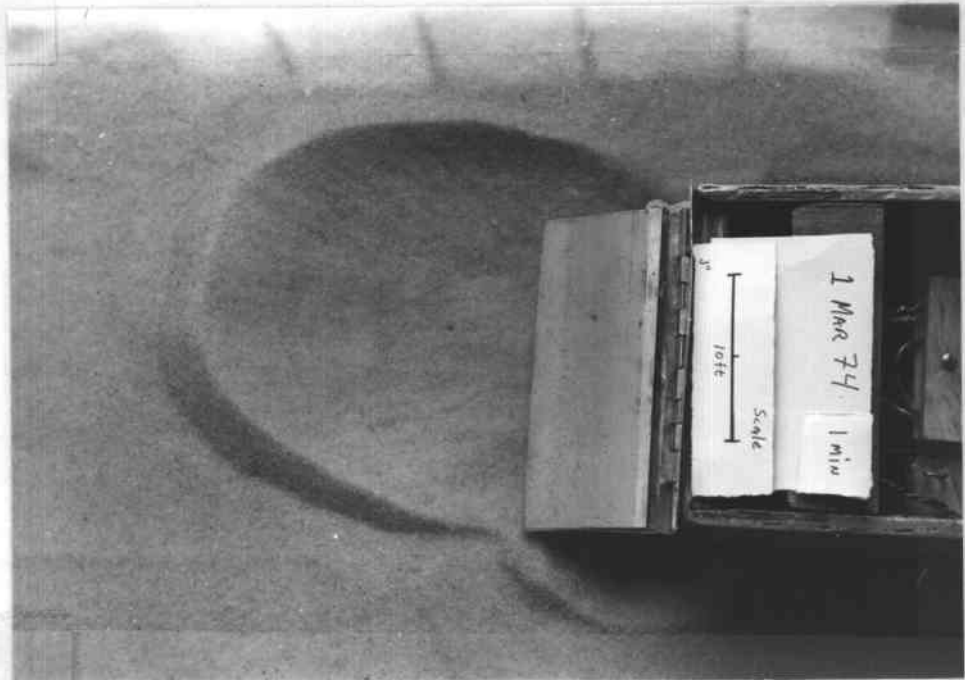
Appendix Figure 3-8. Scour pattern after six minutes of operation, conditions as above. No further change was noticed in hole configuration.



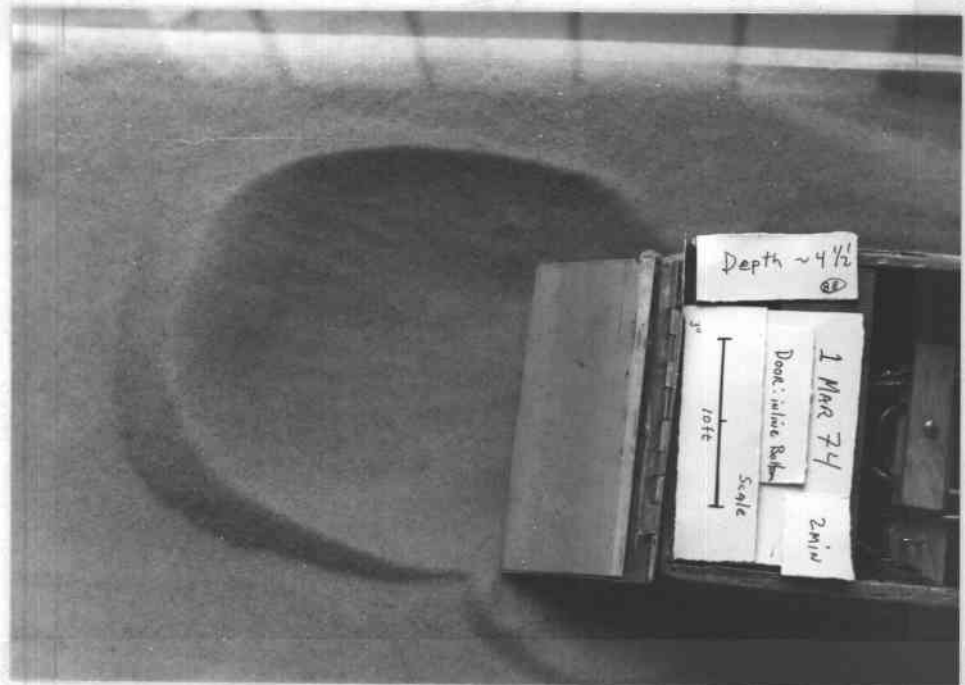
Appendix Figure 3-1.



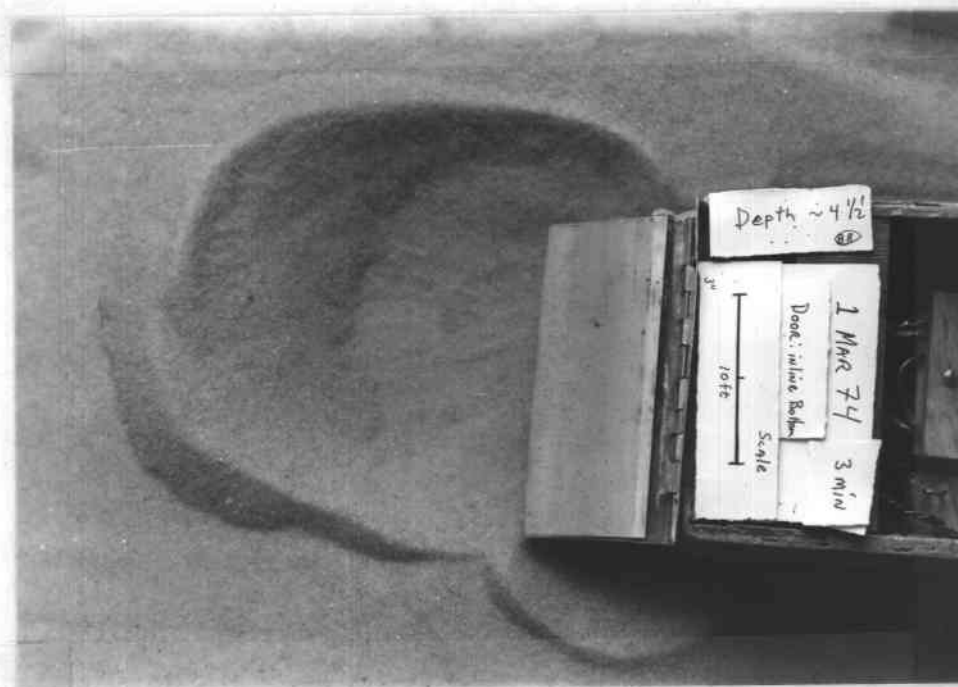
Appendix Figure 3-2.



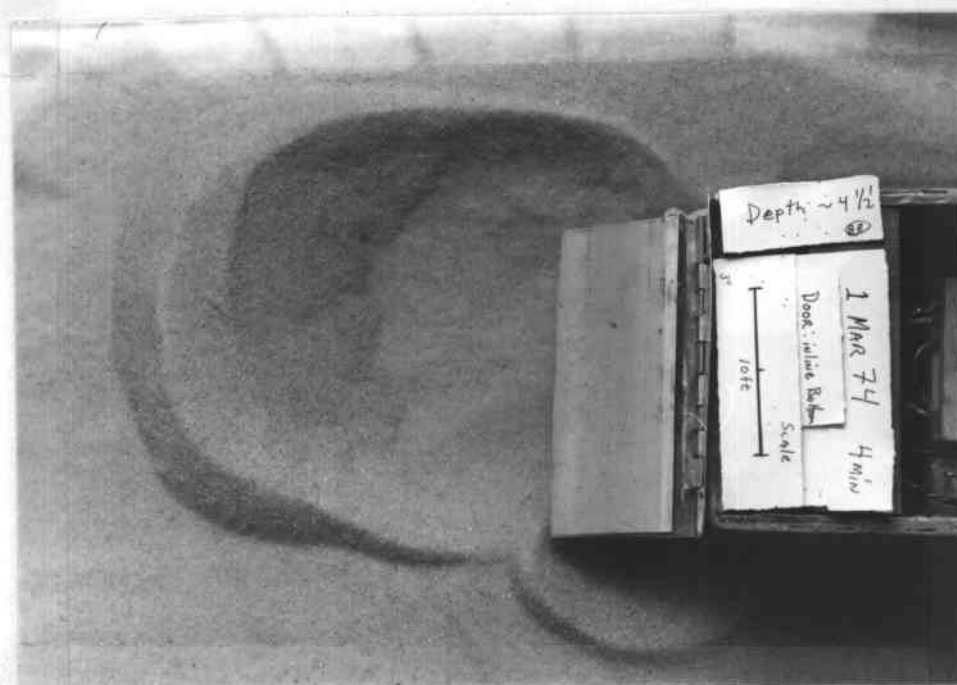
Appendix Figure 3-3.



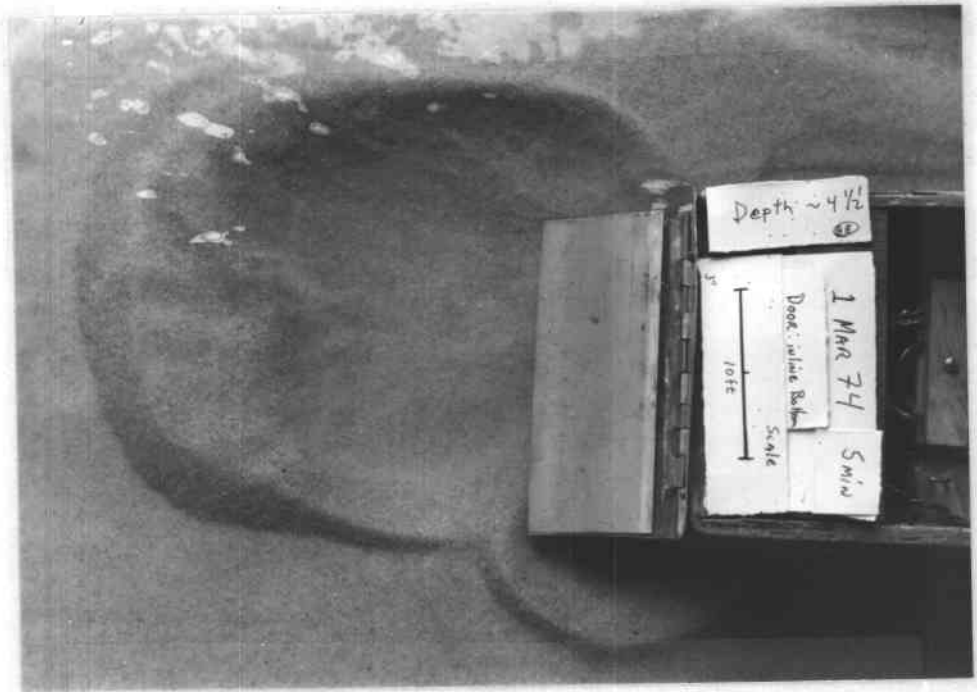
Appendix Figure 3-4.



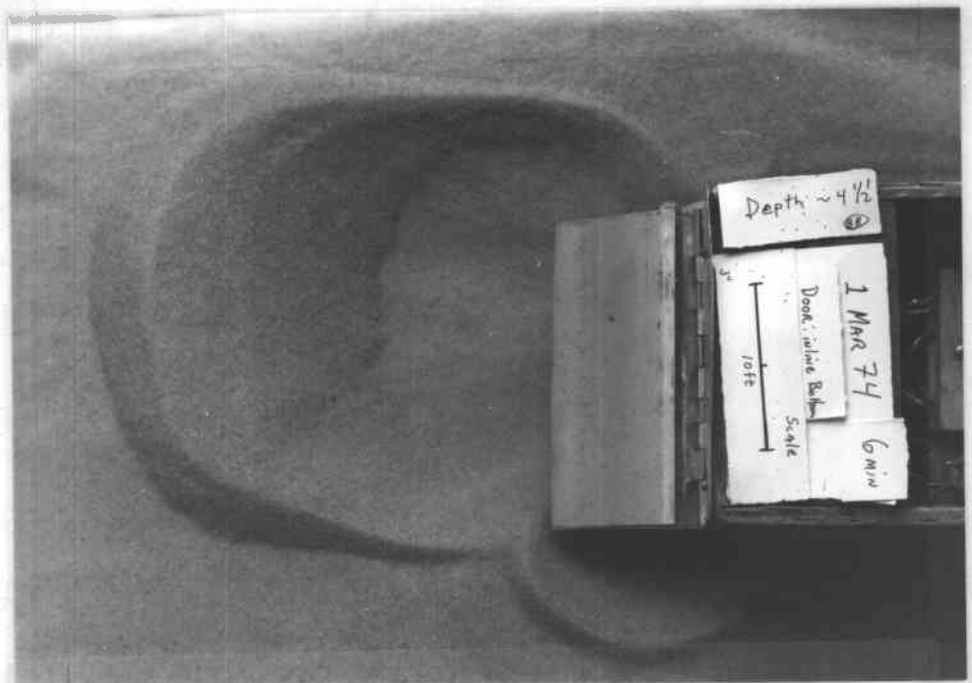
Appendix Figure 3-5.



Appendix Figure 3-6.



Appendix Figure 3-7.



Appendix Figure 3-8.

Photographs of 1:12 Scale Model

Tests were conducted at 1500 rpm. All final forms are photographed after 10 minutes of model operation. Flow is from right to left in all photographs. The bed material was washed quartz sand.

Appendix Figure 3-9. Model floating unballasted in test flume. Water line labeled on side of model.

Appendix Figure 3-10. Rick Downs drawing contours for placement of 5 cm nails with a floating point gauge.

Appendix Figure 3-11. View of model deflector door and propellers on the 1:12 scale model of the LCM Sandwich.

Appendix Figure 3-12. Model of LCM Sandwich in position. The 10 mm Ott current meter is in foreground. Model was ballasted with sand for proper draft.

Appendix Figure 3-13. Final scour pattern for depth nearly equal to draft of vessel. 10° deflector door angle, 1:12 scale. Contours are every 2.5 cm starting at mean bed level.

Appendix 3-14. Final scour pattern for depth nearly equal to the vessel's draft. 20° deflector door angle, 1:12 scale. Contours are every 2.5 cm starting at mean bed level.

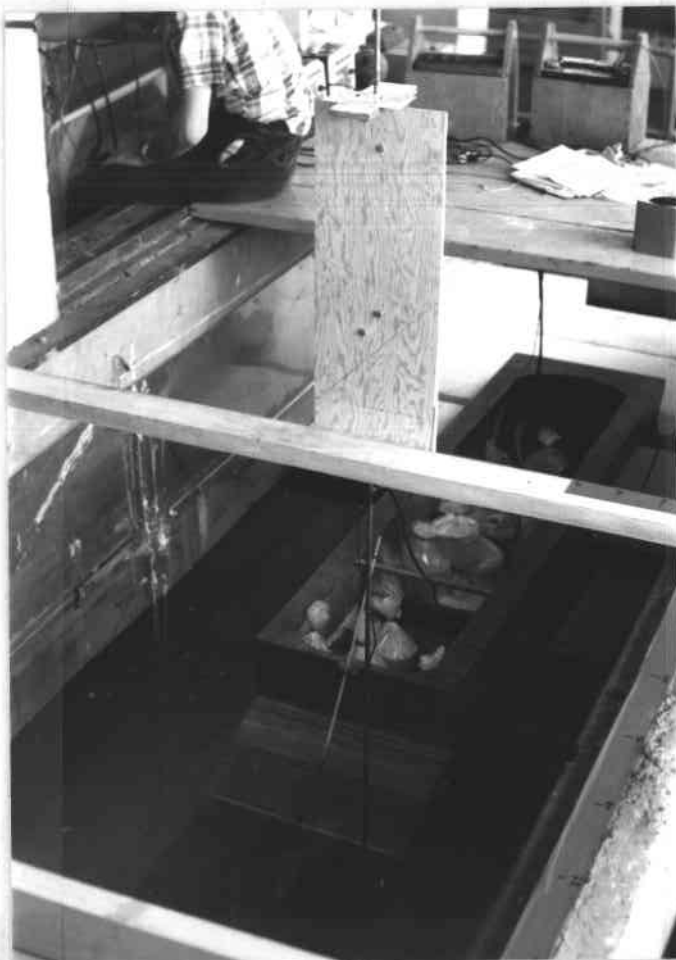
Appendix Figure 3-15. Final scour pattern for 10° deflector door and depth equals twice vessel's draft. Contours are every 2.5 cm beginning at the mean bed level.



Appendix Figure 3-9.



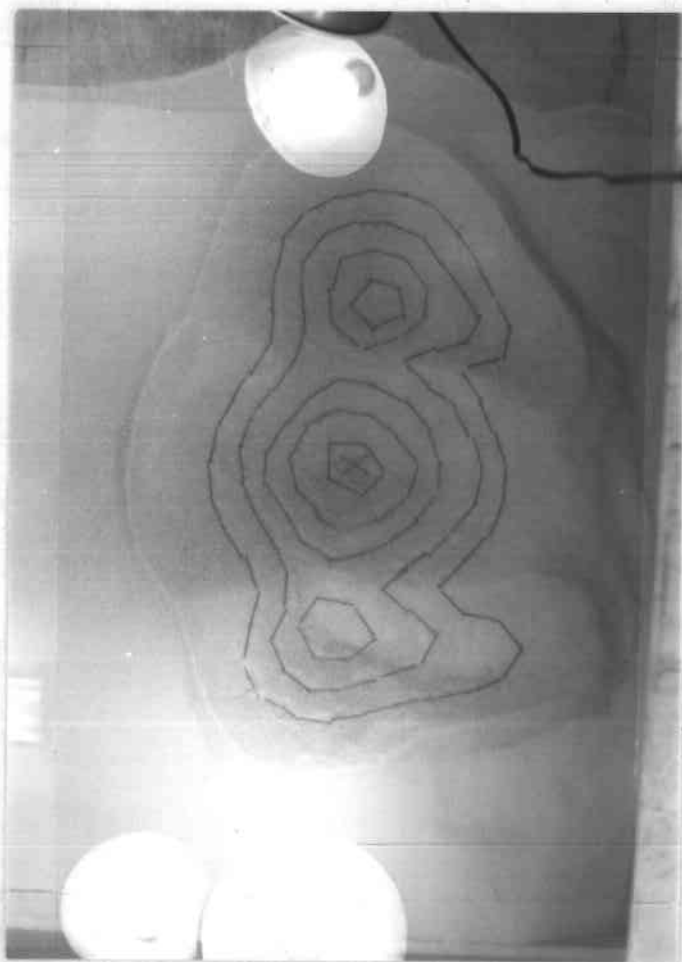
Appendix Figure 3-10.



Appendix Figure 3-11.



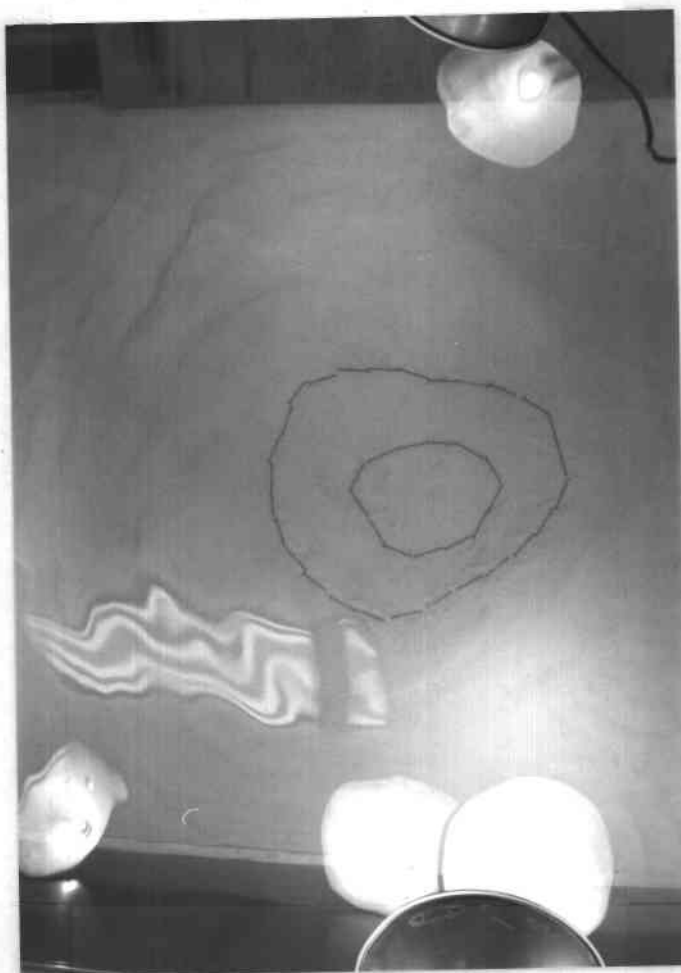
Appendix Figure 3-12.



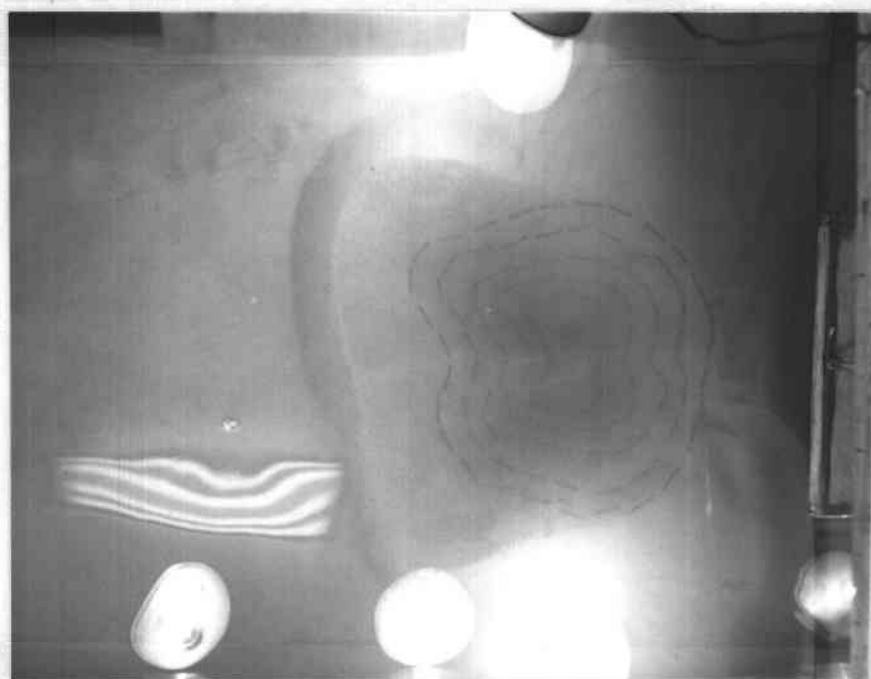
Appendix Figure 3-13.



Appendix Figure 3-14.



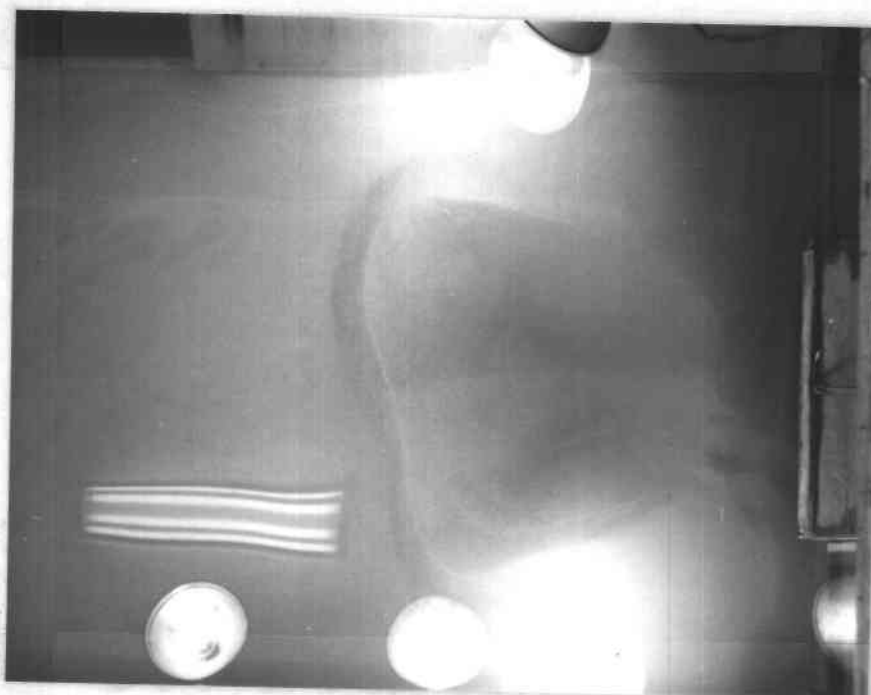
Appendix Figure 3-15.



Appendix Figure 3-16.



Appendix Figure 3-17.



Appendix Figure 3-18.